Molecular networks of periderm development in *Arabidopsis*

Dissertation

der Mathematisch-Naturwissenschaftlichen Fakultät

der Eberhard Karls Universität Tübingen

zur Erlangung des Grades eines

Doktors der Naturwissenschaften

(Dr. rer. nat.)

vorgelegt von

Anna Wunderling

aus Herrenberg

Tübingen

2018

Gedruckt mit Genehmigung der Mathematisch-Naturwissenschaftlichen Fakultät der
Eberhard Karls Universität Tübingen

Tag der mündlichen Qualifikation: 19.10.2018

Dekan:	Dr. Wolfgang Rosenstiel
1. Berichterstatter:	Dr. Laura Ragni
2. Berichterstatter:	Prof. Dr. Gerd Jürgens

Acknowledgements

In the first place I would like to thank Dr. Laura Ragni for admitting me into her new research group at the ZMBP and for the continued guidance as well as the opportunity to take part in international conferences. I would like to express sincere thanks to Prof. Dr. Gerd Jürgens for his advice and assistance with my scientific projects and for the willing agreement to act as second examiner for this dissertation. I want to extend my gratitude to my dear colleagues and former colleagues in the Ragni group for the collaborative work and the amicable atmosphere: Mehdi Ben-Targem, Dagmar Ripper, Andrea Bock, Rebecca Richter, Stefan Mahn, Azahara Barra-Jimenez and Kathrin Sajak. Furthermore, I am very grateful to all my colleagues of the developmental genetics department for the all-time readiness to help with problem solutions and for the evening trips to downtown Tübingen. Finally I would like to thank my family and Sascha for always supporting me.

Table of Contents

1. Summary

A periderm is developed by most dicotyledons and gymnosperms to protect the vascular cylinder against the environment and replaces the epidermis once it cannot accommodate the radial thickening during secondary growth anymore. The periderm consists of the cork cambium producing inwards the phelloderm and outwards the phellem or cork. Phellem cells are highly suberized and develop into dead cells. Despite its biological and economic importance, the molecular mechanisms of periderm development are largely unknown.

To shed light on the periderm development of Arabidopsis, marker lines for phellem and cork cambium cells were developed. Six stages of periderm growth in the root and hypocotyl were defined in this study. At stage 0 the pericycle is surrounded by the endodermis, cortex and epidermis cell layers while at stage 6 the differentiated periderm is the outside tissue of root and hypocotyl. In addition to the periderm development, these stages reveal the fate of the outside layers (endodermis, cortex and epidermis). The loosening of the outside layers follows a specific pattern that involves programmed cell death and cell abscission. Furthermore, this study shows that perturbing the cell number and identity and cell wall composition of these outside layers has an effect on the periderm development, demonstrating that a mechanical interaction occurs between the periderm cells and the outer layers. In contrast, there seems to be some kind of competition between the lateral root formation and the periderm development. In this regard, it was demonstrated that auxin plays an important role in the periderm development and many auxin-dependent early LR regulators are expressed in the periderm and are involved in its development.

2. Zusammenfassung

Ein Periderm schützt den vaskulären Zylinder der meisten Dikotylen und Gymnospermen vor Umwelteinflüssen und ersetzt die Epidermis, sobald sich diese nicht mehr an das sekundäre Wachstum der Pflanze anpassen kann. Das Periderm besteht aus drei unterschiedlichen Gewebetypen: Das Korkkambium gibt nach innen das Phelloderm und nach außen das Phellem oder Kork ab. Phellemzellen sind stark suberinisiert und sterben mit der Zeit ab. Trotz der biologischen und wirtschaftlichen Bedeutung von Kork sind die molekularen Mechanismen der Peridermentwicklung weitgehend unbekannt.

Um der Peridermentwicklung in Arabidopsis auf den Grund zu gehen, wurden in dieser Dissertation Markerlinien für das Phellem und Korkkambium entwickelt und sechs verschiedene Stadien des Peridermwachstums in Wurzel und Hypokotyl definiert. Im Stadium 0 ist der Perizykel von Endodermis-, Kortex- und Epidermiszellschichten umgeben während im Stadium 6 das ausdifferenzierte Periderm das äußerste Gewebe der Wurzel und des Hypokotyls bildet. Zusätzlich zur Peridermentwicklung enthüllen diese Stadien das Schicksal der äußeren Zellschichten (Endodermis, Kortex und Epidermis). Das Ablösen dieser äußeren Zellschichten folgt einem bestimmten Muster, welches den programmierten Zelltod sowie Zellabszission einschließt. Außerdem fanden wir heraus, dass die Eigenschaften und Zellwandkomponenten der äußeren Zellschichten einen Einfluss auf die Peridermentwicklung haben. Dies weist auf die Existenz einer mechanischen Interaktion zwischen Peridermzellen und den äußeren Zellschichten hin. Im Gegensatz dazu scheint eine Konkurrenz zwischen lateraler Wurzelbildung und der Peridermentwicklung vorzuliegen. In diesem Zusammenhang konnten wir zeigen, dass Auxin eine wichtige Rolle in der Peridermentwicklung spielt. Viele auxinabhängige, frühe Regulatoren der lateralen Wurzelbildung werden im Periderm exprimiert und sind an dessen Entwicklung beteiligt.

3. List of publications

Published articles

3.1 Novel tools for quantifying secondary growth

Anna Wunderling, Mehdi Ben Targem, Pierre Barbier de Reuille and Laura Ragni

Journal of Experimental Botany, Jan. 2017, Vol. 68(1): 89-95. DOI: 10.1093/jxb/erw450

3.2 A molecular framework to study periderm formation in Arabidopsis

Anna Wunderling, Dagmar Ripper, Azahara Barra-Jimenez, Stefan Mahn, Kathrin Sajak, Mehdi Ben Targem, Laura Ragni

New Phytologist, March 2018, Vol. 219: 216–229. DOI: 10.1111/nph.15128

Manuscript draft

3.3 Auxin signaling regulates the periderm development in *Arabidopsis thaliana*

Anna Wunderling, Dagmar Ripper, Stefan Mahn, Joop Vermeer, Laura Ragni

unsubmitted

4. Personal contribution

4.1 Novel tools for quantifying secondary growth (Wunderling et al., 2017)

The article was written together with M. B. T., P. B. R. and L. R.

4.2 A molecular framework to study periderm formation in Arabidopsis

(Wunderling et al., 2018)

The research was designed together with L.R. All experiments were performed by D.R., A.B-J., S.M., K.S., M.B.T., L.R. and me. Experiments performed by me: root atlas, GUS expression analyses, phellem extension experiments, cross-sections and analyses of roots grown under different conditions and lateral root stages. The data was analyzed and discussed in collaboration with A.B-J. and L.R. L.R. wrote the article with the help of A.B-J and me.

4.3 Auxin signaling regulates the periderm development in Arabidopsis thaliana

(Manuscript draft)

The research was designed together with L.R. All experiments were performed by me except for the fluorescence confocal microscope analyses and generation of the *PER15::mCherry-SYP122* line. The data was analyzed and discussed and the article was written in collaboration with L.R.

5. Introduction

5.1 Secondary growth of plants

Secondary growth, the radial thickening of plant organs, is essential for an efficient long-distance transport of water, solutes and photo-assimilates. But secondary growth also shapes the plant in response to a changing environment and thus enabled the striking success of vascular plants during their evolution (Spicer & Groover, 2010). The production of wood is one process of secondary growth and represents the major source of biomass accumulation in perennial dicotyledons and gymnosperms (Demura & Ye, 2010). Secondary growth is driven by a post-embryonic meristem, the vascular cambium. The vascular cambium is formed of a ring of undifferentiated meristematic cells. Upon cell division, these cells differentiate into xylem cells to the inside, producing wood, and phloem cells to the outside, forming bast. Secondary growth occurs in stems, branches and roots of most woody dicotyledonous plants and gymnosperms (Spicer and Groover, 2010; Ragni and Hardtke, 2014; Zhang et al., 2014). Even in the herbaceous dicotyledonous model plant species *Arabidopsis thaliana* (Arabidopsis), secondary growth of the vasculature can be found in the root, hypocotyl and stem. In the Arabidopsis hypocotyl secondary growth progression is uncoupled from the elongation process and thus can be followed over time. Furthermore, the organization of the vasculature is similar in the Arabidopsis hypocotyl and tree stems. These characteristics render the Arabidopsis hypocotyl a good model to study secondary growth (Chaffey et al., 2002; Ragni and Hardtke, 2014). Secondary growth of the hypocotyl can be divided into two phases based on cell morphology and proliferation rate: an early phase when the xylem mainly comprises water-conducting cells and parenchyma cells and a later phase of xylem expansion in which xylem area increases and fibers differentiate (Chaffey et al., 2002; Sibout et al., 2008). To date, it has been shown that Arabidopsis shares a common regulatory network of the vascular cambium with woody species (Barra-Jimenez & Ragni, 2017). An example is the regulatory module involving the receptor like kinases PHLOEM INTERCALATED WITH XYLEM/TDIF RECEPTOR (PXY/TDR), the small peptide CLAVATA3 (CLV3)/EMBRYO SURROUNDING REGION-RELATED 41/44 (CLE41/CLE44) and the transcription factor (TF) WUSCHEL HOMEOBOX 4 (WOX4). This module controls vascular cambium proliferation in several species including Arabidopsis and poplar (Etchells et al., 2015; Hirakawa & Bowman, 2015; Kucukoglu et al., 2017).

5.2 Periderm in plants

Another lateral meristem, contributing to secondary growth of plants, is the phellogen; also known as cork cambium. The phellogen divides in a strictly bidirectional manner to produce inwards the phelloderm cells and outwards the phellem cells, also called cork (Esau, 1977). The three tissues phellogen, phelloderm and phellem together are referred to as the periderm (Fig. 1). The periderm is a barrier organ that surrounds the vascular cylinder. It replaces the epidermis in stems, branches, and roots of most dicotyledons and gymnosperms once the epidermis can no longer accommodate to radial growth. Similar to the epidermis during primary development, the periderm protects the plant against biotic and abiotic stresses during secondary growth. It effectively restricts gas exchange, water loss and pathogen infestation (Lulai & Freeman, 2001; Groh et al., 2002; Lendzian, 2006). Furthermore, the parenchymatic components of the phelloderm fulfill a function in storing starch (Esau, 1977)

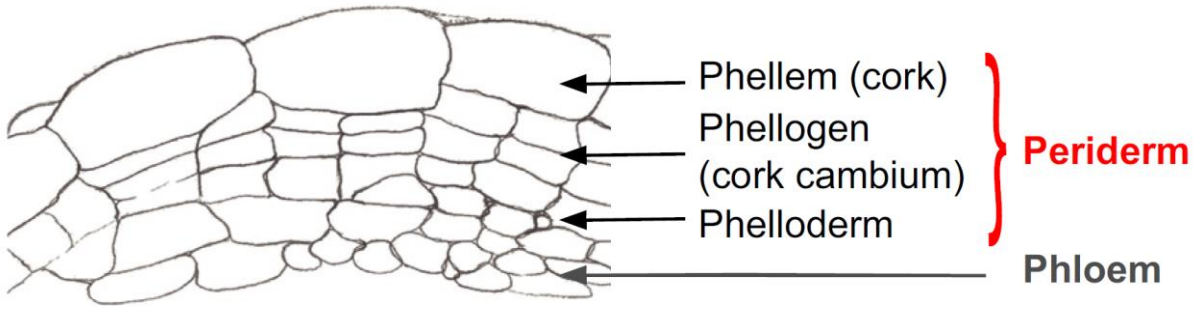

Fig. 1: Schematic representation of the periderm comprising the phellem (cork), the phellogen (cork cambium) and the phelloderm. (Adapted from Wunderling et al., 2018)

In most woody eudicotyledons and gymnosperms a periderm is formed in the root and the stem (Esau, 1977). Also in underground stems, such as the potato tuber, an extensive periderm can be found. In the stem of most trees the first phellogen arises in the sub-epidermal layer. While in the roots of most plant species the phellogen is derived from the pericycle, in some species it arises from the epidermis or phloem (Esau, 1977). The number of cell layers of different periderm tissues varies among species. Usually only 1-2 layers of phelloderm cells are present in the periderm, whereas several cell layers of phellem cells are differentiated (Esau, 1977; Pereira, 2007). In trees, the phellogen can be replaced every year by a new phellogen or can remain active for several years (Esau, 1977; Pereira, 2007). For example the phellogen of cork oak is functional for many years and remains viable throughout the life of a tree while its activity decreases with age (Waisel, 1995; Pereira, 2007). Furthermore, the phellogen activity in trees undergoes seasonal changes and fluctuates with climatic variations (Waisel, 1995; Caritat et al.,

2000; Pereira, 2007). Cold spells and drought lead to a decreased phellogen activity while periods of warm weather result in an increased phellogen activity (Waisel, 1995; Caritat et al., 2000; Pereira, 2007). A special form of periderm is the so called “wound” periderm. It covers damaged or necrotic tissues in case of a mechanical injury, a shedding of branches and leaves (Tucker, 1975; Thomson et al., 1995; Oven et al., 1999; Neubauer et al., 2012; Khanal et al., 2013) or during pathogen infections (Lulai & Corsini, 1998; Thangavel et al., 2016).

The barrier function of the periderm is mainly fulfilled by macromolecules, such as suberin, that are the major components of the phellem cell walls (Pereira, 1988). Because of the economic importance of potato and cork oak, the chemical and physical properties of phellem cell walls have been extensively studied in these plant species. This is due to the relevance of improving potato conservation (Neubauer et al., 2013) and of phellem as a source for wine bottle stoppers as well as building and insulating material (Silva et al., 2005). Suberin extracted from the phellem is also used for industrial applications such as the production of hybrid co-polymers like polyurethanes (Cordeiro et al., 1999), thermoset resins (Torron et al., 2014) and high-resistant fibers (de Geus et al., 2010). Suberin is a complex glycerol based heteropolymer comprised of aliphatic and phenolic fractions and it often has non-covalently associated waxes (Vishwanath et al., 2015). The amount and composition of phellem suberin and waxes varies among species and throughout the plant development, e.g. in the phellem of cork oak the suberin content can reach up to 40% of the dry weight (Pereira, 1988; Pinto et al., 2009; Kosma et al., 2015). Like in xylem cell walls, lignin is also deposited in phellem cell walls but displays a different monolignol composition compared to wood (Marques & Pereira, 2013; Fagerstedt et al., 2015; Lourenco et al., 2016).

The periderm can be isolated from the potato tuber in sufficient amounts for chemical analyses which renders potato a good model species to study suberin biosynthesis and periderm water permeability (Serra et al., 2009a). Reverse genetic studies point out that a reduction of ferulic acids in the potato periderm leads to an increased water permeability and a defective periderm maturation (Serra et al., 2010). Reducing the aliphatic suberin contents results in similar phenotypes; suggesting that both suberin composition and quantity is important for the water barrier function of the phellem (Serra et al., 2009a; Serra et al., 2009b; Serra et al., 2010). Suberin biosynthesis genes have been extensively characterized, also in Arabidopsis, with focus on the chemical composition of the whole root, endodermis and seed coat (Beisson et al., 2007; Hofer et al., 2008; Compagnon et al., 2009; Molina et al., 2009; Domergue et al., 2010; Kosma et al., 2012). It has been shown that *ALIPHATIC SUBERIN FERULOYL TRANSFERASE*

(*ASFT*) as well as *FATTY ACYL-COA REDUCTASES 1* (*FAR1*), *FAR4* and *FAR5* genes are expressed within the phellem cells of the Arabidopsis root (Molina et al., 2009; Vishwanath et al., 2013). However, the suberin lamellae in the periderm are undisturbed in *asft* mutants (Molina et al., 2009).

Despite the progress in understanding the molecular mechanisms underlying vascular cambium development, very few regulators controlling phellogen establishment and activity have been identified so far. The transcription factor (TF) SHORT-ROOT-like 2B (PttSHRL2B) has been shown to regulate phellogen activity in poplar (Miguel et al., 2016) and it has been suggested that the TF QsMYB1 (ortholog of Arabidopsis MYB84), coordinates phellogen activity in response to drought and heat in cork oak (Almeida et al., 2013a; Almeida et al., 2013b). One possible explanation for the lack of knowledge about the periderm could be that it has mainly been studied in non-model species. In contrast, the knowledge about the basic mechanisms of vascular cambium activity is primarily derived from research within Arabidopsis. However, also the periderm can be studied in the root and hypocotyl of Arabidopsis to gain new insights into its development and regulation (Dolan and Roberts, 1995; Chaffey et al., 2002).

5.3 Lateral root formation in Arabidopsis

The periderm development shares a mutual characteristic with lateral root (LR) formation in Arabidopsis as LRs and the periderm both arise from the pericycle (Malamy and Benfey, 1997; Esau, 1977). LRs are derived from pairs of pericycle cells; the so- called LR founder cells. They are located next to the xylem poles (Malamy and Benfey, 1997) and develop close to the root tip within the basal meristem of the root (De Smet et al., 2007; Moreno-Risueno et al., 2010; Van Norman et al., 2013) (Fig. 2). The nuclei of the LR founder cells move towards the common cell walls after the founder cell priming. Both cells divide in an asymmetric anticlinal manner (De Smet et al., 2007; De Rybel et al., 2010; Goh et al., 2012) and the stage I LR primordium is established. A change in the division planes from anticlinal to periclinal results in a two-layered LR primordium and Stage II. More periclinal divisions lead to a multilayered LR primordium (Stage III to VII). This primordium protrudes into the cell layers of the ground tissue and epidermis (Malamy and Benfey, 1997; Lucas et al., 2013). Finally, the LR emerges and the meristem is activated leading to LR elongation.

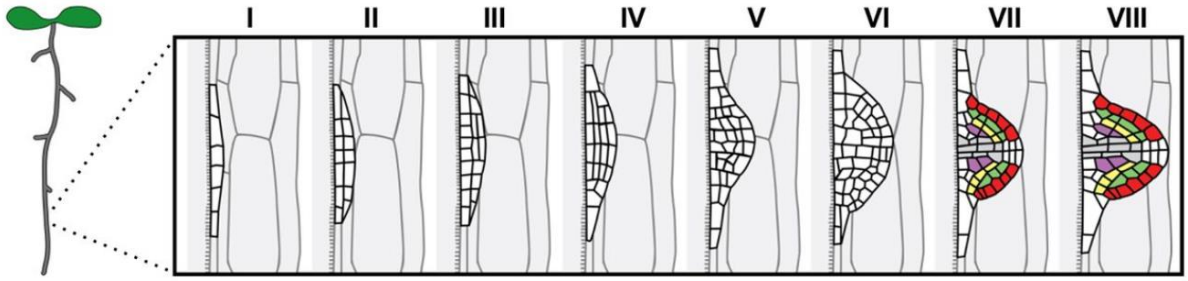

Fig: 2: Eight developmental stages of lateral root formation in Arabidopsis (I-VIII; Adapted from Porco et al., 2016)

The processes of LR formation from LR priming to emergence are controlled by the phytohormone auxin (Lavenus et al., 2013). Thus, LR formation is regulated by auxin signaling modules and each module is formed by co-expressed and interacting Aux/ INDOLE-3-ACETIC ACID INDUCIBLE (Aux/IAA) and AUXIN RESPONSE FACTOR (ARF) proteins regulating auxin responsive genes (De Rybel et al., 2010) (Fig.3). Aux/IAA proteins are short-living, nuclear proteins that repress the expression of ARF genes (Tiwari et al. 2004).

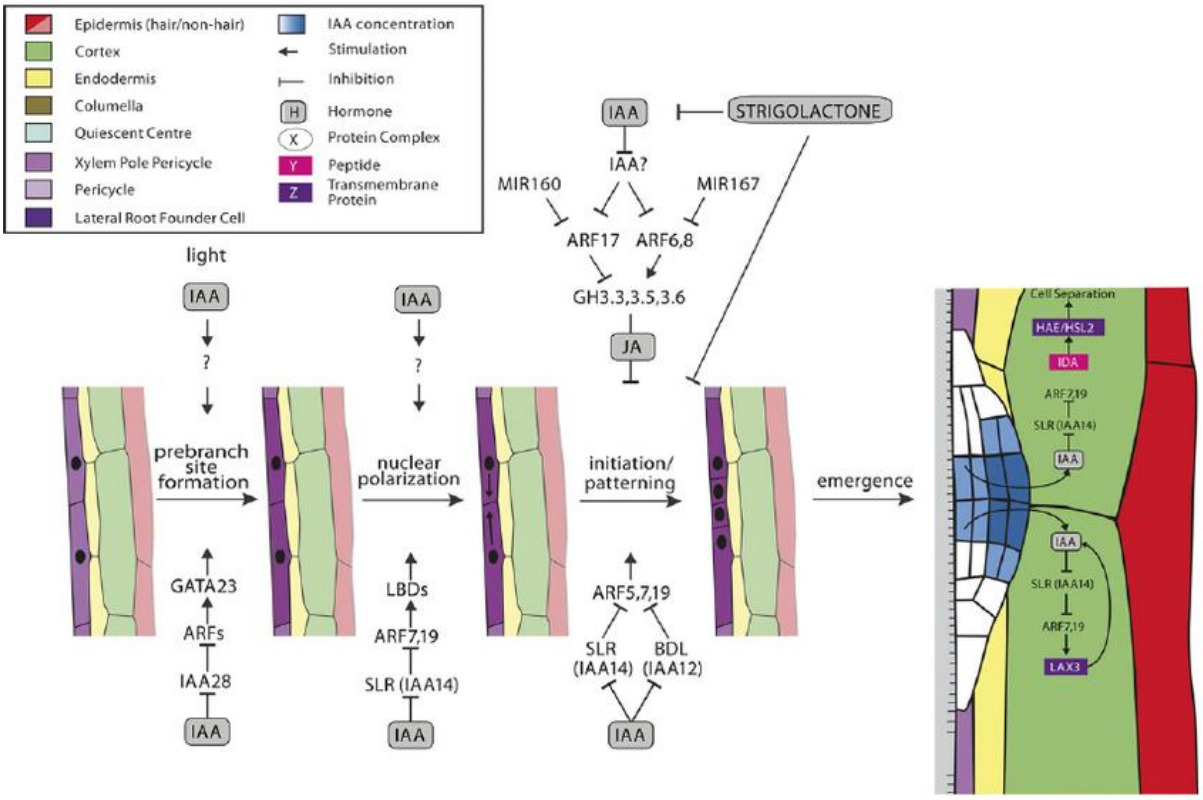

Fig. 3 Regulators of lateral root initiation and patterning. (Adapted and modified from Atkinson et al., 2014)

The following auxin signaling modules are important in the LR regulation of Arabidopsis: LR priming is controlled by an IAA28-dependent auxin signaling module. One target is *GATA23*, encoding a transcription factor that triggers the acquisition of the lateral root founder cell identity (De Rybel et al., 2010). The founder cell polarization is regulated by an auxin signaling module that involves IAA14/SLR, ARF7 and ARF19 (Fukaki et al., 2005; Okushima et al., 2005a, 2007; Wilmoth et al., 2005; Lee et al., 2009; Goh et al., 2012). Signaling targets are genes encoding the LBD transcription factors LBD16, 18, 29, and 33 as well as ARF19 itself (Okushima et al., 2005a, 2007). Together with a third module of IAA12/BDL and ARF5/MP, the IAA14/SLR module is also important for LR initiation and LR primordia patterning (Vanneste et al., 2005; De Smet, 2010). Furthermore, *Aux/IAA* genes *IAA3* (Tian and Reed, 1999), *IAA18* (Uehara et al., 2008), *IAA19* (Tatematsu et al., 2004), and *IAA28* (Rogg et al., 2001) were found to be related to lateral root formation.

6. Objectives

Molecular mechanisms of periderm development are largely uninvestigated and should be revealed within this study. So far the periderm has been examined mainly in trees like poplar and cork oak or in potato. However, the periderm can also be studied in the root and hypocotyl of Arabidopsis (Dolan and Roberts, 1995; Chaffey et al., 2002). In this thesis the molecular mechanisms of periderm development should be investigated in the Arabidopsis root and hypocotyl.

In most plant species the periderm arises from the pericycle, an inner cell layer, and will finally build the outside tissue of roots, stems and branches (Esau, 1977). In order to determine molecular regulators of the periderm development in Arabidopsis, periderm reporter lines were generated and their expression patterns explored. Additionally, these reporter lines were used to establish an atlas with stages of periderm development. Here, the fate of the outside cell layers (endodermis, cortex/inner and outer cortex and epidermis) surrounding the pericycle of Arabidopsis has to be considered as well. Furthermore, it should be examined if and in which way the pericycle/periderm and the outside layers communicate or interact with each other. For that reason, the periderm development of mutant plant lines displaying an impaired ground tissue or altered chemical composition of ground tissue cell walls was analyzed. To gain an even deeper understanding of the molecular frameworks controlling periderm development it was determined whether auxin signaling could be part of the network as auxin plays a role in many plant developmental processes like vascular stem cell initiation (Hardtke and Berleth 1998; Friml et al., 2003) or lateral root formation (Lavenus et al., 2013). Therefore, transgenic auxin concentration (*D2VENUS*) and activity (*DR5*) reporter lines were analyzed regarding to the periderm tissues. Additionally, we examined the periderm development in mutants that display defects in auxin-dependent early LR regulators or harbor an impaired auxin signaling specifically in the pericycle/periderm. Furthermore, periderm development and LR formation share the same characteristic of arising from the pericycle (Esau, 1977; Malamy and Benfey, 1997). Since many LR regulators are already published, one aim of this thesis was to show whether these regulators are also involved in the periderm development or if LR and periderm formation are competing processes. In order to answer this question the periderm formation of plant lines showing an impairment in lateral root formation (decreased LR density or absence of LRs) or an over-proliferation of lateral roots was examined.

7. Results and Discussion

7.1 A molecular framework to study periderm formation in *Arabidopsis* (Wunderling et al., 2018)

To improve investigations of periderm development in the future, we aimed to determine the molecular framework underlying periderm formation of Arabidopsis roots and hypocotyls. We found that the Arabidopsis periderm displays characteristics similar to those of woody eudicotyledonous periderms and putative regulators are conserved among species. A main characteristic of phellem cell walls is the high degree of suberization and many suberin biosynthesis genes are expressed in the phellem of cork oak as well as the root and the hypocotyl of Arabidopsis (Molina et al., 2009; Kosma et al., 2012; Vishwanath et al., 2013). We could confirm that that the phellem cell walls of Arabidopsis are suberized and lignified as well and the phellem tissue is even partially composed of dead cells. Also on a molecular level the periderm of Arabidopsis shares characteristics with trees and potato as some regulators are conserved among species. Transcriptomic datasets once revealed that *MYB* and *NAC* transcription factor families are expressed in the phellem of poplar and potato (Soler et al., 2007, 2011; Ginzberg et al., 2009; Rains et al., 2017; Vulavala et al., 2017). For example, *QsMYB1/ MYB84/RAX3* is expressed in the phellem of cork oak and the expression responds to drought and heat stress (Almeida et al., 2013b). We found that the Arabidopsis homologue *MYB84/RAX3* is also expressed in the Arabidopsis periderm and *ANAC78* as member of the NAC TF family is expressed in the periderm and in the phloem of the hypocotyl and root. Additionally the suberin/wax biosynthesis genes *GPAT5*, *KCR1*, *HORST*, *DAISY*, *RALPH* and *ASFT* are expressed in the phellem of cork oak, potato and poplar (Soler et al., 2007, 2011; Serra et al., 2009a,b, 2010; Rains et al., 2017) and we found it also to be expressed in the Arabidopsis phellem of both root and hypocotyl.

For further analyzation of the periderm development, we established marker lines for the phellem and the cork cambium and identified six stages of periderm growth in the root and hypocotyl. The periderm development is temporally separated with an accelerated development in the root compared to the hypocotyl. Furthermore, the periderm development can be analyzed only over time in the hypocotyl but followed gradually along a root. In both, hypocotyl and root, the periderm arises from the pericycle. The pericycle is an inner tissue that is surrounded to the outside by three or four cell layers in root or hypocotyl at stage 0, and becomes the external tissue when periderm cells are differentiated (stage 6). The duration of the periderm development in root and hypocotyl depends on the growing conditions. We identified STAGE

0 as the state before the first division of a pericycle cells occurs but after hypocotyl elongation. The vasculature is already arranged with a central metaxylem and two phloem poles. The pericycle comprises in the hypocotyl 13–14 cells surrounded by eight endodermal cells, approximately eight inner cortex cells, 14 outer cortex cells, and 33–34 epidermis cells. During STAGE 1 the xylem pole pericycle cells undergo their first anticlinal divisions and the cell divisions expand to the neighboring pericycle cells. Simultaneously the endodermal cells become flattened. STAGE 2 is marked by a reduction in endodermal cell number resulting in four to six cells being left at the sites of the xylem poles. At the same time pericycle cells divide periclinally and the pericycle then consists of two cell layers in some regions and is in these regions referred to as the phellogen. The pericycle/periderm of STAGE 3 comprises at least two layers of cells and one or two endodermal cells are still left at the xylem poles. The number of cortical and epidermal cells stays consistent. At STAGE 4 all endodermal cells are gone and the first phellem cells are differentiated from the phellogen. During STAGE 4A, the inner cortex most of the times starts to disappear from the phloem poles and a few more phellem cells are differentiated. In STAGE 4B the inner cortex is missing and a ring of phellem cells is formed. At STAGE 5 the epidermis and outer cortex start to break at one site and get detached from the periderm. Finally, STAGE 6 is marked by a mature periderm as the outer tissue with a completely detached epidermis and cortex. It consists of four to five cell layers comprising the phellem, the phellogen and the phelloderm in the hypocotyl.

The periderm development of the Arabidopsis root mainly follows the same stages but with a few differences in some of the stages probably due to the distinct anatomy compared to the hypocotyl. At STAGE 0 the root has only one cortex cell layer while the hypocotyl has an inner and outer one. Root epidermis and cortex are shed earlier in plant development than in the hypocotyl. The position of each stage and the length of the root part per stage vary by the age of plants and growth conditions. STAGE 0 in roots is positioned directly above the lateral root initiation zone. Similar to the hypocotyl, the root vasculature has a central xylem axis and two phloem poles. The pericycle is surrounded by the endodermis (~ eight cells), the cortex (12–14 cells) and the epidermis (23 cells). STAGE 1 is located in the region above STAGE 0 and the pericycle cells divide anticlinally at the xylem poles. At STAGE 2 one or two endodermal cells are lost most of the times at the phloem poles and the first periclinal divisions of a pericycle cell occur, leading to the two-layered phellogen. There is only one large STAGE 3/4 defined in the root as the characteristics cannot be locally distinguished and the cellular events often happen coincidentally and stochastically. During STAGE 3/4, the pericycle divides periclinally while the number of endodermal cells decreases. The cortex and epidermis break primarily at

the site where the endodermal cells disappeared and phellem cells are differentiating simultaneously at these sites. The periderm of STAGE 5 is completely differentiated while the phellem is still partially covered with patches of epidermis and cortex cells. Finally, at STAGE 6 epidermis and cortex are shed whereas the periderm forms the new, three or four cell layer comprising, outside tissue. We furthermore found that overall, the periderm formation in lateral roots occurs similarly to the main root. Most probably one layer of phelloderm cells is formed in Arabidopsis roots and hypocotyls. In addition to the periderm development, the defined stages reveal the fate of the outside layers (endodermis, cortex and epidermis) demonstrating that the loosening of the outside layers follows a specific pattern that involves cell death and cell abscission. We found that the endodermis cells undergo PCD in the root and hypocotyl as well as the inner cortex in the hypocotyl. The first cells undergoing PCD are located at the sites of the phloem poles and PCD expands from there to neighboring endodermis/inner cortex cells. The last two remaining endodermal cells are generally located at the sites of the original xylem poles. The mature endodermis is a highly suberized tissue and the amount of suberin is modified according to the nutrient availability (Barberon et al., 2016). We found that suberin amount and length of endodermal cells is reduced prior to endodermal PCD. Upon endodermal/inner cortex PCD, the cortex/outer cortex cell layer is abscised from the root and hypocotyl while the cortical/epidermal cell layers get detached. This abscission starts with a breaking point of cortex/outer cortex and epidermis primarily at the site where the endodermal cells disappeared. Simultaneously, phellem cells are differentiating at these sites.

Our results demonstrate that periderm growth is tightly connected to the fate of the outside tissues and particularly to endodermal PCD and cortex/outer cortex cell abscission. The unraveling of the periderm development on a cellular level by defining its stages and the uncovering of the first regulators now facilitates the molecular investigation of the periderm development. Additionally, these results show that insights gained from investigating the Arabidopsis periderm might also be transferable to trees as both have shared characteristics.

7.2 Communication between periderm and ground tissue cells

The loosening of the outside tissues is a controlled mechanism that follows a predetermined pattern during periderm development. A tight connection exists between the periderm development and the fate of the outside tissues, particularly endodermal PCD and the abscission of cortex/outer cortex cell layers. Due to this tight connection, we wondered if these outer layers have an effect on the periderm development. Therefore, we investigated the periderm development of mutants that exhibit ground tissue (endodermis and cortex) defects.

7.2.1 An impaired ground tissue effects the periderm development

To examine if the ground tissue cell layers effect the periderm development, at first we analyzed if mutants with a defective endodermis or cortex also have an altered periderm development. In the *CASPARIAN STRIP MEMBRANE PROTEIN 1::callose synthase 3m* (*CASP1::cals3m*) mutant plasmodesmatal transport between endodermis and pericycle or periderm cells is blocked by an excess of callose deposition in endodermal plasmodesmata (Vermeer et al., 2014). We determined periderm extension in roots by measuring the length of the phellem-covered root part and normalizing it to the root length. This method was used to investigate periderm formation dynamics, as an increased or decreased ratio of phellem length to root length indicates faster or slower periderm development compared to control plants. We found a decreased periderm extension for *CASP1::cals3m* compared to *Col-0* (Fig. 2c) indicating a delayed periderm development. In root cross-sections the phellogen is still visible in *CASP1::cals3m* (Fig. 2h) when a few phellem cells are already differentiated in *Col-0* (Fig. 2g) and the pericycle is still present in *CASP1::cals3m* hypocotyls (Fig. 2f) when a phellogen is already formed in the *Col-0* control plants (Fig. 2l). This confirms the decelerated periderm development of *CASP1::cals3m* mutants.

We next studied the periderm development in *scarecrow* (*scr*) and *short root* (*shr*) mutants. SCR and SHR together control the first asymmetric cell divisions in the ground tissue founder cells and the *scr-3* mutant is characterized by a single layer of ground tissue with a hybrid identity of endodermis and cortex cells (Di Laurenzio et al., 1996; Helariutta et al., 2000; Sozzani et al., 2010). Primary root growth is strongly affected in *scr* because SCR is involved in the maintenance of the root meristem stem cell niche (Di Laurenzio et al., 1996; Goh et al., 2016; Moubayidin et al., 2016). Primary root growth is even more effected in *shr-2* mutants and in addition they exhibit a single layer of ground tissue with cortex characteristics (Benfey et al., 1993). We were able to observe the published *scr-3* (Fig. 2i) and *shr-2* (Fig. 2j) phenotypes showing a single layer of ground tissue cells. The periderm extension was increased in *scr-3* (Fig. 2c) suggesting an accelerated periderm development. This was confirmed by an increased periderm extension in an inducible *pSCR::SCR:GR scr-4* line (Fig. 2f). The periderm extension for *shr* is very variable. Beside, we cannot draw conclusions about the effects of altered outside layers on the periderm of the *shr* mutant because we found *SHR* expression in the periderm and not exclusively in the outer layers. Therefore a direct effect of the *shr* mutation on the periderm could be possible and not only a secondary effect due to the altered outer layers. In *scr-3* root cross-sections, some pericycle cells are still present (Fig. 2i red arrows) but not in

Col-0 (Fig. 2g). In *shr-2* root cross-sections we found missing periderm cells at an original phloem pole (Fig. 2j red arrows). Moreover the *scr-3* and *shr-2* hypocotyls show a starlike vasculature (Fig. 2 m,n black arrows) and disorganized pericycle/periderm tissues with abnormal division planes of periderm cells (Fig. 2 m,n red arrows) compared to Col-0 (Fig. 2k).

However, we can conclude that a blocked plasmodesmatal transport between the endodermis and pericycle or periderm (*CASP1::cals3m)* decelerates the periderm development while messing up the identity of outer cell layers in combination with a reduced number of outer layer cells *(scr-3)* leads to an accelerated and disorganized periderm development. This indicates that a disorganized ground tissue indeed affects the periderm development and the likely existence of a communication between the cell layers or some kind of interaction of the periderm with the ground tissue cell layers.

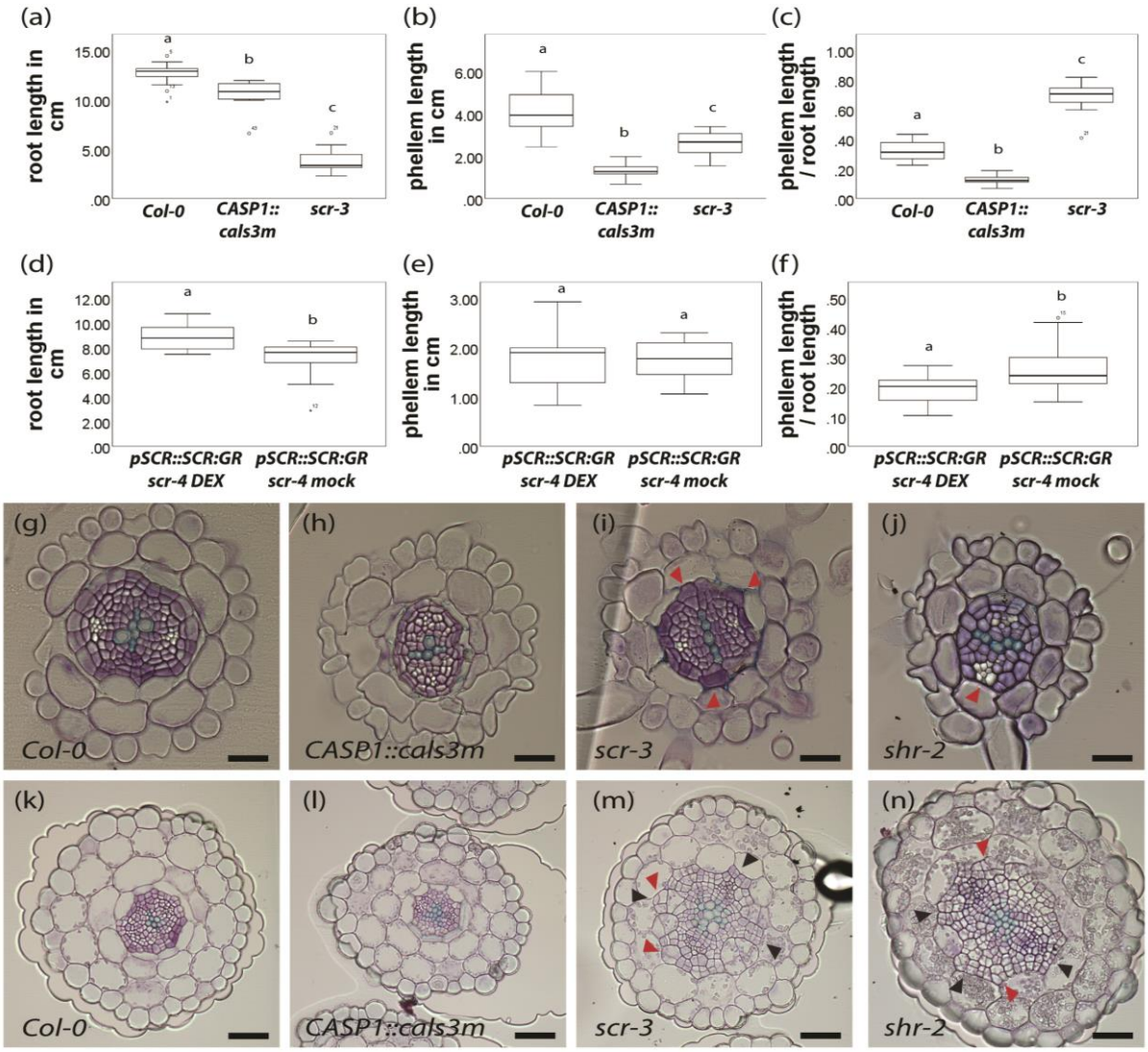

Fig. 4: Altered outer layers effect the periderm development. (a-f) Plots of the root length (a,d), length of the phellem-covered root part (b,e) and ratio of phellem length to root length (c,f) 15-d-old *Col-0*, *CASP1::cals3m* and *scr-3* roots (a-c) and 12-d-old induced and non-induced *pSCR::SCR:GR scr-4* roots (d-f). (g-n) Plastic cross-sections of 9-d-old *Col-0* (g,k), *CASP1::cals3m* (h,l), *scr-3* (i,m) and *shr-2* (j,n) roots (g-j) and hypocotyls (k-n).Box plots: the dark line in the middle of the boxes is the median, the bottom and top of the box indicates the 25^{th} and 75^{th} percentiles, whiskers are within 1.5 times the interquartile range, the empty dots are outliers, the black stars are extreme outliers. (a-f) Student's t-test ($p < 0.05$; n =15 (a-c), n=11-16 (d-f)). Black scale bars, 50 µm.

7.2.2 An altered cell wall composition influences the periderm

As we found that a communication or interaction occurs between the periderm and the ground tissue cell layers, next we wanted to know if this communication happens on a mechanical and/or molecular level. A mechanical communication could possibly be explained by a space limit or tension due to the outer layers forming a constraint for the increasing number of periderm cells. Hence, we analyzed the periderm of plants with an altered cell wall composition of the endodermis for changes. We wondered if an increased deposition of suberin and lignin in the endodermis cell wall leads to an increased tension or constraint on the pericycle/periderm leading to a decelerated periderm development. We also analyzed mutants that possess an altered chemical composition of cell walls of the outer layers. The *myb36-2* mutant shows an altered casparian strip formation by over-lignification/suberization (Kamiya et al., 2015) while the *esb1* mutation and *casp1-1 casp3-1* double mutation leads to an ectopic lignin deposition around the casparian strip domain and ectopic suberin deposition (Hosmani et al., 2013). We performed periderm extension experiments on the mutants and found for *myb36-2* a tendency towards a decreased periderm extension in 9 out of 11 independent repetitions with one statistically significant decrease (Fig. 3c) (twice not statistically significant increase). So the periderm formation seems to be decelerated in *myb36-2* mutants. In contrast, for the *casp1-1 casp3-1* and *esb1-1* mutants, the periderm extension experiments are very variable (results not shown). The decelerated periderm development in *myb36-2* indicates that an increased suberin and lignin deposition in the casparian strip of the endodermis cell wall leads to an increased tension or constraint on the pericycle/periderm. This suggests that at least the mechanical forces contribute to the communication between the periderm and outer layers. To really draw conclusions about the effect of the increased suberization and lignification of the outer layers on the periderm it will be necessary to confirm the *myb36-2* results by repeating the experiments with different lines that bear mutations in other genes leading to an over-lignification and -suberization.

To further confirm if the mechanical forces indeed have an influence on the communication between the periderm and the outer layers, we investigated the opposite situation of an increased suberin and lignin deposition in the outer layer cell walls, namely a decreased suberin deposition. We thus analyzed lines with mutations in suberin biosynthesis genes leading to a reduced amount of suberin deposition in their cell walls (*gpat5-1*, *horst-1 ralph-1*, *asft-1*). In periderm extension experiments *gpat5-1* shows an increased periderm extension (in 7 biological replicates 4x significantly increased, 3x increase not statistically significant) in the root (Fig. 3f) while in case of *horst-1 ralph-1* (3x significantly increased, 4x increase not statistically significant) and *asft-1* (1x significantly increased, 6x increase not statistically significant) there was a tendency of increased periderm extension compared to the *Col-0* control. Nevertheless, the increased periderm extension of *gpat5-1* and the tendency towards an increased periderm extension of *horst-1 ralph-1* and *asft-1* suggests an accelerated periderm development. This indicates that a decreased suberin content in the outer layer (or endodermis) cell wall leads to a decreased tension or constraint on the pericycle/periderm resulting in an accelerated periderm development. This further confirms that there is a mechanical component of communication between the periderm and outer cell layers.

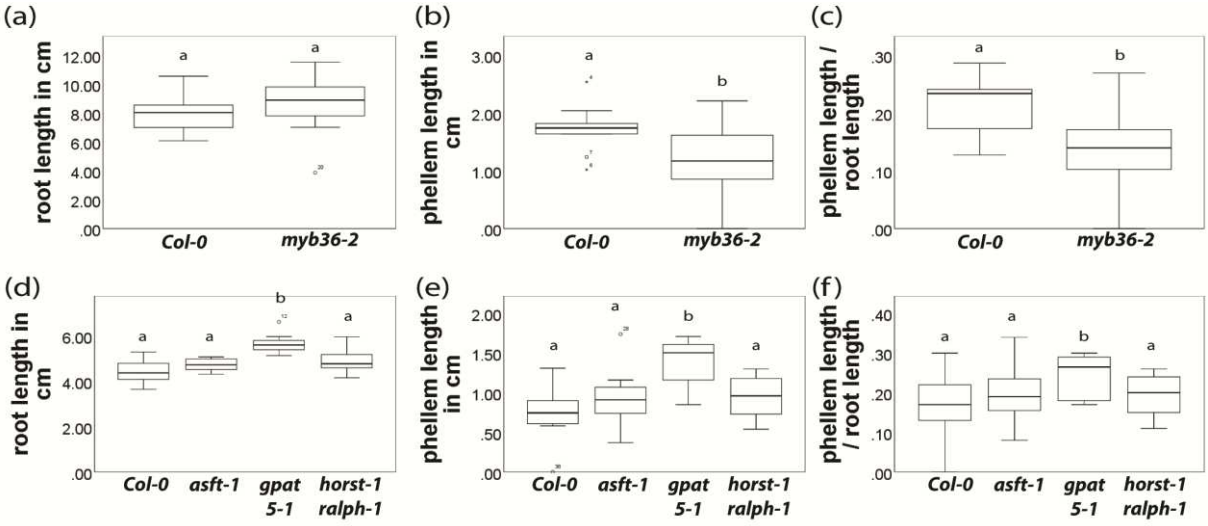

Fig. 5: An altered cell wall composition influences the periderm development. (a-f) Plots of the root length (a,d), length of the phellem-covered root part (b,e) and ratio of phellem length to root length (c,f) of 12-d-old *Col-0* and *myb36* roots (a-c) and of 9-d-old *Col-0*, *horst-1 ralph-1*, *gpat5-1* and *asft-1* roots (d-f). Box plots: the dark line in the middle of the boxes is the median, the bottom and top of the box indicates the 25th and 75th percentiles, whiskers are within 1.5 times the interquartile range, the empty dots are outliers, the black stars are extreme outliers. Student's t-test ($p < 0.05$; n =9-15 (a-c), n=8-10 (d-f)).

7.2.3 Conclusions

Taken together these results demonstrate that there is an interaction or communication between the outer cell layers disappearing upon periderm formation and the pericycle/periderm itself. This communication is on a mechanical level due to space limits and tensions which is indicated by the fact that *CASP1::cals3m* and *scr* mutants having defects in the endodermis or cortex also have a decelerated and accelerated periderm development, respectively. As a matter of fact, this shows that the disorganized ground tissue affects the periderm development and that there might be some kind of communication. The decelerated periderm formation of the *myb36-2* mutant (with an increased suberin/lignin deposition in the casparian strip) as well as the accelerated periderm development of suberin mutants *horst-1 ralph-1*, *gpat5-1* and *asft-1* (with an decreased suberin content in the outer layers) further suggest that this communication between the pericycle/periderm and the outer layers takes place on a mechanical level. Probably the space limit of the outer layers due to the increasing number and space of periderm cells as well as the tension decrease after endodermal PCD acts as mechanical signals. Nevertheless, it still would be interesting to analyze if there is also a molecular component of the interaction additionally to the mechanical signals. This mechanical communication between the cell layers might also be involved in the loosening of the outer tissues as a controlled mechanism that follows a predetermined pattern (Wunderling et al. 2018). It could also play a role in the tight connection between the periderm development and the fate of the outside tissues and particularly endodermal PCD (Wunderling et al. 2018). Already in 2013 it was proposed that lateral root primordia were to some extent shaped by the regulation of the mechanical properties of overlying cell layers (Lucas et al., 2013) analogous to the periderm being shaped by the mechanical properties of the overlying endodermis and cortex cell layers. This fits in line with the proposition of Vermeer et al. (2014) that "pericycle cells perceive a nonresponsive endodermis through an increased resistance to its expansion growth" and this mechanical stress then leads to a block of lateral root initiation. Our results fortify this idea because actually an increased suberin/lignin deposition in the casparian strip leads to a decelerated periderm formation as well as a decreased suberin content in the outer layers results in an accelerated periderm development. It would be interesting to see if the periderm can be completely abolished with an even more increased suberin/lignin deposition in the casparian strip leading to pericycle maintenance. We would expect that the pericycle cells are not even able to divide under increased mechanical stress by the outer layers, as accommodating responses are even required for initiation of cell division during LR formation (Vermeer et al., 2014). Vermeer et al. (2014) also showed that it is specifically the endodermis that plays a key role in lateral root

formation and emergence. This is similar to our findings of the endodermis playing an important role during periderm development.

The periderm-endodermis/cortex interaction that we have uncovered could contribute to examine how plant cells perceive and accommodate to the growth or loss of their neighboring cells. In addition to the periderm development, a similar mechanical communication is essential for lateral root formation (Vermeer et al., Science 2014) and also the growth of the shoot apical meristem is shaped by perceiving mechanical stresses at surface cell layers (Hamant et al., 2008). Mechanical communications might furthermore be of importance in root apical meristems (Potocka et al., 2011) and for secondary vascular growth (Carvalho et al., 2013), as well as for pollen tubes (Burri et al., 2018) and fungi to enter plant tissues (Kumamoto 2008). Generally, the use of mechanical communication by a coordinated accommodation in response to turgor and/or volume loss or increase might be widespread and happen wherever cell division and growth of inner layers occur.

7.2.4 Outlook

In order to prove the interaction or communication between the outer layers and the pericycle/periderm on a mechanical level due to space limits and tensions some experiments have to be repeated with a different setup. To achieve a statistically significant decrease in phellem extension of *myb36-2* it will be necessary to measure the periderm extension of late stages of periderm development or a larger sample size. Furthermore, the experiments have to be replicated with different lines that bear mutations in other genes leading to an over-lignification and –suberization to see if they also show a decrease in phellem extension. Additionally, the experiments with *horst-1 ralph-1* and *asft-1* have to be repeated to achieve a significantly increased periderm extension maybe also by measuring a larger sample size or late stages of periderm development.

7.2.5 Materials and Methods

Plant material and growth

Transgenic plant lines are in Col-0 background unless it is specified otherwise in the text or figures. The plants used for microscopy and periderm extension experiments were grown under continuous light condition in vitro on 1/2MS plates supplemented with 1% sugar. For NAA treatments, plants were transferred after 7 days of growth on 1/2MS 1% sugar to 1/2MS 1% sugar + 0,1 µM NAA / 1µM NAA / mock respectively. *scr-1* (N8539), *shr-2* (N2972), *pH7-CASP1::cals3m* (from Joop Vermeer), *myb36-2* (N355390 or GK-543B11), *esb1* (from David

E.Salt; Kamiya et al., 2015), *horst-1 ralph-1* (from Rocus B.Franke), *gpat5-1* (N673974; Beisson et al., 2007), *asft-1* (N656472; Molina et al., 2009).

Histology and staining

Plastic Root and hypocotyl plastic cross-sections were obtained as described in (Barbier de Reuille & Ragni, 2017) 0.5 mm below or above the hypocotyl-root-junction from the most mature part of a root or directly above the hypocotyl-root-junction in the hypocotyl, stained with 0.1 % toluidine blue and imaged with a Zeiss Axio M2 imager microscope or a Zeiss Axiophot microscope.

Image analyses and statistical analyses

The periderm extension was measured as described in Wunderling et al., 2018. The ratio of phellem length to root length was calculated from at least 15 roots per time point and plant line. The root diameter and periderm cell layers were measured on plastic cross-sections of most mature root parts. All statistical analyses were performed using IBM SPSS Statistics version 24 (IBM). The datasets were at first tested for homogeneity of variances using Levene's Test of Equality of Variances. Then the significant differences between two datasets were calculated using a Welch's t-test in case of a non-homogenous variance or a Student's t-test if the variance is homogeneous. The threshold for significance was set to a p-value < 0.05.

7.3 Auxin signaling regulates periderm development in *Arabidopsis thaliana* (manuscript draft)

Periderm development shares mutual characteristics with LR formation. On the one hand both, LRs and periderm, arise from the pericycle (Wunderling et al., 2018 and Malamy and Benfey, 1997) and on the other hand cell elimination contributes to organ growth during both processes. When phellem cells are differentiating from the phellogen, the overlying endodermal cells undergo PCD (Wunderling et al., 2018) and similarly during LR emergence a subset of endodermal cells overlying the LR primordia undergo cell death (Escamez et al., 2018). Due to these mutual characteristics between periderm and LR development, we investigated if these processes share common molecular regulators.

We demonstrated auxin accumulation at high levels in the phellogen, at lower levels in the phellem and that an auxin response takes place in the phellogen. Furthermore NPA-treatment severely inhibited auxin transport and signaling, leading to a reduced periderm development. In contrast, a high auxin concentrations and increased auxin signaling (by exogenous NAA-

application) promote the periderm development. These results indicate that auxin plays a role in the periderm development.

In support of the previous results, many auxin signaling dependent regulators of the early LR formation were expressed in periderm tissues. These are *GATA23*, *ARF7*, *ARF19*, *ARF8*, *ARF6* and *LBD16*. Consequently, plants displaying defects in the auxin dependent early LR regulators show defects in their periderm development as well. The periderm development is decelerated for *iaa28-1* and *GATA23 RNAi* lines while the periderm of *iaa28-1* and *arf7 arf19* is not able to respond to an exogenous auxin application. Again, these results emphasize that auxin plays a very important, positive role for periderm development. The periderm seems to share some regulators with LR formation, e.g *IAA28*, *GATA23*, *ARF7* and *ARF19*. In contrast to the previous results, we found an increased periderm development in plants with severe defects in LR formation leading to a decreased LR density or absence of LRs (*iaa18*, *slr-1* and *CASP1::shy2-2*). A possible explanation could be no expression of *IAA18* and *IAA14/SLR* in the periderm (preliminary results) and perturbed auxin signaling only in the endodermis in *CASP1::shy2-2*. Additionally, *sur1* displaying an over-proliferation of adventitious roots due to auxin overproduction in the hypocotyl (Pacurar et al., 2014), shows a nearly abolished periderm in hypocotyl and root. Furthermore, plants with impaired auxin-signaling (*shy2.2* Vermeer et al., 2014) specifically in the pericycle (*PER15::shy2-2*), develop LRs but have a severely disorganized periderm. Taken together, our results hint towards a competition between lateral/adventitious root formation and the periderm development possibly with a molecular switch in between both processes.

7.3.1 Outlook

To further investigate the periderm regarding to the role of auxin and lateral root regulators, the following experiments would be interesting to perform. The LR density of *PER15::shy2-2* plants is slightly reduced maybe caused by the residual *shy2-2* expression in endodermis cells as the *PER15* promoter is weakly active in the endodermis (data not shown). Thus, it will be necessary to generate plant lines expressing shy2-2 only in the pericycle and periderm, not in the endodermis to repeat the experiments. These plant lines are generated by cloning a DEX-inducible dominant active shy2-2 version under the control of a *MYB84* promoter with an activation restricted to the pericycle and periderm. As controls, the *GPAT5* (active in the endodermis and phellem) and *GATA23* (active in LRs and the periderm) promoters will be used. Induced *MYB84::shy2-2* lines are expected to show a disorganized periderm but lateral root

growth like non-induced plants. If this is the case, plants of these transgenic lines will be treated with 1µM NAA to analyze if the periderm is still able to respond to auxin.

In case of *sur1* we found an over-proliferation of adventitious roots but not of LRs. The primary roots of these mutants are much shorter than of *Col-0* and the LR density is significantly reduced. Therefore, it would be interesting to find out if the over-production of auxin takes place only in the hypocotyl and not in roots by expressing auxin reporters in *sur1* or treating *sur1* with exogenous applied 1µM NAA.

In addition, it will be necessary to repeat the embedding and phellem extension experiments of *slr-1*, *arf7 arf19* (N24629), *CASP1::shy2-2*, *iaa18-1* (in Ler) *and iaa28-1* (in *Ws*) for a third biological replicate. Also the embedding and phellem extension experiments of the auxin-treatments of *CASP1::shy2-2*, *arf7 arf19*, and *pCASP::shy2-2* have to be repeated for more biological replicates. Here, *PER15:shy2-2 –GR:term*, *GATA23::shy2-2-GR:term* and *Xpp:Shy2-2-GR:term* (provided by Alexis Maizel) will be included as auxin signaling is specifically and inducible impaired in the periderm (*PER15)*, periderm and LRs (*GATA23*) or the xylem pole pericycle (*Xpp* promoter) in these lines. It would further be interesting to measure the phellem extension and to repeat the embedding of *axr1-12*, *alf4-1*, *bdl-2*, *axr-3-1* and *mp-S319*. Moreover embedding and phellem extension experiments should be carried out on *PLASMODESMAL (PD)-LOCALIZED B-1,3 GLUCANASE1* (*PDBG1)* overexpression, *pdbg1,2* double mutant and *PD-CALLOSE BINDING PROTEIN1* (*PDCB1)* overexpression lines. These lines have a reduced (*PdBG1 OE*) or increased (*pdbg1,2*; *PDCB1 OE*) LR primordia density due to defects in the plasmodesmata callose deposition and thus the defects are independent of the auxin signaling pathway in the pericycle/periderm. Finally, it will be important to analyze if other LR regulators like *SLR* are expressed in the periderm.

7.4 Closing remarks

In the course of this study, different aspects of the molecular networks of Arabidopsis periderm were addressed, including the developmental stages and molecular regulators. We gained insight into how the periderm interacts with surrounding tissues and also identified a competition with LR formation.

The periderm development is tightly regulated in Arabidopsis and is effected by seemingly periderm-independent processes. Upon periderm formation, the endodermis and inner cortex cells undergo PCD followed by cortex and epidermis cells being abscised from root and hypocotyl in a predetermined pattern (Wunderling et al., 2018). During these processes cells of

developing periderm tissues interact with cells of the ground tissue, most probably mainly with the endodermis, via a mechanical communication. This mechanical communication could be on the one hand due to a space limit and growing tension because of the outer layers forming a constraint for the increasing number and volume of periderm and vascular cells. On the other hand it could be due to a decreasing tension when the endodermis cells undergo PCD. It remains to be unknown if there is also a communication on a molecular level.

As in many plant processes, like in lateral root formation (Lavenus et al., 2013), vascular stem cell initiation (Hardtke CS, Berleth T 1998; Friml et al., 2003) auxin plays a role in the periderm development as well (Wunderling et al., unpublished). But periderm development has more characteristics in common with LR formation. LRs and the periderm both arise from the pericycle (Wunderling et al. 2018; Malamy and Benfey, 1997), cell elimination contributes to organ growth during both processes (Wunderling et al. 2018; Escamez et al. 2018), and some of the LR regulators (e.g. *IAA28*, *GATA23*, *ARF7*, *ARF19*) are involved in both processes. In contrast, the LR formation and periderm development are also competing processes (Wunderling et al., unpublished).

As we found that auxin plays an important role in the periderm development and a mechanical communication exists between the pericycle/periderm and the outer cell layers, most probably the endodermis, the effect of auxin on the periderm development might partly be indirect due to auxin regulation of aquaporins or ion channels in the endodermis. This is indicated by the finding of Péret et al. (2012) that the auxin-mediated regulation of aquaporins contributes to LR emergence (Péret et al., 2012). It would be interesting to specifically manipulate aquaporins (e.g. *PIP2;1*) or ion channels in the endodermis and study their effects on endodermal shrinkage and periderm development.

An example for a response to mechanical stimuli is the strong and rapid upregulation of *Arabidopsistouch3* (*TCH3*) in response to touch and wind (Antosiewicz et al., 1995). Elevated levels of TCH3 were found in the developing periderm but are "restricted to the most internal one or two cells of the periderm" (Antosiewicz et al., 1995) (looks like the phellogen). TCH3 accumulates at high levels in periderm regions of developing LRs and is most abundant in periderm cells located at the opposite sides of LRs (Antosiewicz et al., 1995). Furthermore, TCH3 accumulation closely correlates with the process of cellular expansion and with tissues where an auxin response is thought to take place. Additionally, *TCH3* is up-regulated in response to low levels of exogenous indole-3-acetic acid (IAA) and thus auxin levels may regulate *TCH3* expression (Antosiewicz et al., 1995) during the periderm development. Hence,

TCH3 could possibly be upregulated in response to an increasing constraint before endodermis PCD.

As a next step genes that are important for the periderm development should be determine by unraveling the periderm transcriptome. This could be conducted by micro-dissection of the hypocotyl and mature root periderm and subsequent purification of RNA, followed by RNAseq of mRNA. By comparison with the mRNA of the whole mature root part or the hypocotyl, the periderm-specific transcriptome could be determined.

Then again, it would be interesting to investigate how molecular signals such as plant hormones and reactive oxygen species but also environmental stress conditions, like drought, heat or osmotic stress may modulate periderm development and response of molecular periderm regulators. It was already published that environmental stress has an effect on the suberin deposition in the plant root endodermis (Aroca et al., 2012; Domergue et al., 2010) and periderm (Beckman, 2000; Lulai et al., 2016). Aroca et al. (2012) proposed that environmental stresses may modify a number of cellular properties, which may change the concentration of reactive oxygen species (ROS) or hormones. This may in the end modify suberin deposition and aquaporin activity of the root endodermis leading to a root water uptake regulation (Aroca et al., 2012). Yadav et al. (2014) found that for the formation of an effective suberin barrier in the root endodermis and seed coats of Arabidopsis, ATP binding cassette (ABC)G half-transporters (*ABCG2*, *ABCG6*, and *ABCG20*) are required and *abcg2 abcg6 abcg20* triple mutant plants show a decreased suberin content. Roots of these triple mutants were more permeable to water and salt with a distorted lamellar structure of the suberin and reduced proportions of aliphatic components as well as few lateral roots and early secondary growth in primary roots (Yadav et al., 2014). It would be interesting to analyze this triple mutant or ABCG overexpression lines for a periderm phenotype, also under stress conditions. Furthermore *FAR1, FAR4* and *FAR5* (expressed in the Arabidopsis periderm) are transcriptionally induced in the root endodermal cells by wounding and salt stress (Domergue et al., 2010). Additionally, it was proposed by Beckman (2000) that environmental stress leads to an accumulation of IAA and ethylene resulting in growth responses to produce a peridermal defense. In 2016 it was shown by Lulai et al. that wounding induces changes in cytokinin and auxin content in potato tuber followed by a wound periderm formation. Furthermore, plant hormones like jasmonic acid (JA) and abscisic acid (ABA) as well as chemical substances e.g. the metal cadmium or salts like Phosphite compounds, have been shown to either induce periderm formation or molecular modifications of the periderm in Arabidopsis, potato and *Merwilla plumbea* (Eshraghi et al.

2011; Lulai and Suttle 2009; Lux et al., 2011; Olivieria et al., 2012). In total these experiments suggest that also plant hormones like JA, ABA and cytokinin or substances such as cadmium and phosphite as well as environmental stress might have an effect on periderm development in Arabidopsis and it would be interesting to examine how treatments with differnet hormones/substances/stresses effect the periderm.

Remarkably, a periderm is formed in all mutant lines we tested in this study, even with multiple knock- out lines of candidate genes in periderm regulation (*MYB* and *NAC* TFs, results not shown), and under all available growing conditions. Thus, the periderm seems to be crucial for plant survival and there are possibly a lot of back-up strategies to ensure periderm formation.

8. References

Almeida T, Menendez E, Capote T, Ribeiro T, Santos C, Goncalves S. 2013a. Molecular characterization of Quercus suber MYB1, a transcription factor up-regulated in cork tissues. *J Plant Physiol* **170**, 172-178.

Almeida T, Pinto G, Correia B, Santos C, Goncalves S. 2013b. QsMYB1 expression is modulated in response to heat and drought stresses and during plant recovery in Quercus suber. *Plant Physiol Biochem* **73**, 274-281.

Antosiewicz DM, Polisensky DH, Braam J. 1995. Cellular localization of the Ca2+ binding TCH3 protein of Arabidopsis. *The Plant Journal* **8**(5), 623-636.

Aroca R, Porcel R, Ruiz-Lozano JM. 2012. Regulation of root water uptake under abiotic stress conditions. *Journal of Experimental Botany* **63**(1), 43–57.

Atkinson JA, Rasmussen A, Traini R, Voß U, Sturrock C, Mooney SJ, Wells DM, Bennett MJ. 2014. Branching Out in Roots: Uncovering Form, Function, and Regulation. *Plant Physiology* **166**, 538–550

Barberon M, Vermeer JE, De Bellis D, Wang P, Naseer S, Andersen TG, Humbel BM, Nawrath C, Takano J, Salt DE et al. 2016. Adaptation of root function by nutrient-induced plasticity of endodermal differentiation. *Cell* **164**:447–459.

Barra-Jimenez A, Ragni L. 2017. Secondary development in the stem: when Arabidopsis and trees are closer than it seems. *Curr Opin Plant Biol* **35**, 145-151.

Beckman CH. 2000. Phenolic-storing cells: keys to programmed cell death and periderm formation in wilt disease resistance and in general defence responses in plants? *Physiological and Molecular Plant Pathology* **57**, 101-110.

Beisson F, Li Y, Bonaventure G, Pollard M, Ohlrogge JB. 2007. The acyltransferase GPAT5 is required for the synthesis of suberin in seed coat and root of Arabidopsis. *Plant Cell* **19**, 351-368.

Benfey PN1, Linstead PJ, Roberts K, Schiefelbein JW, Hauser MT, Aeschbacher RA. 1993. Root development in Arabidopsis: four mutants with dramatically altered root morphogenesis. *Development* **119(1)**:57-70.

Burri JT, Vogler H, Läubli NF, Hu C, Grossniklaus U, Nelson BJ. 2018. Feeling the force: how pollen tubes deal with obstacles. *New Phytol*. **220**(1):187-195.

Caritat A, Gutierrez E, Molinas M. 2000. Influence of weather on cork-ring width. *Tree Physiology* **20**, 893-900.

Carvalho A, Paiva J, Louzada J, Lima-Brito J. 2013. The Transcriptomics of Secondary Growth and Wood Formation in Conifers. *Mol Biol Int* doi: 10.1155/2013/974324

Chaffey N, Cholewa, E.., Regan, S., Sundberg, B. 2002. Secondary xylem development in Arabidopsis: a model for wood formation. *Physiol Plant* **114**, 594–600.

Compagnon V, Diehl P, Benveniste I, Meyer D, Schaller H, Schreiber L, Franke R, Pinot F. 2009. CYP86B1 is required for very long chain omega-hydroxyacid and alpha, omega - dicarboxylic acid synthesis in root and seed suberin polyester. *Plant Physiol* **150**, 1831-1843.

Cordeiro N, Belgacem MN, Gandini A, Pascoal Neto C. 1999. Urethanes and polyurethanes from suberin 2: synthesis and characterization. *Industrial Crops and Products* **10**, 1-10.

de Geus M, van der Meulen I, Goderis B, van Hecke K, Dorschu M, van der Werff H, Koning CE, Heise A. 2010. Performance polymers from renewable monomers: high molecular weight poly(pentadecalactone) for fiber applications. *Polymer Chemistry* **1**, 525.

De Rybel B, Mahonen AP, Helariutta Y, Weijers D. 2016. Plant vascular development: from early specification to differentiation. *Nat Rev Mol Cell Biol* **17**, 30-40.

De Rybel B, Vassileva V, Parizot B, Demeulenaere M, Grunewald W, Audenaert D, Van Campenhout J, Overvoorde P, Jansen L, Vanneste S, Moller B, Wilson M, Holman T, Van Isterdael G, Brunoud G, Vuylsteke M, Vernoux T, De Veylder L, Inze D, Weijers D, Bennett MJ, Beeckman T. 2010. A novel aux/IAA28 signaling cascade activates GATA23-dependent specification of lateral root founder cell identity. *Curr Biol* **20**, 1697-1706.

De Smet I, Lau S, Voss U, Vanneste S, Benjamins R, Rademacher EH, Schlereth A, De Rybel B, Vassileva V, Grunewald W, Naudts M, Levesque MP, Ehrismann JS, Inze D, Luschnig C, Benfey PN, Weijers D, Van Montagu MC, Bennett MJ, Jurgens G, Beeckman T. 2010.

Bimodular auxin response controls organogenesis in Arabidopsis. *Proc Natl Acad Sci U S A* **107**, 2705-2710.

De Smet I, Tetsumura T, De Rybel B, Frei dit Frey N, Laplaze L, Casimiro I, Swarup R, Naudts M, Vanneste S, Audenaert D, Inze D, Bennett MJ, Beeckman T. 2007. Auxin-dependent regulation of lateral root positioning in the basal meristem of Arabidopsis. *Development* **134**, 681-690.

Demura T, Ye ZH. 2010. Regulation of plant biomass production. *Curr Opin Plant Biol* **13**, 299-304.

Di Laurenzio L, Wysocka-Diller J, Malamy JE, Pysh L, Helariutta Y, Freshour G, Hahn MG, Feldmann KA, Benfey PN. 1996. The SCARECROW gene regulates an asymmetric cell division that is essential for generating the radial organization of the Arabidopsis root. *Cell* **86**: 423–433.

Dolan L, Roberts K. 1995. Secondary thickening in roots of Arabidopsis thaliana: anatomy and cell surface changes. *New Phytologist* **131**, 121-128.

Domergue F, Vishwanath SJ, Joubes J, Ono J, Lee JA, Bourdon M, Alhattab R, Lowe C, Pascal S, Lessire R, Rowland O. 2010. Three Arabidopsis fatty acyl-coenzyme A reductases, FAR1, FAR4, and FAR5, generate primary fatty alcohols associated with suberin deposition. *Plant Physiol* **153**, 1539-1554.

Esau, K. 1977. *Anatomy of seed plants*. New York, NY, USA: John Wiley&Sons.

Escamez S, Bollhoner B, Hall H, André D, Berthet B, Voß U, Lers A, Maizel A, Bennett M, Tuominen H. Cell death in cells overlying lateral root primordia contributes to organ growth in Arabidopsis. *bioRxiv* preprint first posted online Feb. 20, 2018; doi: http://dx.doi.org/10.1101/268433

Eshraghi L, Anderson J, Aryamanesh N, Shearer B, McComb J, Hardyaand GEStJ, O'Brien PA. 2011. Phosphite primed defence responses and enhanced expression of defence genes in Arabidopsis thaliana infected with Phytophthora cinnamomi L. *Plant Pathology* **60**, 1086–1095.

Etchells JP, Mishra LS, Kumar M, Campbell L, Turner SR. 2015. Wood Formation in Trees Is Increased by Manipulating PXY-Regulated Cell Division. *Curr Biol* **25**, 1050-1055.

Fagerstedt KV, Saranpaa P, Tapanila T, Immanen J, Serra JA, Nieminen K. 2015. Determining the Composition of Lignins in Different Tissues of Silver Birch. *Plants (Basel)* **4**, 183-195.

Freeman ECLaTP. 2001. The Importance of Phellogen Cells and their Structural Characteristics in Susceptibility and Resistance to Excoriation in Immature and Mature Potato Tuber (Solanum tuberosum L.) Periderm. *Annals of Botany* **Volume 88**, 555-561.

Fukaki H, Nakao Y, Okushima Y, Theologis A, Tasaka M. 2005. Tissue-specific expression of stabilized SOLITARY-ROOT/IAA14 alters lateral root development in Arabidopsis. *Plant J* **44**, 382-395.

Furuta KM, Hellmann E, Helariutta Y. 2014. Molecular control of cell specification and cell differentiation during procambial development. *Annu Rev Plant Biol* **65**, 607-638.

Goh T, Joi S, Mimura T, Fukaki H. 2012. The establishment of asymmetry in Arabidopsis lateral root founder cells is regulated by LBD16/ASL18 and related LBD/ASL proteins. *Development* **139**, 883-893.

Goh T, Toyokura K, Wells DM, Swarup K, Yamamoto M, Mimura T, Weijers D, Fukaki H, Laplaze L, Bennett MJ, Guyomarc'h S. 2016. Quiescent center initiation in the Arabidopsis lateral root primordia is dependent on the SCARECROW transcription factor. *Development* **143**: 3363–3371.

Groh B, Hubner C, Lendzian KJ. 2002. Water and oxygen permeance of phellems isolated from trees: the role of waxes and lenticels. *Planta* **215**, 794-801.

Hamant O1, Heisler MG, Jönsson H, Krupinski P, Uyttewaal M, Bokov P, Corson F, Sahlin P, Boudaoud A, Meyerowitz EM, Couder Y, Traas J. 2008. Developmental patterning by mechanical signals in Arabidopsis. *Science.* **322(5908)**:1650-5.

Helariutta Y, Fukaki H, Wysocka-Diller J, Nakajima K, Jung J, Sena G, Hauser MT, Benfey PN. 2000. The SHORT-ROOT gene controls radial patterning of the Arabidopsis root through radial signaling. *Cell* **101**: 555–567.

Hirakawa Y, Bowman JL. 2015. A Role of TDIF Peptide Signaling in Vascular Cell Differentiation is Conserved Among Euphyllophytes. *Front Plant Sci* **6**, 1048.

Hofer R, Briesen I, Beck M, Pinot F, Schreiber L, Franke R. 2008. The Arabidopsis cytochrome P450 CYP86A1 encodes a fatty acid omega-hydroxylase involved in suberin monomer biosynthesis. *J Exp Bot* **59**, 2347-2360.

Hosmani PS1, Kamiya T, Danku J, Naseer S, Geldner N, Guerinot ML, Salt DE. 2013. Dirigent domain-containing protein is part of the machinery required for formation of the lignin-based Casparian strip in the root. *Proc Natl Acad Sci U S A* **110(35)**:14498-503.

Jouannet V, Brackmann K, Greb T. 2015. (Pro)cambium formation and proliferation: two sides of the same coin? *Curr Opin Plant Biol* **23**, 54-60.

Kamiya T, Borghi M, Wang P, Danku JMC, Kalmbach L, Hosmani PS, Naseer S, Fujiwara T, Geldner N, Salt DE. 2015. The MYB36 transcription factor orchestrates Casparian strip formation. *PNAS* **112 (33)**: 10533-10538.**Khanal BP, Grimm E, Knoche M**. 2013. Russeting in apple and pear: a plastic periderm replaces a stiff cuticle. *AoB Plants* **5**, pls048.

Kosma DK, Molina I, Ohlrogge JB, Pollard M. 2012. Identification of an Arabidopsis fatty alcohol:caffeoyl-Coenzyme A acyltransferase required for the synthesis of alkyl hydroxycinnamates in root waxes. *Plant Physiol* **160**, 237-248.

Kosma DK, Rice A, Pollard M. 2015. Analysis of aliphatic waxes associated with root periderm or exodermis from eleven plant species. *Phytochemistry* **117**, 351-362.

Kucukoglu M, Nilsson J, Zheng B, Chaabouni S, Nilsson O. 2017. WUSCHEL-RELATED HOMEOBOX4 (WOX4)-like genes regulate cambial cell division activity and secondary growth in Populus trees. *New Phytologist* **215**, 642-657.

Kumamoto CA. 2008. Molecular mechanisms of mechanosensing and their roles in fungal contact sensing. *Nat Rev Microbiol* **6**(9): 667–673.

Lavenus J, Goh T, Roberts I, Guyomarc'h S, Lucas M, De Smet I, Fukaki H, Beeckman T, Bennett M, Laplaze L. 2013. Lateral root development in Arabidopsis: fifty shades of auxin. *Trends Plant Sci* **18**, 450-458.

Lee HW, Kim NY, Lee DJ, Kim J. 2009. LBD18/ASL20 regulates lateral root formation in combination with LBD16/ASL18 downstream of ARF7 and ARF19 in Arabidopsis. *Plant Physiol* **151**, 1377-1389.

Lendzian KJ. 2006. Survival strategies of plants during secondary growth: barrier properties of phellems and lenticels towards water, oxygen, and carbon dioxide. *J Exp Bot* **57**, 2535-2546.

Lourenco A, Rencoret J, Chemetova C, Gominho J, Gutierrez A, Del Rio JC, Pereira H. 2016. Lignin Composition and Structure Differs between Xylem, Phloem and Phellem in Quercus suber L. *Front Plant Sci* **7**, 1612.

Lucas M, Kenobi K, von Wangenheim D, Vobeta U, Swarup K, De Smet I, Van Damme D, Lawrence T, Peret B, Moscardi E, Barbeau D, Godin C, Salt D, Guyomarc'h S, Stelzer EH, Maizel A, Laplaze L, Bennett MJ. 2013. Lateral root morphogenesis is dependent on the mechanical properties of the overlaying tissues. *Proc Natl Acad Sci U S A* **110**, 5229-5234.

Lulai EC, Corsini DL. 1998. Differential deposition of suberin phenolic and aliphatic domains and their roles in resistance to infection during potato tuber (Solanum tuberosum L.) wound-healing. *Physiological and Molecular Plant Pathology* **53**, 209–222.

Lulai C and Suttle JC. 2009. Signals involved in tuber wound-healing Edward. *Plant Signaling & Behavior* **4:7**, 620-622.

Lulai EC, Suttle JC, Olson LL, Neubauer JD, Campbell LG, Campbell MA. 2016. Wounding induces changes in cytokinin and auxin content in potato tuber, but does not induce formation of gibberellins. *Journal of Plant Physiology* **191**, 22-28.

Lux A, Vaculík M, Martinka M, Lišková D, Kulkarni MG, Stirk WA, Van Staden J. 2011. Cadmium induces hypodermal periderm formation in the roots of the monocotyledonous medicinal plant Merwilla plumbea. *Annals of Botany* **107**(2), 285–292.

Malamy JEB, P.N. 1997. Organization and cell differentiation in lateral roots of Arabidopsis thaliana. *Development* **124**, 33-44.

Marques AV, Pereira H. 2013. Lignin monomeric composition of corks from the barks of Betula pendula, Quercus suber and Quercus cerris determined by Py–GC–MS/FID. *Journal of Analytical and Applied Pyrolysis* **100**, 88-94.

Miguel A, Milhinhos A, Novak O, Jones B, Miguel CM. 2015. The SHORT-ROOT-like gene PtSHR2B is involved in Populus phellogen activity. *J Exp Bot*.

Molina I, Li-Beisson Y, Beisson F, Ohlrogge JB, Pollard M. 2009. Identification of an Arabidopsis feruloyl-coenzyme A transferase required for suberin synthesis. *Plant Physiol* **151**, 1317-1328.

Moreno-Risueno MA, Busch W, Benfey PN. 2010. Omics meet networks - using systems approaches to infer regulatory networks in plants. *Curr Opin Plant Biol* **13**, 126-131.

Moubayidin L, Salvi E, Giustini L, Terpstra I, Heidstra R, Costantino P, Sabatini S. 2016. A SCARECROW-based regulatory circuit controls Arabidopsis thaliana meristem size from the root endodermis. *Planta* **243**: 1159–1168.

Neubauer JD, Lulai EC, Thompson AL, Suttle JC, Bolton MD. 2012. Wounding coordinately induces cell wall protein, cell cycle and pectin methyl esterase genes involved in tuber closing layer and wound periderm development. *J Plant Physiol* **169**, 586-595.

Neubauer JD, Lulai EC, Thompson AL, Suttle JC, Bolton MD, Campbell LG. 2013. Molecular and cytological aspects of native periderm maturation in potato tubers. *J Plant Physiol* **170**, 413-423.

Okushima Y, Fukaki H, Onoda M, Theologis A, Tasaka M. 2007. ARF7 and ARF19 regulate lateral root formation via direct activation of LBD/ASL genes in Arabidopsis. *Plant Cell* **19**, 118-130.

Okushima Y, Overvoorde PJ, Arima K, Alonso JM, Chan A, Chang C, Ecker JR, Hughes B, Lui A, Nguyen D, Onodera C, Quach H, Smith A, Yu G, Theologis A. 2005. Functional genomic analysis of the AUXIN RESPONSE FACTOR gene family members in Arabidopsis thaliana: unique and overlapping functions of ARF7 and ARF19. *Plant Cell* **17**, 444-463.

Olivieri FP, Feldman ML, Machinandiarena MF, Lobato MC, Caldiz DO, Daleo GR, Andreu AB. 2012. Phosphite applications induce molecular modifications in potato tuber periderm and cortex that enhance resistance to pathogens. *Crop Protection* **32**, 1-6

Oven P, Torelli N, Shortle WC, Zupančič M. 1999. The formation of a ligno-suberised layer and necrophylactic periderm in beech bark (Fagus sylvatica L.). *Flora* **194**, 137-144.

Pacurar DI, Pacurar ML, Bussell JD, Schwambach J, Pop TI, Kowalczyk M, Gutierrez L, Cavel E, Chaabouni S, Ljung K, Fett-Neto AG, Pamfil D, Bellini C. 2014. Identification of new adventitious rooting mutants amongst suppressors of the Arabidopsis thaliana superroot2 mutation. J Exp Bot **65(6)**:1605-18.

Pereira H. 1988. Chemical composition and variability of cork from Quercus suber L. *Wood Science and Technology* **22**, 211-218.

Pereira H. 2007. *Cork: Biology, Production and Uses*. Amsterdam: Elsevier.

Péret B, Li G, Zhao J, Band LR, Voß U, Postaire O, Luu D-T, Da Ines O, Casimiro I, Lucas M, Wells DM, Lazzerini L, Nacry P, King JR, Jensen OE, Schäffner AR, Maurel C, Bennett MJ. 2012. Auxin regulates aquaporin function to facilitate lateral root emergence. *Nature Cell Biology* **14**, 991–998.

Porco S, Larrieu A, Du Y, Gaudinier A, Goh T, Swarup K, Swarup R, Kuempers B, Bishopp A, Lavenus J, Casimiro I, Hill K, Benkova E, Fukaki H, Brady SM, Scheres B, Péret B, Bennett MJ. 2016. Lateral root emergence in Arabidopsis is dependent on transcription factor LBD29 regulation of auxin influx carrier LAX3. *Development* **143**, 3340-3349.

Potocka I, Szymanowska-Pułka J, Karczewski J, Nakielsk J. 2011. Effect of mechanical stress on Zea root apex. I. Mechanical stress leads to the switch from closed to open meristem organization. *J Exp Bot* **62**(13): 4583–4593.

Pinto PCRO, Sousa AF, Silvestre AJD, Neto CP, Gandini A, Eckerman C, Holmbom B. 2009. Quercus suber and Betula pendula outer barks as renewable sources of oleochemicals: A comparative study. *Industrial Crops and Products* **29**, 126-132.

Ragni L, Hardtke CS. 2014. Small but thick enough--the Arabidopsis hypocotyl as a model to study secondary growth. *Physiol Plant* **151**, 164-171.

Rains MK, Gardiyehewa de Silva ND, Molina I. 2017. Reconstructing the suberin pathway in poplar by chemical and transcriptomic analysis of bark tissues. *Tree Physiology* **1**: 1–22.

Schreiber L, Franke R, Hartmann K. 2005. Wax and suberin development of native and wound periderm of potato (Solanum tuberosum L.) and its relation to peridermal transpiration. *Planta* **220**, 520-530.

Serra O, Hohn C, Franke R, Prat S, Molinas M, Figueras M. 2010. A feruloyl transferase involved in the biosynthesis of suberin and suberin-associated wax is required for maturation and sealing properties of potato periderm. *Plant J* **62**, 277-290.

Serra O, Soler M, Hohn C, Franke R, Schreiber L, Prat S, Molinas M, Figueras M. 2009a. Silencing of StKCS6 in potato periderm leads to reduced chain lengths of suberin and wax compounds and increased peridermal transpiration. *J Exp Bot* **60**, 697-707.

Serra O, Soler M, Hohn C, Sauveplane V, Pinot F, Franke R, Schreiber L, Prat S, Molinas M, Figueras M. 2009b. CYP86A33-targeted gene silencing in potato tuber alters suberin composition, distorts suberin lamellae, and impairs the periderm's water barrier function. *Plant Physiol* **149**, 1050-1060.

Sibout R, Plantegenet S, Hardtke CS. 2008. Flowering as a condition for xylem expansion in Arabidopsis hypocotyl and root. *Curr Biol* **18**, 458-463.

Silva S, Sabino M, Fernandes E, Correlo V, Boesel L, Reis R. 2005. Cork: properties, capabilities and applications. *International Materials Reviews* **50**: 345–365.

Soler M, Serra O, Molinas M, Huguet G, Fluch S, Figueras M. 2007. A Genomic approach to suberin biosynthesis and cork differentiation. *Plant Physiology* **144**: 419–431.

Sozzani R, Cui H, Moreno-Risueno MA, Busch W, Van Norman JM, Vernoux T, Brady SM, Dewitte W, Murray JA, Benfey PN. 2010 Spatiotemporal regulation of cell-cycle genes by SHORTROOT links patterning and growth. *Nature* **466**: 128–132.

Spicer R, Groover A. 2010. Evolution of development of vascular cambia and secondary growth. *New Phytol* **186**, 577-592.

Thangavel T, Tegg RS, Wilson CR. 2016. Toughing It Out--Disease-Resistant Potato Mutants Have Enhanced Tuber Skin Defenses. *Phytopathology* **106**, 474-483.

Thomson N, Evert RF, Kelman A. 1995. Wound healing in whole potato tubers: a cytochemical, fluorescence, and ultrastructural analysis of cut and bruise wounds. *Canadian Journal of Botany* **73**: 1436–1450.

Tiwari SB, Hagen G, Guilfoyle TJ. 2004. Epub 2004. Aux/IAA proteins contain a potent transcriptional repression domain. *Plant Cell* **16(2)**: 533-43.

Torron S, Semlitsch S, Martinelle M, Johansson M. 2014. Polymer Thermosets from Multifunctional Polyester Resins Based on Renewable Monomers. *Macromolecular Chemistry and Physics* **215**, 2198-2206.

Tucker SC. 1975. Wound regeneration in the lamina of magnoliaceous leaves. *Canadian Journal of Botany* **53**: 1352–1364.

Van Norman JM, Xuan W, Beeckman T, Benfey PN. 2013. To branch or not to branch: the role of pre-patterning in lateral root formation. *Development* **140**, 4301-4310.

Vanneste S, De Rybel B, Beemster GT, Ljung K, De Smet I, Van Isterdael G, Naudts M, Iida R, Gruissem W, Tasaka M, Inze D, Fukaki H, Beeckman T. 2005. Cell cycle progression in the pericycle is not sufficient for SOLITARY ROOT/IAA14-mediated lateral root initiation in Arabidopsis thaliana. *Plant Cell* **17**, 3035-3050.

Vermeer JE, von Wangenheim D, Barberon M, Lee Y, Stelzer EH, Maizel A, Geldner N. 2014. A spatial accommodation by neighboring cells is required for organ initiation in Arabidopsis. *Science* **343**:178-83.

Vishwanath SJ, Delude C, Domergue F, Rowland O. 2015. Suberin: biosynthesis, regulation, and polymer assembly of a protective extracellular barrier. *Plant Cell Rep* **34**, 573-586.

Vishwanath SJ, Kosma DK, Pulsifer IP, Scandola S, Pascal S, Joubes J, Dittrich-Domergue F, Lessire R, Rowland O, Domergue F. 2013. Suberin-associated fatty alcohols in Arabidopsis: distributions in roots and contributions to seed coat barrier properties. *Plant Physiol* **163**, 1118-1132.

Waisel Y. 1995. Developmental and functional aspects of the periderm. In: Iqbal M, ed. The *cambial derivatives*. Stuttgart, Germany: Gebruder Borntraeger Verlagsbuchhandlung, 293–315.

Wilmoth JC, Wang S, Tiwari SB, Joshi AD, Hagen G, Guilfoyle TJ, Alonso JM, Ecker JR, Reed JW. 2005. NPH4/ARF7 and ARF19 promote leaf expansion and auxin-induced lateral root formation. *Plant J* **43**, 118-130.

Wunderling A, Ripper D, Barra-Jimenez A, Mahn S, Sajak K, Targem MB, Ragni L. 2018. A molecular framework to study periderm formation in Arabidopsis. *New Phytol* **219**, 216-229.

Yadav V, Molina I, Ranathunge K, Indira ueralta Castillo I, Rothstein SJ, Reeda JW. 2014. ABCG Transporters Are Required for Suberin and Pollen Wall Extracellular Barriers in Arabidopsis. *The Plant Cell* **26**: 3569–3588.

Zhang J, Nieminen K, Serra JA, Helariutta Y. 2014. The formation of wood and its control. *Curr Opin Plant Biol* **17**, 56-63.

9. Appendix

9.1 Wunderling et al., 2017 (Review)

9.2 Wunderling et al., 2018

9.3 Wunderling et al., unsubmitted (manuscript draft)

9.1 Novel tools for quantifying secondary growth

Anna Wunderling, Mehdi Ben Targem, Pierre Barbier de Reuille and Laura Ragni

Journal of Experimental Botany, Jan. 2017, Vol. 68(1): 89-95. DOI: 10.1093/jxb/erw450

Journal of Experimental Botany, Vol. 68, No. 1 pp. 89–95, 2017
doi:10.1093/jxb/erw450 Advance Access publication 12 December 2016

REVIEW PAPER

Novel tools for quantifying secondary growth

Anna Wunderling[1], Mehdi Ben Targem[1], Pierre Barbier de Reuille[2] and Laura Ragni[1,*]

[1] ZMBP, University of Tübingen, Auf der Morgenstelle 32, D-72076 Tübingen, Germany
[2] University of Bern, Altenbergrain 21, CH-3013 Bern, Switzerland

* Correspondence: laura.ragni@zmbp.uni-tuebingen.de

Received 20 July 2016; Editorial decision 9 November 2016; Accepted 9 November 2016

Editor: Simon Turner, University of Manchester

Abstract

Secondary growth occurs in dicotyledons and gymnosperms, and results in an increased girth of plant organs. It is driven primarily by the vascular cambium, which produces thousands of cells throughout the life of several plant species. For instance, even in the small herbaceous model plant Arabidopsis, manual quantification of this massive process is impractical. Here, we provide a comprehensive overview of current methods used to measure radial growth. We discuss the issues and problematics related to its quantification. We highlight recent advances and tools developed for automated cellular phenotyping and its future applications.

Key words: Arabidopsis, automated cellular phenotyping, machine learning, quantitative histology, secondary growth.

Introduction

Secondary growth, the radial thickening of plant organs, is a large-scale process: thousands of cells are produced by the vascular cambium throughout the life of most woody dicotyledonous plants and gymnosperms (Spicer and Groover, 2010; Ragni and Hardtke, 2014; Zhang *et al.*, 2014). It occurs in the root, hypocotyl and stem of the herbaceous model species *Arabidopsis thaliana* (Arabidopsis). However, even in this relatively small model plant, soon after secondary growth begins, cell abundance is too large to perform manual quantifications effectively (Sankar *et al.*, 2014).

Vascular anatomical disposition differs throughout the plant kingdom, depending on the species, the organ considered, and even the developmental stage. For instance, during secondary growth in Arabidopsis, the root and hypocotyl rearrange their vasculature from a diarch symmetry (with two opposite initial phloem and xylem poles) to a fully radial symmetry (with a ring of cambial cells that produces inward daughter cells, which will differentiate into xylem and outward daughter cells that will develop into phloem) (Esau, 1977; Dolan and Roberts, 1995; Chaffey *et al.*, 2002; Ragni and Hardtke, 2014). In contrast, in the stem, secondary growth arises with the formation of the fascicular cambia in the 7–8 collateral bundles and later with the formation of an interfascicular cambium, which connects the bundles (Esau, 1977; Altamura *et al.*, 2001; Ragni and Hardtke, 2014).

Another lateral meristem that contributes to the increase in girth of plant organs is the cork cambium or phellogen. It produces the phelloderm on the inner side and the cork or phellem tissues on the outer side. In many plant species, cork cells develop into suberized dead cells at maturity. Together with the phellogen, the phelloderm and phellem form the periderm (Esau, 1977). The periderm replaces the epidermis in stems, branches, and roots of most dicotyledons, and gymnosperms once the latter can no longer accommodate radial growth. The periderm acts as a protective barrier against biotic and abiotic stress (Pereira, 2011). Furthermore, the parenchymatic components of the phelloderm fulfill a function in storing starch (Esau, 1977).

The periderm can be studied in the root and hypocotyl of Arabidopsis (Dolan and Roberts, 1995; Chaffey *et al.*, 2002). Working with the Arabidopsis hypocotyl offers several advantages because radial growth progression can be easily followed over time (as elongation and secondary growth are uncoupled) and the disposition of the vasculature is reminiscent of trees. Together these features make the Arabidopsis hypocotyl a good model to study secondary growth (Chaffey *et al.*, 2002; Ragni and Hardtke, 2014). Briefly, hypocotyl secondary growth can be divided into two phases based on cell morphology and proliferation rate: an early phase in which xylem mainly comprises water-conducting cells and parenchyma, and a later phase of so-called xylem expansion in which xylem occupancy is increased and fibers differentiate (Chaffey *et al.*, 2002; Sibout *et al.*, 2008).

Many factors controlling vascular secondary growth have been identified (see the following reviews for more detail: Furuta *et al.*, 2014; Zhang *et al.*, 2014; Jouannet *et al.*, 2015; De Rybel *et al.*, 2016). However, not all the players are known, and the spatio-temporal regulation of radial growth is far from being understood. In this review, we will provide an overview of the issues posed by secondary growth quantification. Moreover, we will present approaches and tools that have the potential to advance the field.

Current approaches for the quantification of secondary growth

In tree species, overall secondary growth is traditionally quantified as stem diameter at reference internode positions, while more accurate analyses are achieved by measuring tissue widths, number of cells per tissue files, distances between tissues (i.e. distance from the outer bark to the pith), or a combination of these measurements (such as the ratio between the width of the wood and the stem radius) (Nieminen *et al.*, 2008; Etchells *et al.*, 2015; Miguel *et al.*, 2016). Similarly, in the model plant Arabidopsis, overall secondary growth is quantified as diameter or the area of the different organs (the stem, the root, and the hypocotyl) (Altamura *et al.*, 2001; Chaffey *et al.*, 2002).

More specific parameters can be used to quantify Arabidopsis stem radial growth as the number of cells per vascular bundle, the tangential over radial ratio of vascular bundles, the lateral extension of the tissue produced by the interfascicular cambium, and the acropetal progression of interfascicular cambium initiation along the stem (Sehr *et al.*, 2010; Agusti *et al.*, 2011*a*, *b*; Etchells *et al.*, 2012, 2013) (Fig. 1A). For the Arabidopsis hypocotyl and root, valid alternatives to diameter length are the xylem over total area ratio (xylem occupancy) (Fig. 1B) or the xylem over phloem area ratio (Sibout *et al.*, 2008). More insights on xylem composition can be obtained by macerating woody samples to estimate the relative number of different cell types and their characteristics, such as shape and size (Franklin, 1945; Chaffey *et al.*, 2002; Muñiz *et al.*, 2008; Ragni *et al.*, 2011) or by measuring the so-called 'xylem 1' (vessels and parenchyma) and 'xylem 2' (fibers and vessels) (Fig. 1C) (Chaffey *et al.*, 2002; Liebsch *et al.*, 2014).

Challenges of secondary growth quantification

Many of the previously mentioned approaches only coarsely describe radial growth and do not capture its complexity at the morphological and temporal level. For instance, a reduction of hypocotyl area does not always reflect an overall reduction in cell proliferation. It could be due to small changes in cell sizes that cannot be easily detected by eye, or by an increased/decreased proliferation rate in one specific tissue. Along the same lines, both the presence of larger xylem vessels and more cell divisions could account for higher xylem occupancy in the hypocotyl radial section (Sankar *et al.*, 2014; Lehmann and Hardtke, 2016). To be able to account for these growth patterns, it is necessary to track and quantify growth at a cellular level (Sankar *et al.*, 2014).

However, manual quantification of secondary growth morphodynamics is impractical even in the tiny Arabidopsis plant, as there are >15 000 cell files in a mature hypocotyl. Moreover, the quantification of vascular morphodynamics is hampered not only by the scale of the process but also by the inaccessibility of certain tissues due to their deep location

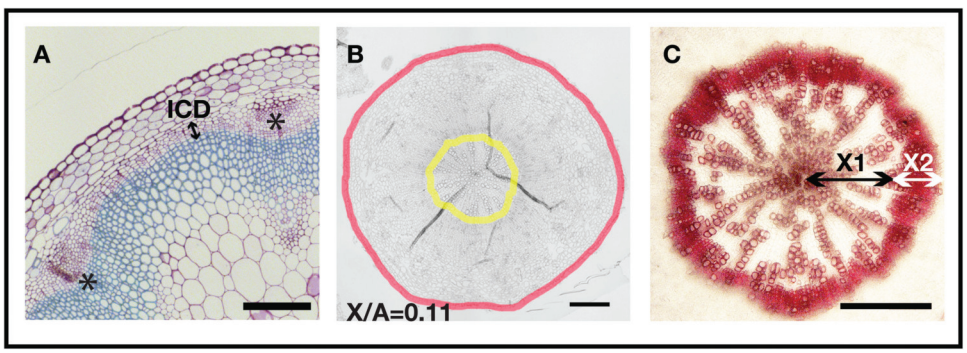

Fig. 1. Examples of secondary growth quantification. Cross-sections of plastic-embedded Arabidopsis: (A) Col-0 stem, 0.5 cm from the base of a 9-week-old plant; (B) Col-0 hypocotyl at 12 d after flowering. X/A, ratio between the xylem area and the total area; ICD, interfascicular cambium-derived tissue; * vascular bundle. (C) Vibratome section of Arabidopsis hypocotyl (Col-0, 15 d after flowering) stained with phluoroglucinol (in red) showing how 'xylem 1' (X1) and 'xylem 2' (X2) are measured. Scale bar=200 μm.

such as the xylem. Consequently, live imaging is challenging, and the majority of the measurements are achieved on cross-sections of embedded fixed samples. Thus, temporal resolution is also limited by sample preparation.

A further aspect to consider is that severe defects in radial growth often coincide with decreased plant viability. This renders the isolation of such plants challenging and the interpretation of those results even more difficult, as it is arduous to distinguish the direct contribution to secondary growth from pleiotropic effects. Thus, many studies rely on weak alleles or partially redundant contexts, in which plant fitness is not affected and phenotypes are mild. Therefore, quantification of secondary growth will benefit from novel tools for automated cellular phenotyping (Sankar *et al.*, 2014; Lehmann and Hardtke, 2016).

Finally, it is important to emphasize that secondary growth studies in Arabidopsis should be normalized to the developmental stage rather than to absolute age, as flowering greatly influences secondary growth progression. For instance, it triggers xylem expansion and fiber formation in the root and in the hypocotyl (Sibout *et al.*, 2008; Ragni *et al.*, 2011; Ragni and Hardtke, 2014).

Quantitative histology

In the last few years, the increasing volume of genotyping data, generated using low-cost sequencing technology, has shifted attention from more efficient genotyping to more automated and precise phenotyping. However, while high-throughput plant phenotyping is well developed for laboratory and field experiments in model and crop plants, automated cellular phenotyping is still a novel field and it has only recently been applied to secondary growth (Sankar *et al.*, 2014; Hall *et al.*, 2016; Lehmann and Hardtke, 2016). Sankar *et al.* (2014) define 'quantitative histology' as an automated identification/quantification of cell types and cellular morphological descriptors in a tissue.

Several pipelines, such as RootScan, RootAnalyzer, PHIV-RootCell, and the method of Montengro-Johnson and colleagues exist for the characterization and quantification of primary root growth (Burton *et al.*, 2012; Chopin *et al.*, 2015; Lartaud *et al.*, 2015; Montenegro-Johnson *et al.*, 2015). These tools were developed to classify rice, wheat, and Arabidopsis roots, respectively. To ensure a high quality classification, these methods exploit *a priori* knowledge of root architecture (Burton *et al.*, 2012; Chopin *et al.*, 2015; Lartaud *et al.*, 2015; Montenegro-Johnson *et al.*, 2015). This renders their usage very specific and not easy to adapt to other species or organs. More recently, two methods for automating cell extraction, quantitative shape analysis and cell type classification (in any 2D tissue of interest), were developed independently (Sankar *et al.*, 2014; Hall *et al.*, 2016). Relying on generic machine learning (ML) methods, these protocols can be generalized and applied to tissues other than those used in the respective studies. For this reason, these methods can really form the basis of the so-called 'quantitative histology'.

In more detail, both approaches rely on similar methodology, splitting the task into four steps: (i) image acquisition; (ii) image pre-processing; (iii) image segmentation and feature extraction; and (iv) cell type classification (Sankar *et al.*, 2014; Hall *et al.*, 2016) (Table 1; Fig. 2).

Image acquisition is one of the most critical steps, and its importance has often been underestimated. The quality and the nature of the pictures acquired greatly influence the ease with which the other steps in the pipeline can be performed (i.e. images that are suited for segmentation required less pre-processing). A related point is the standardization of the image acquisition process among experiments; parameters will not change if the images are acquired in the same way and in the same conditions, allowing large-scale samples. Due to the fact that live imaging of thick organs, such as the hypocotyl during secondary growth, is still impossible with conventional microscopy, both methods rely on grayscale images of cross-sections of fixed samples. Thus, an additional step of sample preparation is required. The approach of Sankar *et al.* (2014) uses high-resolution images of plastic-embedded sections of fixed material, acquired using the tiling/stitching function of a microscope with a motorized stage (Fig. 2A). In contrast, Hall and colleagues use laser scanning confocal images of vibratome sections in which cell borders were outlined by fluorescent staining of the cell wall (Hall *et al.*, 2016). Both strategies have advantages and disadvantages. Sample preparation for the first approach is easier at young developmental stages, and image resolution is higher, whereas the segmentation/pre-processing processes are slightly more difficult compared with confocal images (confocal images have less background and shadows). Moreover, only the procedure of Hall and colleagues allows the measurement of an additional fluorescent signal. A minor limitation of both protocols and still a general issue of secondary growth quantification is that radial growth is normally measured in cross-sections, and thus only in 2D (Lehmann and Hardtke, 2016).

After acquisition, the pre-processing transforms the images to improve the segmentation. This step is tightly linked to the

Table 1. *Key steps of 'quantitative histology' methods for secondary growth*

Step	Description	Sankar *et al.* (2014)	Hall *et al.* (2016)
0	Sample preparation	Microtome sections Plastic-embedded tissue	Vibratome sections Calcofluor white staining
1	Image acquisition	Light microscopy Stitching/tiling	Laser confocal microscopy
2	Image pre-processing	Gamma contrast Gaussian blur	Gaussian blur
3	Segmentation and features extraction	Watershed algorithm Morphometric features	Watershed algorithm Morphometric features Fluorescence signal intensity
4	Cell type classification	Machine learning (SVM)	Machine learning (random Forest)

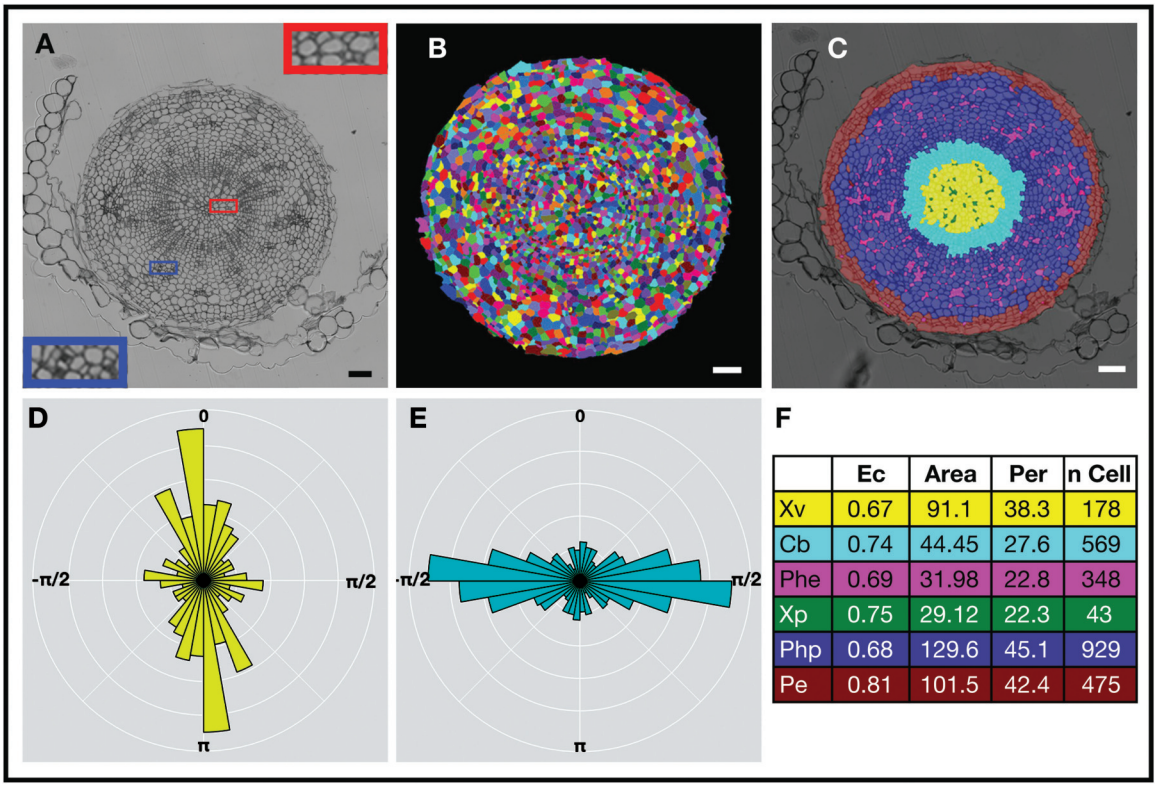

	Ec	Area	Per	n Cell
Xv	0.67	91.1	38.3	178
Cb	0.74	44.45	27.6	569
Phe	0.69	31.98	22.8	348
Xp	0.75	29.12	22.3	43
Php	0.68	129.6	45.1	929
Pe	0.81	101.5	42.4	475

Fig. 2. Example of the 'quantitative histology' approach. In (A–C) the same Arabidopsis hypocotyl section (Col-0 21 d after germination) is presented. (A) Row image, red box magnification showing details of the xylem, blue box magnification showing details of phloem. (B) Image after pre-processing and segmentation with a watershed algorithm; each color basin represents one cell. (C) Labeled image using a machine learning (ML) approach. Every color represents a cell type: yellow, xylem vessels (Xv); cyan, cambium (Cb); magenta, phloem elements (Phe); green, xylem parenchyma (Xp); blue, phloem parenchyma (Php); brown, periderm (Pe). (D) Rose diagram of the incline angles of the xylem vessels measured in (C). For instance, a value of 0 represents radial/anticlinal orientation, and a value of π/2 represents orthoradial/periclinal orientation. (E) Rose diagram of the incline angles of the cambial cells measured in (C). (F) Average of some features [eccentricity (Ec), area, perimeter (Per)] and cell numbers (n Cell) for each cell type measured in (C). Scale bar=100 μm.

imaging method and to the segmentation algorithm used. Both methods apply a series of filters to remove or reduce noise and reinforce the contrast. For instance, Sankar *et al.* (2014) use a Gaussian blur to filter out high-frequency noise, followed by a gamma adjustment to improve the general contrast of the image, while Hall *et al.* (2016) use only a blur for denoizing.

The segmentation is the process in which objects (in our case cells) are identified and extracted from the background and from each other. More precisely, a label is assigned to every pixel of the image, and pixels with the same label share certain characteristics (i.e. belong to the same cell). The two approaches rely on a common algorithm for the segmentation of grayscale images: the watershed algorithm (Fig. 2B) (Vincent and Soille, 1991; Yoo *et al.*, 2002; Barbier de Reuille *et al.*, 2005, 2015; Pound *et al.*, 2012). Briefly, the watershed algorithm is based on the geographical concept of the watershed and catchment basin. In geography, a catchment basin is a region of a map in which water flows into the same lake or basin, while the watersheds are the limits at which water would enter different catchment basins. An image can be seen as a topographical surface where high pixel intensity corresponds to 'high' regions and low pixel intensity refers to 'low' regions; thus we can apply the same geographical definitions to this virtual map. For instance, if the cell wall is brighter than the cell content, we can identify cells as catchment basins for the segmentation process (Fig. 2B) (Vincent and Soille, 1991).

The accuracy of the segmentation is critical, as mis-segmented cells are likely to be wrongly classified. After the segmentation, cellular features/descriptors such as cell area, cell perimeter, position of the cell, and cell eccentricity are computed for every cell. The computation of the features is achieved using conceptually similar toolboxes (Pau *et al.*, 2010) (http://www.diplib.org/main). Moreover, the incline angle—the angle formed by the major axis of the cell with the radius of the sample—is calculated in both protocols (Sankar *et al.*, 2014; Hall *et al.*, 2016). In addition, Hall *et al.* (2016) measured cell lumen area, and the cell wall area.

Cell type classification is achieved through an ML approach (Fig. 2C). The basic principle of ML is to teach computers to: (i) analyze existing data effectively; (ii) extract underlying similarity/differences; and (iii) generate a classifier/pattern to apply to new data (Bastanlar and Ozuysal, 2014; Ma *et al.*, 2014; Libbrecht and Noble, 2015; Angermueller *et al.*, 2016; Singh *et al.*, 2016). The first step is the creation of a training set, a set of images that is used to learn the model, in which the cell types of interest are manually labeled. The second step is the choice of the features that better describe each class of cells. Then, different algorithms for supervised classification can be used to create the classifier. Sankar and colleagues used a Support Vectors Machine (SVM)

algorithm, whereas Hall and colleagues reported to have better performances using a random Forest algorithm (please refer to the followingreviews for a comprehensive overview on ML algorithms: Bastanlar and Ozuysal, 2014; Ma *et al.*, 2014; Libbrecht and Noble, 2015; Angermueller *et al.*, 2016; Singh *et al.*, 2016). Then, the classifier performances are tested against the so-called test set, a fraction of the training set, until they are satisfactory (several rounds of optimization may be necessary). Finally, the classifier is used to label cells (identify the different cell types) on a running set (a set of segmented images that was not manually labeled) (Fig. 2C). Sankar and colleagues also proposed an automated filter to correct mislabeled cells. Indeed, they reported that at later developmental stages, in some cases xylem identity was assigned to phloem parenchymatic cells. In such cases an automated quality check, based on manually created masks of the total area and of the xylem area, was implemented and used (Sankar *et al.*, 2014).

In summary, the final output of the two approaches regarding identification of the cell type is rather comparable as both methods allow the quantification of similar features and cell types with accuracy >85% (Fig. 2F). However, the choice of the method should be dictated by the research focus/interests. For instance, we recommend the method of Hall and colleagues to study problems related to cell wall integrity, whereas we suggest the method of Sankar *et al*. for temporal analyses (developmental series with several time points).

Current and futures applications of 'quantitative histology'

A proof of concept of 'quantitative histology' approaches is the detailed characterization of two Arabidopsis accessions that display differences in secondary growth progression: Ler and Col-0 (Ragni *et al.*, 2011). The characterization of the morphodynamics between Ler and Col-0 revealed that overall secondary growth is more prominent in Col-0, whereas xylem occupancy is higher in Ler. This is not primarily due to cell size, although xylem cells in Ler are slightly bigger, but rather due to a decrease in phloem proliferation in Ler (Sankar *et al.*, 2014). Another remarkable observation is that the spatio-temporal dynamics of the incline angles reflect the different phases of secondary growth of the Arabidopsis hypocotyl. For instance, at young stages (15 d), the inclines are uniformly distributed. At ~20 d, xylem cells are radial and cambial cells orthoradial, and the overall distribution starts to be bi-modal (Fig. 2D, E) (Sankar *et al.*, 2014). In addition, this type of analysis pointed out some unexpected findings such as that the cambium produces more overall phloem than xylem, even though xylem occupancy is increasing during plant development, and that the enhanced xylem occupancy in Ler is not due to an increase of xylem cell numbers but mainly due to a decrease in phloem area.

Hall *et al.* (2016) validated their approach characterizing *knotted1-like 1* (*knat1*)/*brevipedicellus* (*bp*) loss-of-function mutants. The *knat1* mutant is suitable for a test as it exhibits reduced fiber cell number, combined with a decrease in xylem vessel area and altered cell wall deposition (Liebsch *et al.*, 2014). In addition, they quantified xylan abundance across different cell types, coupling the intensity of a fluorescent signal (immunostaining of the xylan) with the cell type classification and the morphometric data. Other components of the cell walls (such as cellulose, lignin, and callose), which can be visualized by immunolabeling techniques, could be easily measured together with the cell morphological descriptors, paving the way for the analyses of the chemical composition of the cell wall with spatial resolution (Hall *et al.*, 2016).

Another future application is to combine the automated cellular phenotyping with genome-wide association studies (GWAS). Strikingly, natural variation is still a largely untapped resource for the study of secondary growth. However, a large degree of variability in radial growth-related traits was observed in the hypocotyl of a small collection of Arabidopsis accessions, confirming the potential of this approach (Sibout *et al.*, 2008; Ragni *et al.*, 2011). Another aspect of secondary growth that can be further explored with more accurate phenotyping techniques is how secondary growth is modulated during changes of environmental conditioned and abiotic stresses.

So far, Sankar *et al.* (2014) and Hall *et al.* (2016) have tested their approaches only in the Arabidopsis hypocotyls. However, we expect to see the 'quantitative histology' approaches exploited in other plant species (tomato, poplar, etc.), as they are quite versatile and easy to adapt. For instance, we foresee minor tuning of the segmentation and machine learning parameters for the application to other organisms (as long as the images can be easily segmented). In addition, Hall *et al.* (2016) provide their method as a MATLAB package, with a graphical interface, and thus it does not require any coding by the user. Along the same lines, the 'quantitative histology' approach by Sankar *et al.* (2014) was recently implemented in the open source platform LithoGraphX [www.lithographx.org; a fork of MorphoGraphX (Barbier de Reuille *et al.*, 2015)] to render it accessible to biologists. Other advantages of the implementation on this platform are: (i) the reduced computational time for the segmentation process; (ii) the possibility to use several types of images as input (laser confocal images, grayscale images, and color images) and several pre-processing tools; and (iii) the choice between the two ML algorithms (Barbier de Reuille and Ragni, 2017). Moreover, in LithoGraphX it is possible to perform the Hall *et al*. approach or other protocols, as LithoGraphX was initially developed for the analyses of confocal images and offers a variety of tools for measuring fluorescent signal intensity.

A possible future implementation is to add tissue-specific features to improve cell type classification of problematic tissues. For instance, phloem companion cells and sieve elements are difficult to distinguish from one another (Sankar *et al.*, 2014). In fact the morphology of these cell types is nearly identical, which hampers the ML recognition process. Adding tissue-specific features such as the number of neighboring cells, cell wall thickness, or a particular stain should resolve this problem.

Conclusions and perspectives

In summary, it is fair to conclude that secondary growth characterization will benefit from precise quantification at the

cellular level. 'Quantitative histology' paves the way towards the study of secondary growth with good spatio-temporal resolution: it facilitates the measurement of complex traits and mild phenotypes. We foresee that automated cellular phenotyping will boost natural variation studies and will soon be applied to other species.

To date, the rate-limiting step of 'quantitative histology' methods is sample preparation/image acquisition. This is especially true for secondary growth studies where sample preparation is laborious and not yet automatized. Any improvements in this direction will contribute to render the 'quantitative histology' approaches routine protocols. A major breakthrough will be to image live secondary growth progression. This will open the door to the study of secondary growth in 3D and 4D.

Acknowledgements

This work was supported by a DFG grant (RA-2590/1-1) and by the SystemsX.ch, the Swiss Initiative in Systems Biology. LR is indebted to the Baden-Württemberg Stiftung for the financial support of this research project by the Elite programme for Postdocs. We thank Dr Azahara Barra-Jiménez and Dr Kristine Hill for critical reading.

References

Agusti J, Herold S, Schwarz M, *et al*. 2011*a*. Strigolactone signaling is required for auxin-dependent stimulation of secondary growth in plants. Proceedings of the National Academy of Sciences, USA **108,** 20242–20247.

Agusti J, Lichtenberger R, Schwarz M, Nehlin L, Greb T. 2011*b*. Characterization of transcriptome remodeling during cambium formation identifies MOL1 and RUL1 as opposing regulators of secondary growth. PLoS Genetics **7,** e1001312.

Altamura MM, Possenti M, Matteucci A, Baima S, Ruberti I, Morelli G. 2001. Development of the vascular system in the inflorescence stem of Arabidopsis. New Phytologist **151,** 381–389.

Angermueller C, Pärnamaa T, Parts L, Stegle O. 2016. Deep learning for computational biology. Molecular Systems Biology **12,** 878.

Barbier de Reuille P, Bohn-Courseau I, Godin C, Traas J. 2005. A protocol to analyse cellular dynamics during plant development. The Plant Journal **44,** 1045–1053.

Barbier de Reuille P, Ragni L. 2017. Vascular morphodynamics during secondary growth. Methods in Molecular Biology **1544**, in press.

Barbier de Reuille P, Routier-Kierzkowska A-L, Kierzkowski D, *et al*. 2015. MorphoGraphX: a platform for quantifying morphogenesis in 4D. eLife **4,** 05864.

Baştanlar Y, Ozuysal M. 2014. Introduction to machine learning. Methods in Molecular Biology **1107,** 105–128.

Burton AL, Williams M, Lynch JP, Brown KM. 2012. RootScan: software for high-throughput analysis of root anatomical traits. Plant and Soil **357,** 189–203.

Chaffey N, Cholewa E, Regan S, Sundberg B. 2002. Secondary xylem development in Arabidopsis: a model for wood formation. Physiologia Plantarum **114,** 594–600.

Chopin J, Laga H, Huang CY, Heuer S, Miklavcic SJ. 2015. RootAnalyzer: a cross-section image analysis tool for automated characterization of root cells and tissues. PLoS One **10,** e0137655.

De Rybel B, Mähönen AP, Helariutta Y, Weijers D. 2016. Plant vascular development: from early specification to differentiation. Nature Reviews. Molecular Cell Biology **17,** 30–40.

Dolan L, Roberts K. 1995. Secondary thickening in roots of *Arabidopsis thaliana*: anatomy and cell surface changes. New Phytologist **131,** 121–128.

Esau K. 1977. Anatomy of seed plants. Chichester, UK: Wiley.

Etchells JP, Mishra LS, Kumar M, Campbell L, Turner SR. 2015. Wood formation in trees is increased by manipulating PXY-regulated cell division. Current Biology **25,** 1050–1055.

Etchells JP, Provost CM, Mishra L, Turner SR. 2013. WOX4 and WOX14 act downstream of the PXY receptor kinase to regulate plant vascular proliferation independently of any role in vascular organisation. Development **140,** 2224–2234.

Etchells JP, Provost CM, Turner SR. 2012. Plant vascular cell division is maintained by an interaction between PXY and ethylene signalling. PLoS Genetics **8,** e1002997.

Franklin GL. 1945. Preparation of thin sections of synthetic resins and wood–resin composites, and a new macerating method for wood. Nature **155,** 51.

Furuta KM, Hellmann E, Helariutta Y. 2014. Molecular control of cell specification and cell differentiation during procambial development. Annual Review of Plant Biology **65,** 607–638.

Hall HC, Fakhrzadeh A, Luengo Hendriks CL, Fischer U. 2016. Precision automation of cell type classification and sub-cellular fluorescence quantification from laser scanning confocal images. Frontiers in Plant Science **7,** 119.

Jouannet V, Brackmann K, Greb T. 2015. (Pro)cambium formation and proliferation: two sides of the same coin? Current Opinion in Plant Biology **23,** 54–60.

Lartaud M, Perin C, Courtois B, *et al*. 2015. PHIV-RootCell: a supervised image analysis tool for rice root anatomical parameter quantification. Frontiers in Plant Science **5,** 790.

Lehmann F, Hardtke CS. 2016. Secondary growth of the Arabidopsis hypocotyl–vascular development in dimensions. Current Opinion in Plant Biology **29,** 9–15.

Libbrecht MW, Noble WS. 2015. Machine learning applications in genetics and genomics. Nature Reviews. Genetics **16,** 321–332.

Liebsch D, Sunaryo W, Holmlund M, *et al*. 2014. Class I KNOX transcription factors promote differentiation of cambial derivatives into xylem fibers in the Arabidopsis hypocotyl. Development **141,** 4311–4319.

Ma C, Zhang HH, Wang X. 2014. Machine learning for Big Data analytics in plants. Trends in Plant Science **19,** 798–808.

Miguel A, Milhinhos A, Novák O, Jones B, Miguel CM. 2016. The SHORT-ROOT-like gene PtSHR2B is involved in Populus phellogen activity. Journal of Experimental Botany **67,** 1545–1555.

Montenegro-Johnson TD, Stamm P, Strauss S, Topham AT, Tsagris M, Wood AT, Smith RS, Bassel GW. 2015. Digital single-cell analysis of plant organ development using 3DCellAtlas. The Plant Cell **27,** 1018–1033.

Muñiz L, Minguet EG, Singh SK, Pesquet E, Vera-Sirera F, Moreau-Courtois CL, Carbonell J, Blázquez MA, Tuominen H. 2008. ACAULIS5 controls Arabidopsis xylem specification through the prevention of premature cell death. Development **135,** 2573–2582.

Nieminen K, Immanen J, Laxell M, *et al*. 2008. Cytokinin signaling regulates cambial development in poplar. Proceedings of the National Academy of Sciences, USA **105,** 20032–20037.

Pau G, Fuchs F, Sklyar O, Boutros M, Huber W. 2010. EBImage—an R package for image processing with applications to cellular phenotypes. Bioinformatics **26,** 979–981.

Pereira H. 2011. Cork: biology, production and uses. Amsterdam: Elsevier Science.

Pound MP, French AP, Wells DM, Bennett MJ, Pridmore TP. 2012. CellSeT: novel software to extract and analyze structured networks of plant cells from confocal images. The Plant Cell **24,** 1353–1361.

Ragni L, Hardtke CS. 2014. Small but thick enough—the Arabidopsis hypocotyl as a model to study secondary growth. Physiologia Plantarum **151,** 164–171.

Ragni L, Nieminen K, Pacheco-Villalobos D, Sibout R, Schwechheimer C, Hardtke CS. 2011. Mobile gibberellin directly stimulates Arabidopsis hypocotyl xylem expansion. The Plant Cell **23,** 1322–1336.

Sankar M, Nieminen K, Ragni L, Xenarios I, Hardtke CS. 2014. Automated quantitative histology reveals vascular morphodynamics during Arabidopsis hypocotyl secondary growth. eLife **3,** e01567.

Sehr EM, Agusti J, Lehner R, Farmer EE, Schwarz M, Greb T. 2010. Analysis of secondary growth in the Arabidopsis shoot reveals a positive role of jasmonate signalling in cambium formation. The Plant Journal **63,** 811–822.

Sibout R, Plantegenet S, Hardtke CS. 2008. Flowering as a condition for xylem expansion in Arabidopsis hypocotyl and root. Current Biology **18,** 458–463.

Singh A, Ganapathysubramanian B, Singh AK, Sarkar S. 2016. Machine learning for high-throughput stress phenotyping in plants. Trends in Plant Science **21,** 110–124.

Spicer R, Groover A. 2010. Evolution of development of vascular cambia and secondary growth. New Phytologist **186,** 577–592.

Vincent L, Soille P. 1991. Watersheds in digital spaces: an efficient algorithm based on immersion simulations. IEEE Transactions on Pattern Analysis and Machine Intelligence **13,** 583–598.

Yoo TS, Ackerman MJ, Lorensen WE, Schroeder W, Chalana V, Aylward S, Metaxas D, Whitaker R. 2002. Engineering and algorithm design for an image processing Api: a technical report on ITK–the Insight Toolkit. Studies in Health Technology and Informatics **85,** 586–592.

Zhang J, Nieminen K, Serra JA, Helariutta Y. 2014. The formation of wood and its control. Current Opinion in Plant Biology **17,** 56–63.

9.2 A molecular framework to study periderm formation in Arabidopsis

Anna Wunderling, Dagmar Ripper, Azahara Barra-Jimenez, Stefan Mahn, Kathrin Sajak, Mehdi Ben Targem, Laura Ragni

New Phytologist, March 2018, DOI: 10.1111/nph.15128

New Phytologist

A molecular framework to study periderm formation in Arabidopsis

Anna Wunderling[1], Dagmar Ripper[1], Azahara Barra-Jimenez[1], Stefan Mahn[1], Kathrin Sajak[1], Mehdi Ben Targem[1] and Laura Ragni[1]

ZMBP-Center for Plant Molecular Biology, University of Tübingen, Auf der Morgenstelle 32, D-72076 Tübingen, Germany

Author for correspondence:
Laura Ragni
Tel: +49 (0)7071 29 76677
Email: laura.ragni@zmbp.uni-tuebingen.de

Received: *18 December 2017*
Accepted: *19 February 2018*

New Phytologist (2018) **219:** 216–229
doi: 10.1111/nph.15128

Key words: *Arabidopsis thaliana*, endodermis, periderm, phellem, programmed cell death (PCD), secondary growth.

Summary

- During secondary growth in most eudicots and gymnosperms, the periderm replaces the epidermis as the frontier tissue protecting the vasculature from biotic and abiotic stresses. Despite its importance, the mechanisms underlying periderm establishment and formation are largely unknown.
- The herbaceous *Arabidopsis thaliana* undergoes secondary growth, including periderm formation in the root and hypocotyl. Thus, we focused on these two organs to establish a framework to study periderm development in a model organism.
- We identified a set of characteristic developmental stages describing periderm growth from the first cell division in the pericycle to the shedding of the cortex and epidermis. We highlight that two independent mechanisms are involved in the loosening of the outer tissues as the endodermis undergoes programmed cell death, whereas the epidermis and the cortex are abscised. Moreover, the phellem of Arabidopsis, as in trees, is suberized, lignified and peels off. In addition, putative regulators from oak and potato are also expressed in the Arabidopsis periderm.
- Collectively, the periderm of Arabidopsis shares many characteristics/features of woody and tuberous periderms, rendering *Arabidopsis thaliana* an attractive model for cork biology.

Introduction

Secondary growth, the increase in girth of plant organs, is not only a prerequisite for efficient long-distance transport of water, solutes and photo-assimilates but also shapes the plant body in response to an ever-changing environment. In fact, the emergence of radial thickening contributed to the striking success of vascular plants during evolution (Spicer & Groover, 2010). Moreover, wood represents the major source of biomass accumulation in perennial dicotyledons and gymnosperms (Demura & Ye, 2010). The post-embryonic meristem that drives this process is the vascular cambium. The vascular cambium consists of a ring of undifferentiated meristematic cells that upon division differentiate into xylem (wood) and phloem (bast). Another lateral meristem that contributes to radial thickening and to the protection of the vascular cylinder is the phellogen, also known as cork cambium. The phellogen divides in a strictly bidirectional manner, producing inward the phelloderm and outward the phellem (cork). These three tissues, phellogen, phelloderm and phellem, are collectively referred to as periderm (Fig. 1a).

The periderm is a frontier tissue and its main function is to protect the plant against biotic and abiotic stress, similar to the epidermis during primary development. In particular, it effectively restricts: gas exchange, water loss and pathogen attack (Lulai & Freeman, 2001; Groh *et al.*, 2002; Lendzian, 2006).

Most woody eudicots and gymnosperms form a periderm in the root and the stem, and likewise, underground stems such as potato tubers form an extensive periderm. In the stem of most trees, the first phellogen is formed in the sub-epidermal layer, but in certain species it arises from the epidermis or the phloem. By contrast, in most roots the periderm derives from the pericycle (Esau, 1977). The number of cell layers comprising the periderm varies among species. Usually only one to two layers of phelloderm cell are present in the periderm, whereas several cell layers of phellem differentiate (Esau, 1977; Pereira, 2007). In trees, the phellogen can remain active for several years and/or it can be replaced each year by a new phellogen (Esau, 1977; Pereira, 2007). The phellogen of cork oak, for example, is functional for many years and remains viable throughout the life of a tree, although its activity decreases with age (Waisel, 1995; Pereira, 2007). Furthermore, phellogen activity in trees undergoes seasonal changes and it fluctuates with climatic variations (Waisel, 1995; Caritat *et al.*, 2000; Pereira, 2007). For instance, cold spells and drought cause a decrease in phellogen activity, whereas periods of warm weather result in high activity (Waisel, 1995; Caritat *et al.*, 2000; Pereira, 2007). A 'wound' periderm develops close to damaged or necrotic tissue after mechanical injury (e.g. shedding of branches and leaves) (Tucker, 1975; Thomson *et al.*, 1995; Oven *et al.*, 1999; Neubauer *et al.*, 2012; Khanal *et al.*, 2013) or pathogen infection (Lulai & Corsini, 1998; Thangavel *et al.*, 2016).

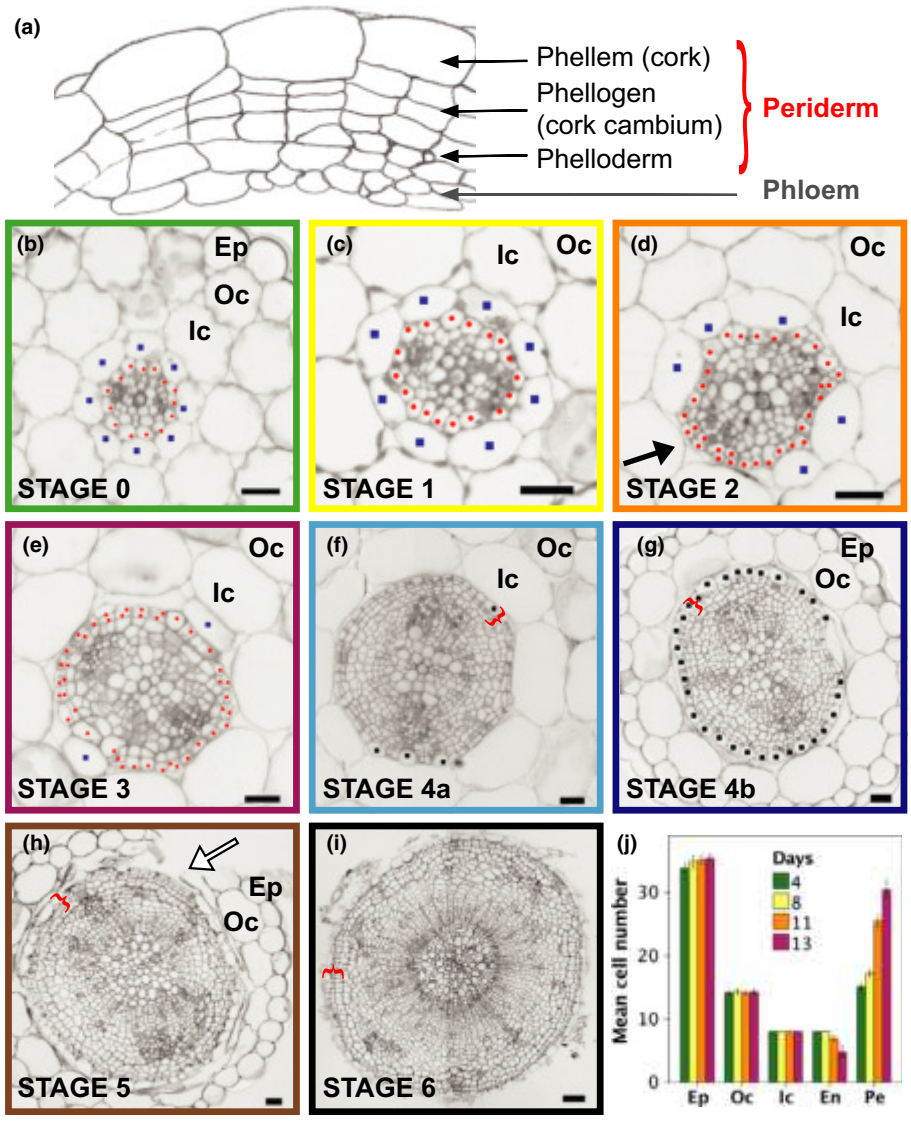

Fig. 1 The six stages of periderm development in the *Arabidopsis thaliana* hypocotyl. (a) Illustration of the periderm, which comprises the phellem/cork, the phellogen/cork cambium and the phelloderm. (b–i) Plastic cross-sections of Col-0 hypocotyls, grown in soil under long day (LD) conditions at different time points: (b) 4 d after sowing (das), (c) 8 das, (d) 11 das, (e) 13 das, (f) 16 das, (g) 18 das, (h) 21 das and (i) 27 das. (b) STAGE 0, the stage before the pericycle starts to divide. (c) STAGE 1, the pericycle divides anticlinally and endodermal cells become flatter. (d) vSTAGE 2 is characterized by four to six endodermal cells and by periclinal division in the pericycle, which we refer to as phellogen. (e) STAGE 3: only two endodermal cells in correspondence of the xylem poles subsist. (f) STAGE 4A is characterized by a lack of endodermis and by the differentiation of the first phellem cells. (g) STAGE 4b lacks the inner cortex and exhibits a ring of phellem cells. (h) During STAGE 5, the cortex and the epidermis break and become detached (white arrow). (i) At STAGE6 the periderm is the outside tissue that protects the vasculature. (j) Quantification of cell number in the epidermis (Ep), outer cortex (Oc), inner cortex (Ic), endodermis (En) and pericycle/periderm (Pe) at different time points (mean cell number ± 2 SE). Blue squares, endodermal cells; red dots, pericycle/periderm; black dots, phellem cells; red brackets, periderm. Bars, 20 μm.

To fulfill its barrier role, specialized macromolecules such as suberin are the major components of the phellem cell wall (Pereira, 1988). The chemical and physical properties of phellem have been extensively studied in potato and cork oak, due to the economic importance of improving potato conservation (Neubauer *et al.*, 2013) and of phellem as a material for wine bottle corks and building/insulating. Suberin extracted from the phellem also has industrial applications (Silva *et al.*, 2005) such as the production of hybrid co-polymers (e.g. polyurethanes) (Cordeiro *et al.*, 1999), thermoset resins (Torron *et al.*, 2014) and high-resistance fibers (de Geus *et al.*, 2010). Suberin is a complex glycerol-based heteropolymer, comprising aliphatic and phenolic fractions and often noncovalently associated waxes (reviewed by Vishwanath *et al.*, 2015). The amount/composition of phellem suberin and waxes varies among species and throughout development; for example, in cork oak it can reach up to 40% of the dry weight (Pereira, 1988; Pinto *et al.*, 2009; Kosma *et al.*, 2015). Lignin is also deposited in the cell wall of the phellem, but it displays a different monolignol composition compared to wood (Marques & Pereira, 2013; Fagerstedt *et al.*, 2015; Lourenco *et al.*, 2016).

Potato has proven to be a good model to study suberin biosynthesis and periderm water permeability, as periderm can be easily isolated from the tuber in sufficient amounts for chemical analyses. Furthermore, it is possible to measure peridermal transpiration rates (Schreiber *et al.*, 2005). In fact, reverse genetic studies indicate that a reduction of ferulic acid in the potato periderm results in an increased water permeability and defective periderm maturation (Serra *et al.*, 2010). Reducing aliphatic suberin contents results in similar phenotypes, suggesting that both suberin composition and quantity are important for water barrier function (Serra *et al.*, 2009a,b, 2010). Suberin biosynthesis genes have been extensively characterized also in Arabidopsis, with particular regard to the chemical composition of the whole root, the endodermis and the seed coat (Beisson *et al.*, 2007; Hofer *et al.*, 2008; Compagnon *et al.*, 2009; Molina *et al.*, 2009; Domergue *et al.*, 2010; Kosma *et al.*, 2012). Furthermore, it has been shown that *ALIPHATIC SUBERIN FERULOYL TRANSFERASE* (*ASFT*)

and *FATTY ACYL-COA REDUCTASES 1* (*FAR1*), *FAR4* and *FAR5* are expressed in the phellem of roots (Molina *et al.*, 2009; Vishwanath *et al.*, 2013). However, the suberin lamella in the periderm is not disturbed in *asft* mutants (Molina *et al.*, 2009)

Despite the huge progress in understanding the molecular mechanisms underlying cambium and vascular development, very few regulators controlling phellogen establishment and activity have been identified. As far as we know, only the transcription factor (TF) *SHORT-ROOT-like 2B* (*PttSHRL2B*) has been shown to regulate phellogen activity in poplar (Miguel *et al.*, 2016), whereas it has been suggested that the TF *QsMYB1* (ortholog of Arabidopsis MYB84) coordinates phellogen action in response to drought and heat (Almeida *et al.*, 2013a,b). One possible explanation for this lack of knowledge is that periderm has been mainly studied in nonmodel/amenable species. In contrast to periderm development, our current understanding of the basic mechanisms of cambium activity in woody species is mainly derived from pioneering works in Arabidopsis. In fact, this herbaceous eudicot model plant undergoes secondary growth in the stem, root and hypocotyl and shares common regulatory networks with woody species (reviewed by Barra-Jimenez & Ragni, 2017). The most striking example is the regulatory module involving the receptor-like kinases PHLOEM INTERCALATED WITH XYLEM/TDIF RECEPTOR (PXY/TDR), the small peptide CLV3/EMBRYO SURROUNDING REGION 41/44 (CLE41/CLE44) and the TF WUSCHEL HOMEOBOX 4 (WOX4), which controls cambium proliferation in several species including poplar (Etchells *et al.*, 2015; Hirakawa & Bowman, 2015; Kucukoglu *et al.*, 2017).

Here, we propose a framework to study periderm growth in *Arabidopsis thaliana*. We provide a suite of tools to study periderm development, including tissue-specific reporters. In particular, we define distinct stages of periderm growth, considering periderm ontogenesis and the fate of the surrounding tissues. We thus show that periderm growth is tightly connected to the development of the outside tissues and particularly to endodermal programmed cell death (PCD). Finally, we highlight that the Arabidopsis periderm displays characteristics similar to those of a woody eudicot periderm, and that putative regulators are conserved among species. These results are setting the stage for mechanistic insights into periderm growth.

Materials and Methods

Plant material and growth

All lines used are in *A. thaliana* Col-0 background unless otherwise specified. All plants used for confocal microscopy were grown *in vitro* on ½ MS 1% sugar plates under continuous light, unless it is otherwise specified. For the other experiments, light and growing conditions are stated in the text/figure. *GPAT5:mCITRINE-SYP122* (Barberon *et al.*, 2016), *UBQ10:eYFP-NPSN12* (*W131Y*) (Geldner *et al.*, 2009), *ASFT:NLS-GFP-GUS*, *GPAT5:NLS-GFP-GUS*, *KCR1:NLS-GFP-GUS*, *RALPH(CYP86B1):NLS-GFP-GUS*, *FAR4:NLS-GFP-GUS*, *HORST:NLS-GFP-GUS*, *DAISY:NLS-GFP-GUS* (Naseer *et al.*, 2012) and *CASP1:CASP1-mCherry* (Vermeer *et al.*, 2014) were gifts from N. Geldner (University of Lausanne, Switzerland). *ESB1:ESB1-mCherry* was kindly provided by D. Salt (University of Aberdeen, UK) and is described by Hosmani *et al.* (2013). *FAR1:GUS*, *FAR5:GUS* were described by Domergue *et al.* (2010) and kindly provided by F. Domergue (CNRS, FR). *PASPA3:H2A-GFP*, *Rxml:H2A-GFP*, *SCPL48:H2A-GFP*, *DPM4:H2A-GFP*, *EXI1:H2A-GFP* were gifts from M. Nowack (VIB, Belgium) and are described by Fendrych *et al.* (2014; Olvera-Carrillo *et al.*, 2015). The *soc1 ful1* mutants were described by Melzer *et al.* (2008). *SCR:H2B-2xmCherry* (N2106153) was obtained from the NASC and is described by Marques-Bueno *et al.* (2016). The *CASP2:NLS-GFP-GUS* was obtained by the NASC (N69050) and described by Liberman *et al.* (2015).

Histology and staining

Thin plastic sections were obtained as described by Barbier de Reuille & Ragni (2017) and stained with 0.1% toluidine blue and imaged with a Zeiss Axio M2 imager microscope or a Zeiss Axiophot microscope. Vibratome sections (50–80 µm) were obtained, embedding the hypocotyl and/or the root in 6% agarose block, and then cut with a Leica VT-1000 vibratome and collected/visualized in water. For suberin staining, Fluorol yellow 088 (FY) (sc-215052; Santa Cruz, CA, USA) staining was performed as described by Naseer *et al.* (2012). For lignin staining, 0.5% Basic Fuchsin (Sigma) aqueous solution was applied to the root or hypocotyl for 5 min, and samples were then rinsed and mounted in 10% glycerol. Phloroglucinol staining was performed applying a ready solution (26337.180; VWR, Radnor, PA, USA) directly to the vibratome section. For pectin staining, ruthenium red (R2751; Sigma), 0.01% aqueous solution was applied to fresh vibratome sections for 4 min, and sections were then rinsed and mounted in 10% glycerol. Clearing, before autofluorescence detection of the casparian strips, was performed as described by Naseer *et al.* (2012). GUS assays were performed as described by Beisson *et al.* (2007).

Confocal microscopy

All confocal images where acquired as whole-mounts unless specified in the figure legend that vibratome sections were used. Images were acquired with a Leica SP8 with resonant scan or with a Zeiss LSM880 microscope. For FY, green fluorescent protein (GFP) and fluorescein diacetate (FDA): excitation wavelength (ex.) 488 nm; emission (em.) 490–510 nm for yellow fluorescent protein (YFP) and mCitrine: ex. 514 nm; em. 520–540 nm; for propidium iodide (PI), mCherry and Basic Fuchsin: ex. 561 nm; em. 570–630 nm; for phellem autofluorescence: ex. 405 nm; em. 420–500 nm or ex. 405 nm; em. 420–460 nm if combined with GFP or YFP; for phelloderm autofluorescence: ex. 561 nm; em. 576–625 nm. Three-dimensional reconstructions and Ortho Views of a Z-stack were obtained using the ZEN BLACK PRO software.

Image analyses and statistical analyses

The number of cells in the different tissues was quantified using the plug-in Cell Counter of Fiji (Schindelin *et al.*, 2012), and cell eccentricity was measured using LithographX (www.lithographx.org) and according to the protocol described by Barbier de Reuille & Ragni (2017). To measure the length of root covered by phellem, whole roots were mounted in water on a microscope slide. Using light microscopy, the point closest to the root tip, where phellem cells begin to be the outside tissue, was marked on the coverslip. The whole root was then traced on the coverslip and the coverslips were subsequently scanned. Phellem length and root length were then measured with the software Fiji (Schindelin *et al.*, 2012). The ratio of phellem length : root length was calculated from at least 15 roots per time point and plant line. To quantify phellem and endodermis cell length and area, Z-stacks of the reporter line *GPAT5:mCITRINE-SYP122* were used. Images were exported with the Ortho View function from the Zen Black pro software and measured with Fiji (Schindelin *et al.*, 2012). More than 50 cells from at least three independent roots were measured per time point and/or root part. At least three independent experiments were performed and the graphs of one representative experiment each are presented. Statistical analyses were performed using IBM spss Statistics version 24. We first tested all datasets for homogeneity of variances using Levene's Test of Equality of Variances. We calculated the significant differences between two datasets using a Welch's *t*-test (not homogenous variance) or a Student's *t*-test (homogeneous variance). The significance threshold was set to $P < 0.05$ (shown by a red asterisk in the figures).

Molecular cloning

The *MYB84* and the *ANAC78* promoters were amplified from genomic DNA with the primers: A-pMYB84F (AACAGGTCT CAACCTCGTGGACTTGGACTTGTTTA) Br-pMYB84R (AACAGGTCTCATGTTACTTGTACTCCTAGTGAAGTC TTG) and A-pANAC78F (AACAGGTCTCAACCTGATCAT TTCAAAGGCATTGTGT) Br-pANAC78R (AACAGGTCTC ATGTTCAATCGGTGAAAACCAGAACTTG), respectively, and cloned into pGG-A0 using the GreenGate technology (Lampropoulos *et al.*, 2013). The β-glucuronidase coding sequence was recloned into pGG-D0. To obtain the lines *MYB84:NLS-GFP-GUS*, *MYB84:NLS-3xGFP* and *ANAC78:NLS-GFP-GUS*, the final GreenGate reaction was performed including some of the published and publicly available modules: NLS, 3XGFP and GFP (Lampropoulos *et al.*, 2013).

Results

Periderm is formed in the root and in the hypocotyl of *Arabidopsis thaliana* under various environmental conditions

To set up a framework to study periderm development, we first investigated in which organs/conditions a periderm is established in Arabidopsis. In Arabidopsis plants that had undergone extensive secondary growth, the hypocotyl was fully covered by the phellem (Supporting Information Fig. S1a), whereas in mature primary root, the periderm covered the uppermost part spanning *c.* 20–30% of the root length (Fig. S1b,c). Likewise, a periderm surrounded the oldest part of lateral roots (Fig. S1d). Although most gymnosperms and eudicots produce a periderm in the stem, no periderm has been reported in the Arabidopsis stem (Altamura *et al.*, 2001; Agusti *et al.*, 2011; Mazur & Kurczynska, 2012). Consistently, a periderm was not observed at the base of the stem of 12-wk-old plants of commonly used Arabidopsis strains such as Col-0, Ler and Ws (Fig. S1e–h). No periderm was detected in the stem of the 24-wk-old *soc1 ful1* double mutant (grown under long day (LD) conditions), which is characterized by extended secondary growth and life span (Fig. S1j–l) (Melzer *et al.*, 2008; Davin *et al.*, 2016). Because the periderm is not present in the Arabidopsis stem, we continued periderm characterization focusing on the root and hypocotyl.

We analyzed whether periderm development is influenced by photoperiods or growing conditions in the Arabidopsis root and hypocotyl. Plants grown *in vitro* (on medium supplemented with (Fig. S2a) or without (Fig. S2b) sugar) in soil (Fig. S2c,d) and under several light conditions (continuous light (CL) (Fig. S2a,b,e), LD (Fig. S2c,f) or short day (SD) conditions (Fig. S2d)) produced a periderm. In general, periderm development reflected plant growth progression: for instance, a periderm was established earlier in plants grown in CL than in LD conditions and in media supplemented with sugar than in media without sugar (Fig. S2). In Arabidopsis, flowering has a major influence on secondary growth progression, as it triggers the 'xylem expansion' phase (xylary fiber production and higher xylem-to-phloem ratio) (Sibout *et al.*, 2008). Therefore, we analyzed the temporal relationship between xylem expansion and periderm growth. Under all tested conditions, the periderm was differentiated before flowering occurred and thus establishment of the periderm precedes xylem expansion (Fig. S2g).

Periderm formation follows a predetermined pattern, which can be summarized by six distinct stages

Periderm development in the hypocotyl and in the root was temporally separated, formation occurring much more slowly in the hypocotyl than in the root (Figs 1, S1b,c). As a result, in an 8-d-old plant, the hypocotyl displayed no phellem (Fig. 1c), whereas in the mature part of the primary root (close to the hypocotyl–root junction) some phellem cells were present (Fig. S1b,c). Moreover, as a root represents a gradient of secondary growth, periderm development can be followed along the same root (Fig. 2a), whereas in the hypocotyl it can be analyzed only over time series with plants in different developmental stages (Fig. 1). In both organs the periderm arises from the pericycle – an inner tissue – surrounded by three to four cell layers and it becomes the external tissue once it is fully differentiated. We therefore characterized periderm growth throughout development, considering the fate of the surrounding tissues.

We were able to identify six characteristic stages of periderm development in the hypocotyl and we found that the duration of

each stage was influenced by the growing conditions (Fig. S3a–h). STAGE 0 was designated as the stage before the first division in the pericycle (after hypocotyl elongation occurred). Here, the vasculature was already arranged with a central metaxylem and two phloem poles. The pericycle comprised *c.* 13–14 cells and it was surrounded by eight endodermal, approximately eight inner cortex, *c.* 14 outer cortex and *c.* 33–34 epidermis cells. In the hypocotyl, this stage was present for instance in 3- to 6-d-old plants grown in LD conditions (Fig. 1b,j). In the course of STAGE 1, the pericycle starts to divide (Fig. 1c,j). The first anticlinal divisions occurred at the xylem pole pericycle cells (Fig. S3i). Shortly thereafter, the divisions expanded to the rest of the pericycle cells. Simultaneously, the endodermal cells became flatter, as shown by a decrease in their eccentricity (Figs 1c, S3j). We defined STAGE 2 as the stage marked by a reduction in the number of endodermal cells (the endodermis comprises four to six cells) as well as by pericycle proliferation (Fig. 1d,j). In more detail, the endodermal cells located at the sites of the phloem poles were missing. The pericycle began to divide periclinally and thus, in some regions, it was possible to distinguish two layers of cells, which hereafter we refer to as phellogen. We classified a periderm to be in STAGE 3 when only one/two endodermal cells located at the xylem poles were still present and the periderm comprised at least two layers of cells. Interestingly, the number of

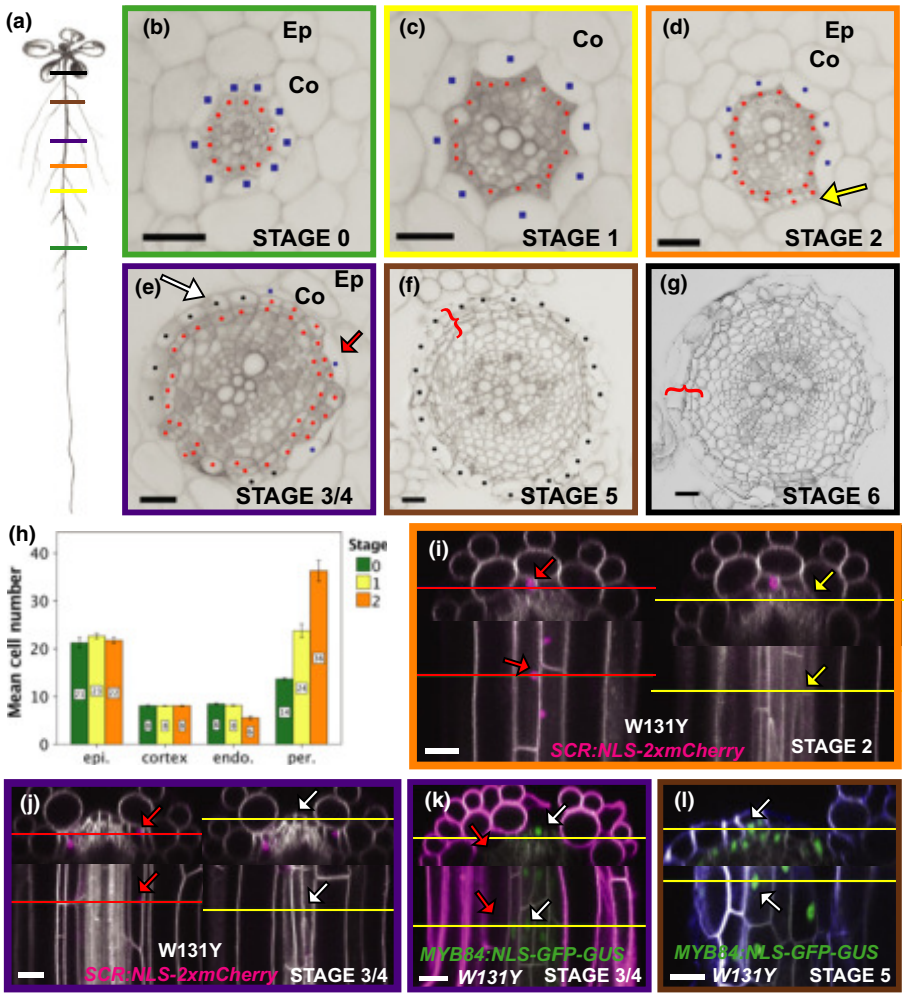

Fig. 2 Periderm development in the *Arabidopsis thaliana* root. (a) Illustration of an Arabidopsis root showing the positions corresponding to the different stages. (b–g) Cross-sections of 14-d-old roots (plastic embedding) at different positions of the root corresponding to STAGES 0–6. (b) STAGE 0: the stage before the pericycle starts to divide. (c) STAGE 1: the pericycle divides anticlinally. (d) STAGE 2 is characterized by a reduction in endodermal cells and pericycle proliferation. (e) STAGE 3/4: the cortex and the epidermis break and the periderm is the outmost tissue, whereas some endodermal cells are still present on the opposite side. (f) STAGE 5: the endodermis is no longer present and a ring of phellem cells is visible. (g) STAGE 6: the periderm is the outside tissue. Ep, epidermis; Co, cortex; blue squares, endodermal cells; red dots, pericycle/phellogen cells; black dots, phellem cells; red brackets, periderm. The yellow arrow indicates the absence of an endodermal cell, the red arrow points toward the remaining endodermal cells and the white arrow shows the emerging phellem. (h) Quantification of the cell number in different tissues (epidermis, cortex, endodermis and pericycle) at different periderm stages (0–2). Cross-sections of plants from independent experiments were measured ($n = 33$ STAGE 0; $n = 52$ STAGE 1; and $n = 31$ STAGE 2; error bars are ± 2 SE). (i, j) Ortho View of Z-stacks of *SCR:NLS-2xmCherry W131Y* roots at the positions corresponding to (i) STAGE 2 and (j) STAGE 3/4. For each stage, the same cross-section is shown, with the corresponding longitudinal section on endodermal cells (left) and periderm cells (right). (k, l) Ortho View of Z-stacks of *MYB84:NLS-GFP-GUS W131Y* roots at the positions corresponding to (k) STAGE 3/4 and (l) STAGE 5. Bars, 20 μm.

cortical cells and of epidermal cells did not vary (Fig. 1e,j). STAGE 4 was characterized by the absence of the endodermis and the differentiation of first phellem cells from the phellogen. This stage can be divided in two sub-stages: in STAGE 4A, the inner cortex started to disappear from the phloem poles (in the majority of cases; Fig. S3k) and only a few phellem cells are differentiated (Fig. 1f), whereas in STAGE 4B, the inner cortex is missing and a ring of phellem cells starts to be visible (phellem cells are larger and rounder than phellogen cells) (Fig. 1g). At STAGE 5, the epidermis and the outer cortex broke on one side and progressively became detached from the periderm (Fig. 1h). Breaking of the cortex and of the epidermis occurred at random positions (Fig. S3l). Finally, STAGE 6 corresponded to a mature periderm in which the epidermis and the cortex were completely detached, and the periderm was the outer tissue protecting the vasculature (Fig. 1i). In a mature periderm we were able to distinguish four to five cell layers comprising the phellem, the phellogen and the phelloderm.

In roots, periderm development mainly followed the same stages defined for the hypocotyl, although we observed some differences possibly due to the distinct anatomy of the two organs (root at STAGE 0: one cell layer of cortex, hypocotyl at STAGE 0: two cell layers). In fact, the epidermis and the cortex broke and were shed earlier in development of the root. The exact position of each stage within the root and the length of the root corresponding to each stage vary with the age of the plant and the growing conditions (Figs S1b,c, S2e,f).

In roots, STAGE 0 occurred in the region with emerged and elongated lateral roots directly above the lateral root initiation zone (Fig. 2a,b). Similar to the hypocotyl, the vasculature of this region was already arranged with a central xylem axis and two phloem poles. In this part of the root, the pericycle was surrounded by the endodermis (approximately eight cells), the cortex (12–14 cells) and the epidermis (*c.* 23 cells) (Fig. 2b,h). In the region above STAGE 0, the pericycle began to divide at the xylem poles (STAGE 1) (Figs 2c, S3m). STAGE 2 is characterized by the loss of one to two endodermal cells at the phloem poles (in most cases) (Figs 2d, S4n) and by the first periclinal division in the pericycle, which from now can be termed phellogen (Fig. 2d).

In contrast to the hypocotyl, in the root we defined only one large stage, STAGE 3/4, as the events defining stage 3 and 4 cannot be precisely distinguished and often occur coincidentally and stochastically. During STAGE 3/4, the pericycle divided periclinally, while the number of endodermal cells decreased. The cortex and the epidermis broke primarily at the site where the endodermal cells disappeared and, at this location, phellem cells began to be visible (Fig. 2e). At STAGE 5, the periderm was fully differentiated and the phellem was the main external tissue, still partially covered with patches of epidermis and cortex (Fig. 2f). Finally, at STAGE 6 the epidermis and the cortex were completely shed and the periderm comprised three to four cell layers (Fig. 2g). Overall, periderm formation in lateral roots occurs similarly to the main root (Figs S1d, S4a–c).

To corroborate the histological analyses we visualized the most distinctive stages by live imaging. We followed endodermis fate using the marker *SCR:H2B-2xmCherry* (Di Laurenzio *et al.*, 1996; Marques-Bueno *et al.*, 2016) and tracked periderm growth in *MYB84:NLS-3xGFP* roots (*MYB84* is the Arabidopsis ortholog of *QSMYB1*). Given that PI does not normally penetrate the endodermis, both reporters were crossed to the ubiquitously expressed plasma membrane marker line *W131Y* (*UBQ10:eYFP-NPSN12*) to outline the different cell types (Geldner *et al.*, 2009; Alassimone *et al.*, 2010). We clearly observed areas of the root where the *SCR* expression domain was interrupted by cells with periderm morphology (Fig. 2i,j) and regions where the periderm marker *MYB84* was flanked by endodermal cells (Fig. 2k), validating our histological analyses. Consistently, in the upper part of the root we could no longer identify endodermal cells (Fig. 2l).

Based solely on morphology and size, phelloderm cells can be difficult to differentiate from phloem parenchyma cells. To address this issue, several staining methods that label phelloderm cells in other species were tested in Arabidopsis. Classical toluidine blue staining, which has been useful in helping to distinguish the three periderm tissues in potato (Sabba & Lulai, 2005), stained uniformly the periderm of Arabidopsis (Fig. S4d). However, a thicker cell wall between two cell layers was visible and may represent the boundary between the periderm and the phloem (Fig. S4e,f). To confirm this, we checked whether we could observe a different degree of esterification of pectins, which is used to distinguish the phelloderm in potato (Sabba & Lulai, 2002), at the presumptive boundary line. In root vibratome sections stained with ruthenium red, a pale red staining was visible in the cell layer below the phellem, whereas it was stronger at the presumptive boundary, supporting our hypothesis (Fig. S4g). These data also fit with the autofluorescence pattern in the red spectrum (ex. 561 nm, em. 570–630 nm), which in roots from 15-d-old plants grown under continuous light showed a strong intracellular autofluorescence mainly in the presumptive phelloderm (Fig. S4h). Together, these results suggested that one layer of phelloderm cells is formed in Arabidopsis, which can be confirmed by the development of tissue-specific markers and/or clonal analyses in the future.

Cortex and epidermis are abscised while endodermis undergoes PCD during periderm growth

We showed that the tissues that surround the periderm are progressively lost following a predefined pattern, so we next investigated the mechanisms underlying this process. In particular, we investigated whether it involves abscission (shedding of plant organs or parts that are no longer necessary), PCD or if the cells simply collapse.

We first studied how the epidermis and the cortex are progressively removed. The breaking of the cortex and epidermis was not an artifact of the embedding methods as we were able to observe it during live cell imaging (Fig. 3a–f). Along a mature root, we observed isolated areas in which the cortex and the epidermis broke and the phellem became the external tissue, followed by a zone where the phellem was the outer tissue with stretches of cortex and epidermis still attached (Fig. 3a,b).

Moreover, most of the epidermal and cortex cells that still surround the periderm after the first break are still alive, as seen by PI and FDA staining (Fig. 3g,h). In fact, PI stains the nuclei of dead cells, whereas FDA becomes fluorescent when cleaved by esterases inside living cells. These results indicate that the epidermis and the cortex are abscised and do not undergo PCD.

We next characterized the course/fate of endodermal cells during periderm growth and assessed the viability of endodermal cells during root development. It was previously shown that 20 min of incubation is sufficient for FDA uptake into the endodermis and stele of the root differentiation zone (Barberon *et al.*, 2016). This was also the case in older root in the regions where lateral roots are emerged and elongated (Figs 4h, S4i). At early STAGE 2, PI was detected in a few nuclei of the endodermis in which FDA was excluded, while the neighboring endodermal cells showed only FDA in the nuclei (Fig. 4a). To better visualize dying vs alive endodermal cells, we repeated the PI staining using the endodermis reporter *CASP2:NLS-GFP-GUS* (*CASPARIAN STRIP DOMAIN PROTEIN 2*) (Roppolo *et al.*, 2011). We observed PI staining in the nuclei of endodermal cells, which were flanked by endodermal cells expressing the *CASP2* reporter, confirming our previous results (Fig. 4b). Furthermore, we analyzed the expression of a set of genes whose expression has been associated with developmental PCD (Fendrych *et al.*, 2014; Olvera-Carrillo *et al.*, 2015). The PCD markers *RIBONUCLEASE 3* (*RNS3*), *EXITUS 1* (*EXI1*) and *DOMAIN OF UNKNOWN FUNCTION679 MEMBRANE PROTEIN 4* (*DMP4*) were broadly expressed in the endodermis from STAGE 1 onwards (as long as the endodermis is present) in both root and hypocotyl and only in the inner cortex of the hypocotyl during STAGE 4 (Figs 4c–e, S4j–l, S5a–f). In summary, these data indicate that the endodermis and the inner cortex (in the hypocotyl) undergo PCD.

Next, we investigated whether the endodermis alters its chemical/physical properties before PCD. The two major features of a mature endodermis are casparian strips (CSs) and suberin lamellae. We first analyzed the expression of the CS markers *ESB1:ESB1-mCherry* (*ENHANCED SUBERIN1*) and *CASP1:CASP1-mcherry* during root development. Both proteins are required for proper CS assembly and accumulate at the plasma membrane domain underlying the CS (casparian strip membrane domain CSD) in the root differentiation zone (Roppolo *et al.*, 2011; Hosmani *et al.*, 2013). A similar pattern was observed for the endodermis in the region of the main root where lateral roots were already emergent and elongated (Figs 4h, S4m,n). Similarly ESB1 still accumulated at the CSD in mature endodermis (region of the root that precedes endodermis PCD; Fig. 4h) (Fig. S4o), whereas CASP1 in the mature endodermis was no longer localized to the CSD (Fig. S4p), suggesting that CSs are maintained throughout endodermis development. To confirm that CSs are not degraded before endodermis PCD, we verified whether the typical autofluorescence pattern of CSs (Alassimone *et al.*, 2010) (Fig. 4f) was present in the mature endodermis (Fig. 4g). No difference in the pattern of autofluorescence of the CSs was observed, suggesting that CSs are still present when the endodermis undergoes PCD. The mature endodermis is a highly suberized tissue, and the amount of suberin is modified according to nutrient availability (Barberon *et al.*, 2016) and in response to hormones. For instance, sulfur and potassium deficiency enhances suberization, whereas iron, magnesium and zinc starvation promotes suberin degradation and reduces the expression of suberin biosynthesis genes (Barberon *et al.*, 2016). Because suberin accumulation in the endodermis is a dynamic

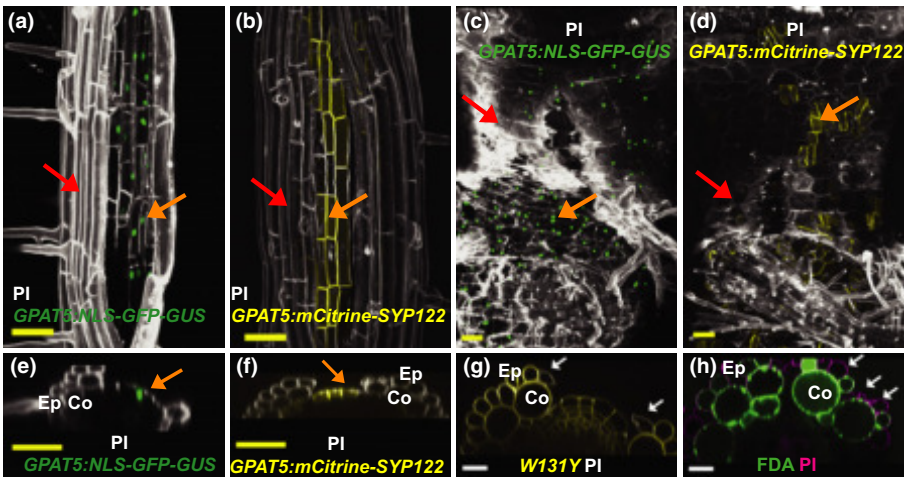

Fig. 3 The epidermis and cortex of Arabidopsis root and hypocotyl are abscised together. (a–d) 3D reconstructions of a Z-stack *GPAT5:NLS-GFP-GUS* and propidium iodide (PI), 13-d-old root. (b) *GPAT5:mCITRINE-SYP122* and PI, 13-d-old root. (c) *GPAT5:NLS-GFP-GUS* and PI, 25-d-old hypocotyl. (d) *GPAT5:mCITRINE-SYP122* and PI, 25-d-old hypocotyl. (e) Cross-section (Ortho View of a Z-stack) of (a). (f) Cross-section (Ortho View of a Z-stack) of (b). The cortex and the epidermis become detached in some areas of the root and the hypocotyl. Phellem cells (orange arrow), expressing the suberin biosynthesis gene *GPAT5*, are the outer tissue in certain regions, whereas the flanking areas remain covered by the epidermis and the cortex (red arrow). (g) Cross-section (Ortho View of a Z-stack) of a 17-d-old root, W131Y and PI. (h) Cross-section (Ortho View of a Z-stack) of a 17-d-old root stained with fluorescein diacetate (FDA) and PI. (g, h) Most epidermis and cortex cells are still alive before detachment. Dead cells (white arrow) do not express the W131Y marker (g) and do not show FDA signal (h, green) but are still stained by PI. Bars: (a–f) 50 μm; (g, h) 20 μm. Ep, epidermis; Co, cortex.

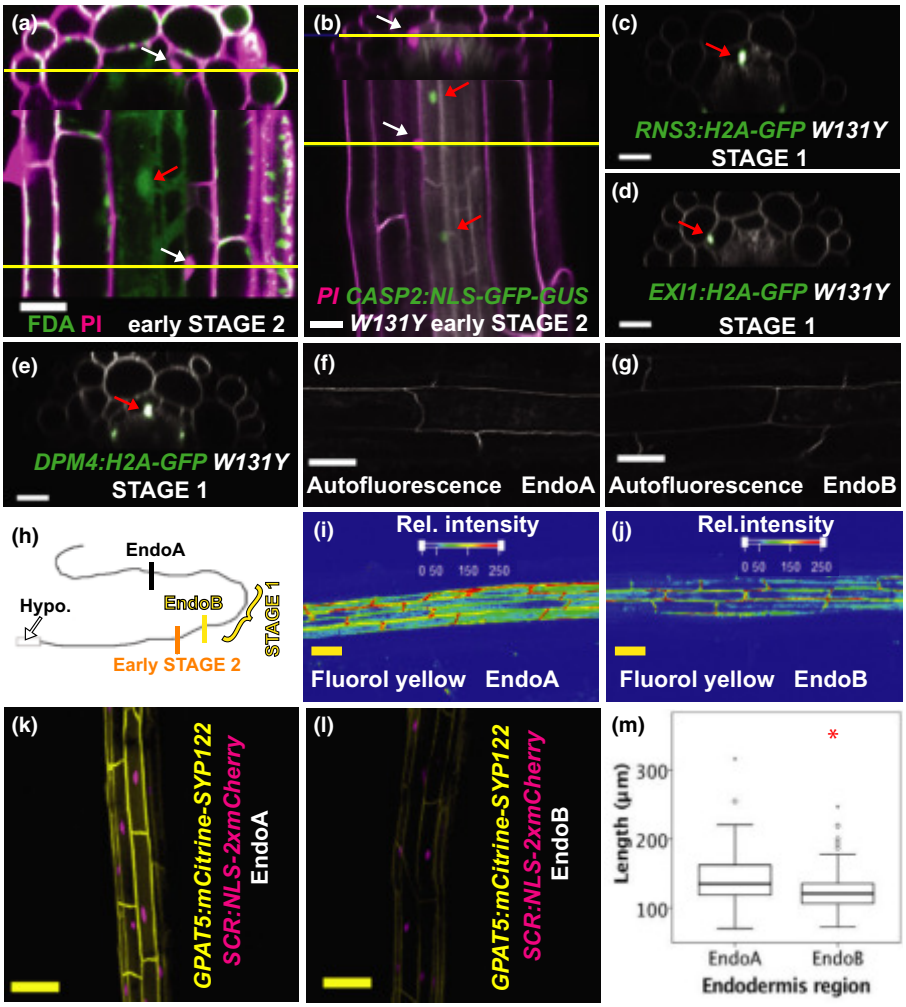

Fig. 4 The endodermis of Arabidopsis undergoes programmed cell death (PCD). (a) Cross and longitudinal sections (Ortho View of a Z-stack) of a 13-d-old root stained with fluorescein diacetate (FDA) and propidium iodide (PI) in early STAGE 2. The endodermis is undergoing PCD, as shown by PI staining of the nuclei (white arrow) and absence of FDA in the endodermis. (b) *CASP2:NLS-GFP-GUS W131Y*. Cross and longitudinal section (Ortho View of a Z-stack) of a 13-d-old root stained with PI. (c) *RNS3:H2A-GFP W131Y*. (d) *EXI1:H2A-GFP W131Y*. (e) *DPM4:H2A-GFP W131Y*. (c–e) Developmental PCD markers are expressed in the endodermis before PCD (red arrows indicate GFP signal in the nuclei of endodermal cells). Cross-sections (Ortho View of a Z-stack) of 14-d-old roots in STAGE 1. (f, g) Autofluorescence of the casparian strips (CSs) in the region of the endodermis where lateral roots emerge and become elongated (f; EndoA) and in the region before PCD (g; EndoB). (h) Scheme of an Arabidopsis root showing the positions along the root where the images where acquired. (i, j) Relative intensity of fluorol yellow (FY) staining in the region of the endodermis where lateral roots emerge and become elongated (i; EndoA) and in the region before PCD (j; EndoB) of a 14-d-old root, showing a reduction of suberin in the more mature part. (k, l) *GPAT5:mCITRINE-SYP122 SCR:NLS-2xmCherry* of 12-d-old roots in the region where lateral roots emerge (k; EndoA) and in the region before PCD (l; EndoB). (m) Quantification of endodermal cell length of 12-d-old roots. Welch's *t*-test (red asterisk: $P \leq 0.001$; $n = 97–39$). Box plot: the dark line in the middle of the boxes is the median, the bottom and top of the boxes indicate the 25th and 75th percentiles, whiskers (T-bars) are within 1.5 times the interquartile range, the empty dots are outliers and the black stars are extreme outliers. Bars: (a–g) 20 µm; (h–l) 50 µm.

process, we investigated whether suberin content varies before endodermis PCD. For this, we analyzed FY staining along the root, from the region of emergence of the lateral roots to where the endodermis undergoes PCD. A small decrease in suberin deposition was observed in the uppermost part of the endodermis (Fig. 4i,j). Consistently, a decrease in the expression of the suberin biosynthesis reporter *GPAT5:mCITRINE-SYP122* was detected in the mature endodermis, suggesting that endodermal PCD is promoted by a reduction of suberin (Fig. 4k,l). We also observed that endodermal cells are shorter in the more mature part of the root. A complication here is that suberin biosynthesis genes are expressed in both cell types, and thus the two cell types are difficult to distinguish at the endodermis–phellem transition zone. Therefore, we confirm a reduction in endodermal cell length before PCD, quantifying cell length in cells expressing both the endodermal marker *SCR:H2B-2xmCherry* and the *GPAT5:mCITRINE-SYP122* (Fig. 4m).

The phellem of *Arabidopsis thaliana* is suberized, lignified and partially composed of dead cells

One of the essential characteristics of phellem is the high degree of suberization, and consequently many suberin biosynthesis genes are expressed in the phellem of cork oak as well as the root

and the hypocotyl of Arabidopsis (Molina *et al.*, 2009; Kosma *et al.*, 2012; Vishwanath *et al.*, 2013) (this work) (Figs 3a–d, S6). FY staining decorated the outside surface of phellem cells in both roots (Fig. 5a) and hypocotyls (Fig. S7a,b). However, suberin is not the only polymer present in the phellem, as lignin impregnates the phellem of trees (Marques & Pereira, 2013; Fagerstedt *et al.*, 2015; Lourenco *et al.*, 2016).

To investigate whether the phellem of Arabidopsis comprises lignin, we stained phellem cells with Basic fuchsin and Phloroglucinol. These two stains revealed the presence of lignin in the phellem and the lignin deposition patterns partially matched the suberin impregnation (Figs 5b,c, S7c–e,g,i). Phellem cells were characterized by a strong extracellular autofluorescence in the blue–green spectrum (ex. 405 nm and em. 425–500 nm) that coincided with the lignin/suberin deposition pattern (Figs 5d, S7d,f–i). This particular chemical composition renders the phellem an impermeable barrier because dyes such as PI were unable to enter the phellem tissue (Fig. 3e,f). Given that the outer phellem cell layers die and peel off in woody species, we investigated whether it also occurs in Arabidopsis. Indeed, the developmental PCD marker genes *RNS3*, *EXI1* and *DPM4* were also expressed in phellem cells (Fig. 5e–g). Moreover, the aspartic protease *PASPA3* and *SERINE CARBOXY- PEPTIDASE-LIKE48* (*SCPL48*) genes were expressed in phellem, as well (Fig. 5h,i). Phellem cell viability was then analyzed by FDA/PI staining, and indicated that most phellem cells were alive as shown by the FDA fluorescence (Fig. 5j). However, we observed a few cells where FDA was excluded while PI stained the nuclei. These cells were larger, suggesting that morphological changes might anticipate phellem cell death (Fig. 5j). Thus, phellem cell size was investigated in more detail. Although phellem cell length was fairly homogeneous (Fig. S7j), when we quantified phellem length in the uppermost region of the root of 12- and 17-d-old plants, we observed a reduction of phellem cell length with age (Fig. 6a–c,e). Consistently, we detected a reduction in cell length when we compared the lower and upper part of the phellem (Fig. 6a,c,d,f). By contrast, phellem cell area was more heterogeneous with most cells having an area of 200–300 μm^2 and few cells with an area larger than 500 μm^2 (Fig. S7j). Moreover, the number of cells with a 'large' area increased with periderm development (Fig. 6g,h). As both cell length and cell area vary during phellem maturation, we estimated the volume. Although phellem cell volume was highly variable (Fig. 6i,j) we observed that cells with an area of > 500 μm^2 were associated with a large volume

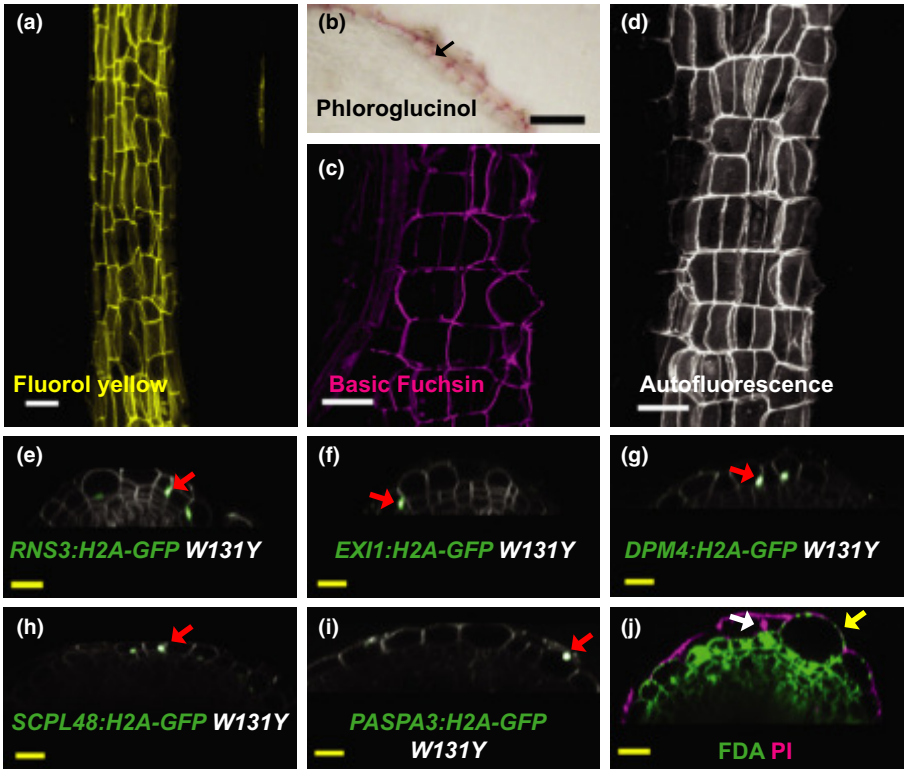

Fig. 5 Chemical composition and morphology of the phellem in the Arabidopsis root. (a) The phellem is suberized as shown by fluorol yellow (FY) staining of the uppermost part of a 17-d-old root (3D reconstruction of a Z-stack). (b) Vibratome section of the uppermost part of a 20-d-old root stained with Phloroglucinol (lignin staining). The black arrow indicates lignin staining of phellem cells. (c) The phellem contains lignin as shown by Basic Fuchsin staining of the uppermost part of a 17-d-old root (3D reconstruction of a Z-stack). (d) Autofluorescence (excitation wavelength (ex.) 405 nm; emission (em.) 420–500 nm) of phellem cell of the uppermost part of a 17-d-old root (3D reconstruction of a Z-stack). (e–i) Developmental PCD markers are expressed in phellem cells (red arrows indicate GFP signal in the nuclei of phellem cells). Cross-sections (Ortho View of a Z-stack) of the phellem region of 12-d-old roots. (e) *RNS3:H2A-GFP W131Y*. (f) *EXI1:H2A-GFP W131Y*. (g) *DPM4:H2A-GFP W131Y*. (h) *SCPL48:H2A-GFP W131Y*. (i) *PASPA3:H2A-GFP W131Y*. (j) Phellem cells die (white arrow) and peel off, as shown by fluorescein diacetate (FDA) and propidium iodide (PI) staining in the uppermost part of a 14-d-old root (Ortho View of a Z-stack). Yellow arrow indicates a large living phellem cell. Bars: (a, c, d) 50 μm; (b) 100 μm; (e–j) 20 μm.

and with the most mature part of the phellem, suggesting that an increase in volume preceded phellem death (Fig. 6i,j).

Conservation of periderm regulators in *Arabidopsis thaliana*

The periderm of Arabidopsis seems to share features with the phellem of trees, but it is not known if this conservation persists at the molecular level. Very few regulators of periderm growth have been identified so far, and no specific expression data for the phellogen and phelloderm exists. Nevertheless, several transcriptome datasets noted the importance of some TF families such as the MYBs and the NACs in phellem (Soler *et al.*, 2007, 2011; Ginzberg *et al.*, 2009; Rains *et al.*, 2017; Vulavala *et al.*, 2017). For instance, in cork oak, *QsMYB1/MYB84/RAX3* is expressed in the phellem and expression responds to drought and heat stress (Almeida *et al.*, 2013b). Moreover, the expression of these genes is enriched in the phellem of poplar (Rains *et al.*, 2017).

We analyzed the expression of *MYB84/RAX3* and *ANAC78* throughout the Arabidopsis periderm. *MYB84/RAX3* was expressed in the whole periderm circumference (Figs 2k,l, 7a,d) whereas *ANAC78* was expressed in the periderm and in the phloem of the hypocotyl and root (Fig. 7b,e). The suberin/wax biosynthesis genes *GPAT5*, *KCR1*, *HORST*, *DAISY*, *RALPH* and *ASFT*, which are expressed in the phellem of oak, potato and poplar (Soler *et al.*, 2007, 2011; Serra *et al.*, 2009a,b, 2010; Rains *et al.*, 2017), were expressed in the Arabidopsis phellem in both root and hypocotyl (Molina *et al.*, 2009) (Figs 7c,f–l, S6a,e). Thus, it seems that a certain degree of conservation exists between Arabidopsis and other species.

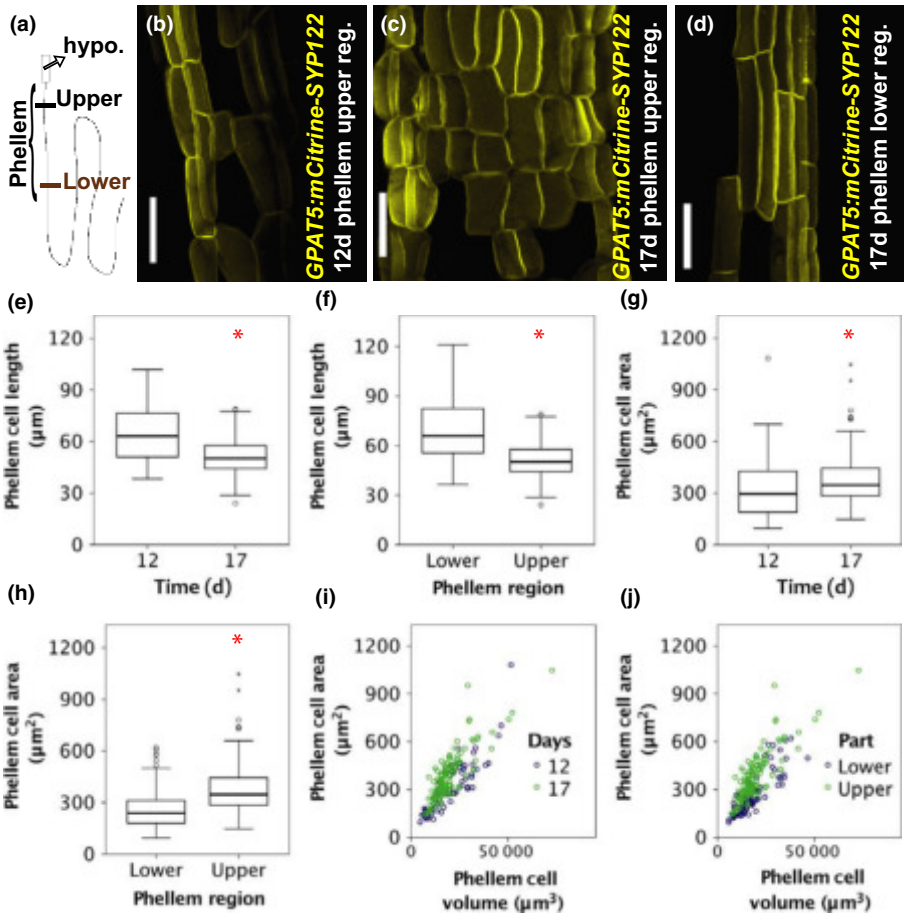

Fig. 6 Phellem cell morphology in Arabidopsis root. (a) Scheme of a root showing the upper and the lower phellem regions. (b–d) 3D reconstructions of Z-stacks of *GPAT5:mCITRINE-SYP122* roots. *GPAT5:mCITRINE-SYP122* is used to visualize phellem cells. Phellem cells at different developmental stages showing how phellem cell length decreases with age. (b) Upper region of the phellem of a 12-d-old root. (c) Upper region of the phellem of a 17-d-old root. (d) Lower region of the phellem of a 17-d-old root. (e) Quantification of phellem cell length measured in the upper region of the phellem of 12- and 17-d-old roots, showing that phellem length decreased during development. Welch's *t*-test (red asterisk: $P \leq 0.001$; $n = 69$–125). (f) Quantification of phellem cell length measured in the upper and lower region of the phellem of 17-d-old roots, showing that phellem cell length decreases with age. Welch's *t*-test (red asterisk: $P \leq 0.001$; $n = 89$–125). (g) Quantification of phellem cell area measured in the upper region of the phellem of 12- and 17-d-old roots, showing that the number of phellem cells of large area increases during development. Student's *t*-test (red asterisk: $P = 0.012$; $n = 69$–125). (h) Quantification of the phellem cell area measured in the upper and lower region of the phellem of 17-d-old roots, showing that the number of phellem cells of large area increases during development. Student's *t*-test (red asterisk: $P = 0.001$; $n = 89$–125). (e–h) Box plots: the dark line in the middle of the boxes is the median, the bottom and top of the box indicates the 25th and 75th percentiles, whiskers (T-bars) are within 1.5 times the interquartile range, the empty dots are outliers and the black stars are extreme outliers. (i, j) Plots of phellem cell volume vs phellem cell area. Bars, 50 µm.

Discussion

Periderm development in *Arabidopsis thaliana* root and hypocotyl

In this study, we set up a means to study periderm biology in *Arabidopsis thaliana*, providing a suite of tools and a detailed characterization of periderm growth in the form of identifiable stages. It was previously reported that a periderm is established in the root and in the hypocotyl of Arabidopsis. Consistently, we show that the stems of the most commonly used Arabidopsis strains lack a periderm. In addition, enhanced longevity and secondary growth do not trigger periderm formation in the stem of *soc1 ful1* plants grown in standard growing conditions, indicating that the epidermis in stems can adapt to a large amount of radial expansion. However, we cannot rule out that in extreme growing conditions or in other strains, which push the life span of *Arabidopsis* even further, a periderm could be produced in the stem.

In Arabidopsis hypocotyl and root, periderm growth is not a minor localized process, as the periderm covers one-third of the length of a mature primary root, the uppermost part of lateral roots and the whole hypocotyl of a flowering plant. Periderm growth occurs under different photoperiods and growing conditions and it mainly follows plant growth progression, in the sense that it is formed earlier in plants in which growth is accelerated. This combination of features makes Arabidopsis a robust model to study the molecular mechanisms of phellogen establishment and maintenance. In both root and hypocotyl, the periderm arises from an inner tissue to become an external barrier, which can be considered to be a complex process. For a better understanding of this process, we visualized periderm growth and defined a set of six stages that cover several intermediate steps from the onset of pericycle divisions that establish the meristematic phellogen to phellem maturation. These stages will help to compare periderm growth in different genetic backgrounds, paving the way for understanding the periderm regulatory network.

In woody species, phellem cells are characterized by lignin in addition to a higher content of suberin and undergo a maturation process that leads to death and peeling off. The presence of lignin, suberin and associated waxes in the phellem gives the

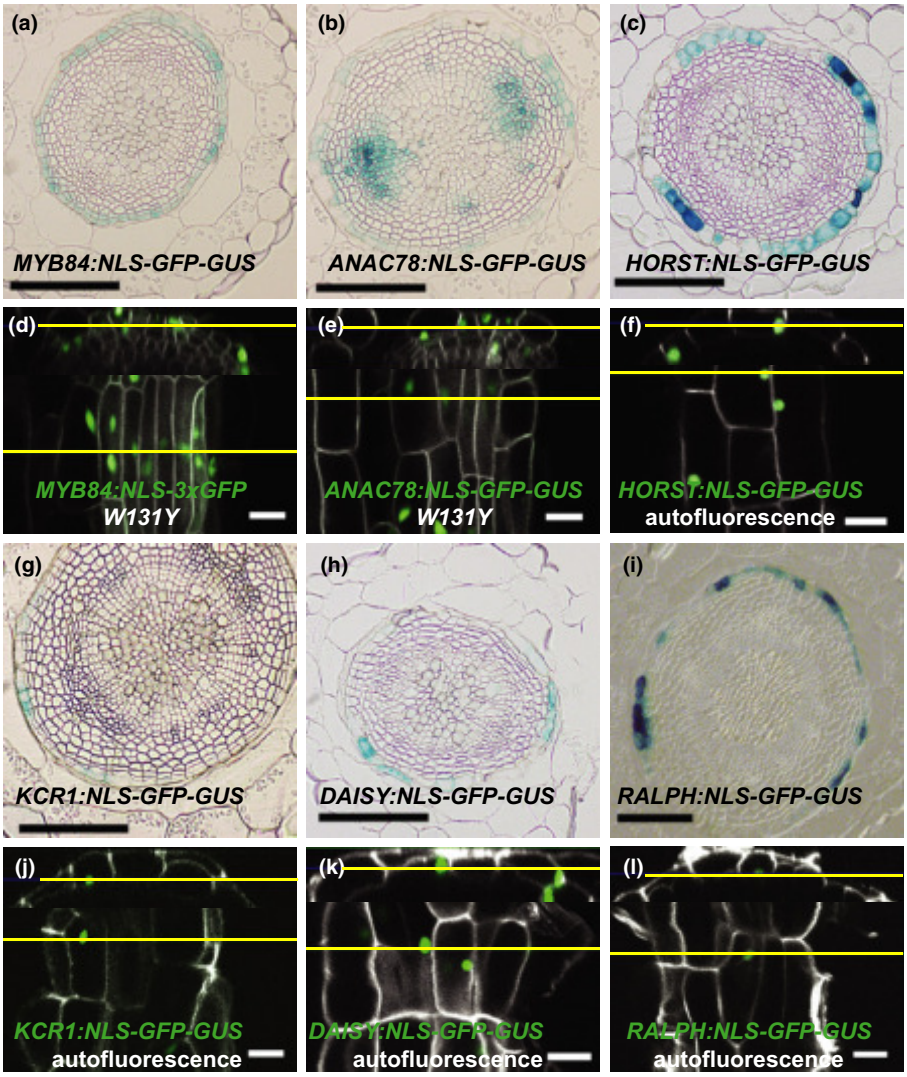

Fig. 7 Periderm-associated gene expression in Arabidopsis. (a–c, g–i) Plastic cross-sections of GUS staining of 17- to 19-d-old hypocotyls (STAGE 4). (d–f, j–l) Cross and longitudinal sections (Ortho View of a Z-stack) of 12- to 15-d-old roots (STAGE 5/6). (d, e) The *MYB84* and the *ANAC78* reporters lines were crossed to the W131Y line, to outline all cells. (f, j–l) Autofluorescence (excitation wavelength (ex.) 405 nm, emission (em.) 420–460 nm) is used to visualize the phellem. (a, d) *MYB84* is specifically expressed in the periderm of the hypocotyl (a) and the root (d). (b, e) *ANAC78* is expressed in the phellem and the phloem of the hypocotyl (b) and the root (e). (c, f) *HORST* is expressed in the phellem of the hypocotyl (c) and the root (f). (g, j) *KCR1* is expressed in the phellem of the hypocotyl (g) and the root (j). (h, k) DAISY is expressed in the phellem of the hypocotyl (h) and the root (k). (i, l) *RALPH* is expressed in the phellem of the hypocotyl (i) and root (l). Bars: (d–f, j–l) 50 μm; (a–c, g–i) 100 μm.

periderm barrier properties. It offers protection against pathogens (Lulai & Corsini, 1998; Thangavel *et al.*, 2016) and it reduces water and solute losses (Beisson *et al.*, 2007). For instance, a somaclonal variant of potato resistant to pathogenic *Streptomyces* is characterized by an increased number of phellem cell layers and suberin deposition (Thangavel *et al.*, 2016).

As in trees, in Arabidopsis, the phellem is highly suberized and many of the genes coding for suberin biosynthesis enzymes are expressed in this tissue (Molina *et al.*, 2009; Vishwanath *et al.*, 2013) (this work) and therefore can be used as reporters for the phellem. Similarly, we show that Arabidopsis phellem is also lignified and it undergoes a maturation process that results in an increase of cell volume and ultimately in cell death, keeping a constant number of phellem cell layers. In summary, Arabidopsis can be used in pioneering works to study phellem biology in response to biotic and abiotic stresses for breeding programs.

Only a few transcription factors are known to regulate phellogen and phellem production in trees. Remarkably they are also expressed in Arabidopsis, suggesting a conserved gene core that controls periderm growth. Among them, *QsMYB1/MYB84/RAX3* is upregulated in the phellem of cork oak upon heat and drought stress (Almeida *et al.*, 2013b) and it also accumulates in the poplar phellem (Rains *et al.*, 2017). In Arabidopsis, it was previously reported that *MYB84/RAX3* regulates axillary meristem formation together with its closest homologs *MYB37/RAX1* and *MYB38/RAX2* (Muller *et al.*, 2006) and it may control lateral root formation (Feng *et al.*, 2004). The specific expression pattern and conservation among species renders *MYB84/RAX3* a good marker to study periderm development and it will be interesting to further study its function in the Arabidopsis root.

PCD shapes periderm growth

Many plant developmental programs, for example xylem vessel and anther differentiation, involve a step of PCD (Olvera-Carrillo *et al.*, 2015). Here, we reveal that PCD is a crucial event during periderm development. As the periderm arises from the pericycle to become the outer protective barrier, the epidermis, the cortex and the endodermis have to accommodate periderm growth and are finally removed. This process follows a predetermined pattern and includes two independent mechanisms: PCD and abscission.

In the root, the endodermis undergoes PCD, whereas the epidermis and the cortex break and are abscised from the periderm. Consistently a set of genes, identified as developmental PCD markers (Olvera-Carrillo *et al.*, 2015), were expressed exclusively in the endodermis and the phellem (which is also dying) and the epidermis and cortex were still alive when they become detached from the periderm. Endodermal PCD is a gradual event as it does not occur in all endodermal cells at the same time and it is preceded by a reduction in cell length and suberin deposition. Remarkably, in the hypocotyl both the endodermis and the inner cortex undergo PCD sequentially, whereas the outer cortex and the epidermis are detached. PCD starts in the endodermal cells located at the phloem poles, it expands to the neighboring endodermal cells, it then occurs in the endodermal cells at the xylem poles and finally it reaches the inner cortex. These successive steps suggest a complex mechanism of regulation and communication between tissues. Mechanical tensions may play a key role, as suggested by the elliptical shapes of the hypocotyl. In fact, the phloem poles (where PCD starts) can be considered as the foci of the ellipse. Future studies directed to the alteration of the physical/chemical properties of the cell walls of the outer tissues may highlight the mechanical regulation of this process. Moreover, the cortex in the hypocotyl represents the ideal cell type to study this communication aspect because the two cell layers of the same tissue (same cell identity) share different fates: the inner cortex undergoes PCD while the outer cortex is abscised.

Acknowledgements

L.R. is indebted to the Baden-Württemberg Stiftung for financial support of this research project by the Elite program for Postdocs. This work was supported by the DFG (grant RA-2590/1-1). We thank Marja Timmermans for critical reading of the manuscript.

Author contributions

A.W. and L.R. designed the research; A.W., D.R., A.B-J., S.M., K.S., M.B.T. and L.R. performed the experiments; A.W., A.B-J. and L.R. analyzed and discussed the data; L.R. wrote the paper with the help of A.W. and A.B-J.

ORCID

Azahara Barra-Jimenez http://orcid.org/0000-0002-4676-2436
Laura Ragni http://orcid.org/0000-0002-3651-8966

References

Agusti J, Lichtenberger R, Schwarz M, Nehlin L, Greb T. 2011. Characterization of transcriptome remodeling during cambium formation identifies *MOL1* and *RUL1* as opposing regulators of secondary growth. *PLoS Genetics* **7**: e1001312.

Alassimone J, Naseer S, Geldner N. 2010. A developmental framework for endodermal differentiation and polarity. *Proceedings of the National Academy of Sciences, USA* **107**: 5214–5219.

Almeida T, Menendez E, Capote T, Ribeiro T, Santos C, Goncalves S. 2013a. Molecular characterization of *Quercus suber* MYB1, a transcription factor up-regulated in cork tissues. *Journal of Plant Physiology* **170**: 172–178.

Almeida T, Pinto G, Correia B, Santos C, Goncalves S. 2013b. *QsMYB1* expression is modulated in response to heat and drought stresses and during plant recovery in *Quercus suber*. *Plant Physiology and Biochemistry* **73**: 274–281.

Altamura MM, Possenti M, Matteucci A, Baima S, Ruberti I, Morelli G. 2001. Development of the vascular system in the inflorescence stem of *Arabidopsis*. *New Phytologist* **151**: 381–389.

Barberon M, Vermeer JE, De Bellis D, Wang P, Naseer S, Andersen TG, Humbel BM, Nawrath C, Takano J, Salt DE *et al.* 2016. Adaptation of root function by nutrient-induced plasticity of endodermal differentiation. *Cell* **164**: 447–459.

Barbier de Reuille P, Ragni L. 2017. Vascular morphodynamics during secondary growth. *Methods in Molecular Biology* **1544**: 103–125.

Barra-Jimenez A, Ragni L. 2017. Secondary development in the stem: when Arabidopsis and trees are closer than it seems. *Current Opinion in Plant Biology* **35**: 145–151.

Beisson F, Li Y, Bonaventure G, Pollard M, Ohlrogge JB. 2007. The acyltransferase GPAT5 is required for the synthesis of suberin in seed coat and root of *Arabidopsis*. *Plant Cell* **19**: 351–368.

Caritat A, Gutiérrez E, Molinas M. 2000. Influence of weather on cork-ring width. *Tree Physiology* **20**: 893–900.

Compagnon V, Diehl P, Benveniste I, Meyer D, Schaller H, Schreiber L, Franke R, Pinot F. 2009. CYP86B1 is required for very long chain omega-hydroxyacid and alpha, omega-dicarboxylic acid synthesis in root and seed suberin polyester. *Plant Physiology* **150**: 1831–1843.

Cordeiro N, Belgacem MN, Gandini A, Pascoal Neto C. 1999. Urethanes and polyurethanes from suberin 2: synthesis and characterization. *Industrial Crops and Products* **10**: 1–10.

Davin N, Edger PP, Hefer CA, Mizrachi E, Schuetz M, Smets E, Myburg AA, Douglas CJ, Schranz ME, Lens F. 2016. Functional network analysis of genes differentially expressed during xylogenesis in *soc1ful* woody Arabidopsis plants. *Plant Journal* **86**: 376–390.

Demura T, Ye Z-H. 2010. Regulation of plant biomass production. *Current Opinion in Plant Biology* **13**: 298–303.

Di Laurenzio L, Wysocka-Diller J, Malamy JE, Pysh L, Helariutta Y, Freshour G, Hahn MG, Feldmann KA, Benfey PN. 1996. The *SCARECROW* gene regulates an asymmetric cell division that is essential for generating the radial organization of the Arabidopsis root. *Cell* **86**: 423–433.

Domergue F, Vishwanath SJ, Joubès J, Ono J, Lee JA, Bourdon M, Alhattab R, Lowe C, Pascal S, Lessire R *et al.* 2010. Three Arabidopsis fatty acyl-coenzyme A reductases, FAR1, FAR4, and FAR5, generate primary fatty alcohols associated with suberin deposition. *Plant Physiology* **153**: 1539–1554.

Esau K. 1977. *Anatomy of seed plants*. New York, NY, USA: John Wiley & Sons.

Etchells JP, Mishra LS, Kumar M, Campbell L, Turner SR. 2015. Wood formation in trees is increased by manipulating PXY-regulated cell division. *Current Biology* **25**: 1050–1055.

Fagerstedt KV, Saranpaa P, Tapanila T, Immanen J, Serra JA, Nieminen K. 2015. Determining the composition of lignins in different tissues of silver birch. *Plants* **4**: 183–195.

Fendrych M, Van Hautegem T, Van Durme M, Olvera-Carrillo Y, Huysmans M, Karimi M, Lippens S, Guerin CJ, Krebs M, Schumacher K *et al.* 2014. Programmed cell death controlled by ANAC033/SOMBRERO determines root cap organ size in *Arabidopsis*. *Current Biology* **24**: 931–940.

Feng C, Andreasson E, Maslak A, Mock HP, Mattsson O, Mundy J. 2004. Arabidopsis MYB68 in development and responses to environmental cues. *Plant Science* **167**: 1099–1107.

Geldner N, Denervaud-Tendon V, Hyman DL, Mayer U, Stierhof YD, Chory J. 2009. Rapid, combinatorial analysis of membrane compartments in intact plants with a multicolor marker set. *Plant Journal* **59**: 169–178.

de Geus M, van der Meulen I, Goderis B, van Hecke K, Dorschu M, van der Werff H, Koning CE, Heise A. 2010. Performance polymers from renewable monomers: high molecular weight poly(pentadecalactone) for fiber applications. *Polymer Chemistry* **1**: 525.

Ginzberg I, Barel G, Ophir R, Tzin E, Tanami Z, Muddarangappa T, de Jong W, Fogelman E. 2009. Transcriptomic profiling of heat-stress response in potato periderm. *Journal of Experimental Botany* **60**: 4411–4421.

Groh B, Hubner C, Lendzian KJ. 2002. Water and oxygen permeance of phellems isolated from trees: the role of waxes and lenticels. *Planta* **215**: 794–801.

Hirakawa Y, Bowman JL. 2015. A role of TDIF peptide signaling in vascular cell differentiation is conserved among euphyllophytes. *Frontiers in Plant Science* **6**: 1048.

Hofer R, Briesen I, Beck M, Pinot F, Schreiber L, Franke R. 2008. The Arabidopsis cytochrome P450 CYP86A1 encodes a fatty acid omega-hydroxylase involved in suberin monomer biosynthesis. *Journal of Experimental Botany* **59**: 2347–2360.

Hosmani PS, Kamiya T, Danku J, Naseer S, Geldner N, Guerinot ML, Salt DE. 2013. Dirigent domain-containing protein is part of the machinery required for formation of the lignin-based Casparian strip in the root. *Proceedings of the National Academy of Sciences, USA* **110**: 14498–14503.

Khanal BP, Grimm E, Knoche M. 2013. Russeting in apple and pear: a plastic periderm replaces a stiff cuticle. *AoB Plants* **5**: pls048.

Kosma DK, Molina I, Ohlrogge JB, Pollard M. 2012. Identification of an Arabidopsis fatty alcohol:caffeoyl-coenzyme A acyltransferase required for the synthesis of alkyl hydroxycinnamates in root waxes. *Plant Physiology* **160**: 237–248.

Kosma DK, Rice A, Pollard M. 2015. Analysis of aliphatic waxes associated with root periderm or exodermis from eleven plant species. *Phytochemistry* **117**: 351–362.

Kucukoglu M, Nilsson J, Zheng B, Chaabouni S, Nilsson O. 2017. *WUSCHEL-RELATED HOMEOBOX4* (*WOX4*)-like genes regulate cambial cell division activity and secondary growth in *Populus* trees. *New Phytologist* **215**: 642–657.

Lampropoulos A, Sutikovic Z, Wenzl C, Maegele I, Lohmann JU, Forner J. 2013. GreenGate – a novel, versatile, and efficient cloning system for plant transgenesis. *PLoS ONE* **8**: e83043.

Lendzian KJ. 2006. Survival strategies of plants during secondary growth: barrier properties of phellems and lenticels towards water, oxygen, and carbon dioxide. *Journal of Experimental Botany* **57**: 2535–2546.

Liberman LM, Sparks EE, Moreno-Risueno MA, Petricka JJ, Benfey PN. 2015. MYB36 regulates the transition from proliferation to differentiation in the Arabidopsis root. *Proceedings of the National Academy of Sciences, USA* **112**: 12099–12104.

Lourenco A, Rencoret J, Chemetova C, Gominho J, Gutierrez A, Del Rio JC, Pereira H. 2016. Lignin composition and structure differs between xylem, phloem and phellem in *Quercus suber* L. *Frontiers in Plant Science* **7**: 1612.

Lulai EC, Corsini DL. 1998. Differential deposition of suberin phenolic and aliphatic domains and their roles in resistance to infection during potato tuber (*Solanum tuberosum* L.) wound-healing. *Physiological and Molecular Plant Pathology* **53**: 209–222.

Lulai EC, Freeman TP. 2001. The importance of phellogen cells and their structural characteristics in susceptibility and resistance to excoriation in immature and mature potato tuber (*Solanum tuberosum* L.) periderm. *Annals of Botany* **88**: 555–561.

Marques AV, Pereira H. 2013. Lignin monomeric composition of corks from the barks of *Betula pendula*, *Quercus suber* and *Quercus cerris* determined by Py–GC–MS/FID. *Journal of Analytical and Applied Pyrolysis* **100**: 88–94.

Marques-Bueno MDM, Morao AK, Cayrel A, Platre MP, Barberon M, Caillieux E, Colot V, Jaillais Y, Roudier F, Vert G. 2016. A versatile Multisite Gateway-compatible promoter and transgenic line collection for cell type-specific functional genomics in Arabidopsis. *Plant Journal* **85**: 320–333.

Mazur E, Kurczynska E. 2012. Rays, intrusive growth, and storied cambium in the inflorescence stems of *Arabidopsis thaliana* (L.) Heynh. *Protoplasma* **249**: 217–220.

Melzer S, Lens F, Gennen J, Vanneste S, Rohde A, Beeckman T. 2008. Flowering-time genes modulate meristem determinacy and growth form in *Arabidopsis thaliana*. *Nature Genetics* **40**: 1489–1492.

Miguel A, Milhinhos A, Novak O, Jones B, Miguel CM. 2016. The SHORT-ROOT-like gene PtSHR2B is involved in *Populus* phellogen activity. *Journal of Experimental Botany* **67**: 1545–1555.

Molina I, Li-Beisson Y, Beisson F, Ohlrogge JB, Pollard M. 2009. Identification of an Arabidopsis feruloyl-coenzyme a transferase required for suberin synthesis. *Plant Physiology* **151**: 1317–1328.

Muller D, Schmitz G, Theres K. 2006. *Blind* homologous *R2R3 Myb* genes control the pattern of lateral meristem initiation in *Arabidopsis*. *Plant Cell* **18**: 586–597.

Naseer S, Lee Y, Lapierre C, Franke R, Nawrath C, Geldner N. 2012. Casparian strip diffusion barrier in *Arabidopsis* is made of a lignin polymer without suberin. *Proceedings of the National Academy of Sciences, USA* **109**: 10101–10106.

Neubauer JD, Lulai EC, Thompson AL, Suttle JC, Bolton MD. 2012. Wounding coordinately induces cell wall protein, cell cycle and pectin methyl esterase genes involved in tuber closing layer and wound periderm development. *Journal of Plant Physiology* **169**: 586–595.

Neubauer JD, Lulai EC, Thompson AL, Suttle JC, Bolton MD, Campbell LG. 2013. Molecular and cytological aspects of native periderm maturation in potato tubers. *Journal of Plant Physiology* **170**: 413–423.

Olvera-Carrillo Y, Van Bel M, Van Hautegem T, Fendrych M, Huysmans M, Simaskova M, van Durme M, Buscaill P, Rivas S, Coll NS *et al.* 2015. A conserved core of programmed cell death indicator genes discriminates developmentally and environmentally induced programmed cell death in plants. *Plant Physiology* **169**: 2684–2699.

Oven P, Torelli N, Shortle WC, Zupančič M. 1999. The formation of a ligno-suberised layer and necrophylactic periderm in beech bark (*Fagus sylvatica* L.). *Flora* **194**: 137–144.

Pereira H. 1988. Chemical composition and variability of cork from *Quercus suber* L. *Wood Science and Technology* **22**: 211–218.

Pereira H. 2007. *Cork biology production and uses*. Amsterdam, the Netherlands: Elsevier.

Pinto PCRO, Sousa AF, Silvestre AJD, Neto CP, Gandini A, Eckerman C, Holmbom B. 2009. *Quercus suber* and *Betula pendula* outer barks as renewable sources of oleochemicals: a comparative study. *Industrial Crops and Products* **29**: 126–132.

Rains MK, Gardiyehewa de Silva ND, Molina I. 2017. Reconstructing the suberin pathway in poplar by chemical and transcriptomic analysis of bark tissues. *Tree Physiology* **1**: 1–22.

Roppolo D, De Rybel B, Denervaud Tendon V, Pfister A, Alassimone J, Vermeer JE, Yamazaki M, Stierhof YD, Beeckman T, Geldner N. 2011. A novel protein family mediates Casparian strip formation in the endodermis. *Nature* **473**: 380–383.

Sabba RP, Lulai EC. 2002. Histological analysis of the maturation of native and wound periderm in potato (*Solanum tuberosum* L.) tuber. *Annals of Botany* **90**: 1–10.

Sabba RP, Lulai EC. 2005. Immunocytological analysis of potato tuber periderm and changes in pectin and extensin epitopes associated with periderm maturation. *Journal of the American Society for Horticultural Science* **130**: 936–942.

Schindelin J, Arganda-Carreras I, Frise E, Kaynig V, Longair M, Pietzsch T, Preibisch S, Rueden C, Saalfeld S, Schmid B *et al.* 2012. Fiji: an open-source platform for biological-image analysis. *Nature Methods* **9**: 676–682.

Schreiber L, Franke R, Hartmann K. 2005. Wax and suberin development of native and wound periderm of potato (*Solanum tuberosum* L.) and its relation to peridermal transpiration. *Planta* **220**: 520–530.

Serra O, Hohn C, Franke R, Prat S, Molinas M, Figueras M. 2010. A feruloyl transferase involved in the biosynthesis of suberin and suberin-associated wax is required for maturation and sealing properties of potato periderm. *Plant Journal* **62**: 277–290.

Serra O, Soler M, Hohn C, Franke R, Schreiber L, Prat S, Molinas M, Figueras M. 2009a. Silencing of *StKCS6* in potato periderm leads to reduced chain lengths of suberin and wax compounds and increased peridermal transpiration. *Journal of Experimental Botany* **60**: 697–707.

Serra O, Soler M, Hohn C, Sauveplane V, Pinot F, Franke R, Schreiber L, Prat S, Molinas M, Figueras M. 2009b. *CYP86A33*-targeted gene silencing in potato tuber alters suberin composition, distorts suberin lamellae, and impairs the periderm's water barrier function. *Plant Physiology* **149**: 1050–1060.

Sibout R, Plantegenet S, Hardtke CS. 2008. Flowering as a condition for xylem expansion in *Arabidopsis* hypocotyl and root. *Current Biology* **18**: 458–463.

Silva S, Sabino M, Fernandes E, Correlo V, Boesel L, Reis R. 2005. Cork: properties, capabilities and applications. *International Materials Reviews* **50**: 345–365.

Soler M, Serra O, Fluch S, Molinas M, Figueras M. 2011. A potato skin SSH library yields new candidate genes for suberin biosynthesis and periderm formation. *Planta* **233**: 933–945.

Soler M, Serra O, Molinas M, Huguet G, Fluch S, Figueras M. 2007. A Genomic approach to suberin biosynthesis and cork differentiation. *Plant Physiology* **144**: 419–431.

Spicer R, Groover A. 2010. Evolution of development of vascular cambia and secondary growth. *New Phytologist* **186**: 577–592.

Thangavel T, Tegg RS, Wilson CR. 2016. Toughing it out – disease-resistant potato mutants have enhanced tuber skin defenses. *Phytopathology* **106**: 474–483.

Thomson N, Evert RF, Kelman A. 1995. Wound healing in whole potato tubers: a cytochemical, fluorescence, and ultrastructural analysis of cut and bruise wounds. *Canadian Journal of Botany* **73**: 1436–1450.

Torron S, Semlitsch S, Martinelle M, Johansson M. 2014. Polymer thermosets from multifunctional polyester resins based on renewable monomers. *Macromolecular Chemistry and Physics* **215**: 2198–2206.

Tucker SC. 1975. Wound regeneration in the lamina of magnoliaceous leaves. *Canadian Journal of Botany* **53**: 1352–1364.

Vermeer JE, von Wangenheim D, Barberon M, Lee Y, Stelzer EH, Maizel A, Geldner N. 2014. A spatial accommodation by neighboring cells is required for organ initiation in Arabidopsis. *Science* **343**: 178–183.

Vishwanath SJ, Delude C, Domergue F, Rowland O. 2015. Suberin: biosynthesis, regulation, and polymer assembly of a protective extracellular barrier. *Plant Cell Reports* **34**: 573–586.

Vishwanath SJ, Kosma DK, Pulsifer IP, Scandola S, Pascal S, Joubes J, Dittrich-Domergue F, Lessire R, Rowland O, Domergue F. 2013. Suberin-associated fatty alcohols in Arabidopsis: distributions in roots and contributions to seed coat barrier properties. *Plant Physiology* **163**: 1118–1132.

Vulavala VKR, Fogelman E, Rozental L, Faigenboim A, Tanami Z, Shoseyov O, Ginzberg I. 2017. Identification of genes related to skin development in potato. *Plant Molecular Biology* **94**: 481–494.

Waisel Y. 1995. Developmental and functional aspects of the periderm. In: Iqbal M, ed. *The cambial derivatives*. Stuttgart, Germany: Gebruder Borntraeger Verlagsbuchhandlung, 293–315.

Supporting Information

Additional Supporting Information may be found online in the Supporting Information tab for this article:

Fig. S1 Periderm formation in Arabidopsis.

Fig. S2 Periderm establishment in the hypocotyl and in the root grown under different conditions.

Fig. S3 Stages of periderm development in the hypocotyl of plants grown under different conditions.

Fig. S4 Periderm formation in lateral roots, phelloderm stainings and programmed cell death in the root endodermis.

Fig. S5 Programmed cell death in the hypocotyl during periderm growth.

Fig. S6 Several suberin biosynthesis genes are expressed in the phellem.

Fig. S7 Chemical composition of hypocotyl phellem cells.

Please note: Wiley Blackwell are not responsible for the content or functionality of any Supporting Information supplied by the authors. Any queries (other than missing material) should be directed to the *New Phytologist* Central Office.

***New Phytologist* Supporting Information**

Article title: A molecular framework to study periderm formation in *Arabidopsis*.

Authors: Anna Wunderling, Dagmar Ripper, Azahara Barra-Jimenez, Stefan Mahn, Kathrin Sajak, Mehdi Ben Targem, Laura Ragni.

Article acceptance date: 19th February 2018

The following Supporting Information is available for this article:

Fig. S1 Periderm formation in *Arabidopsis*.
Fig. S2 Periderm establishment in the hypocotyl and in the root grown under different conditions.
Fig. S3 Stages of periderm development in the hypocotyl of plants grown under different conditions.
Fig. S4 Periderm formation in lateral roots, phelloderm stainings and programmed cell death in the root endodermis.
Fig. S5 Programmed cell death in the hypocotyl during periderm growth.
Fig. S6 Several suberin biosynthesis genes are expressed in the phellem.
Fig. S7 Chemical composition of hypocotyl phellem cells.

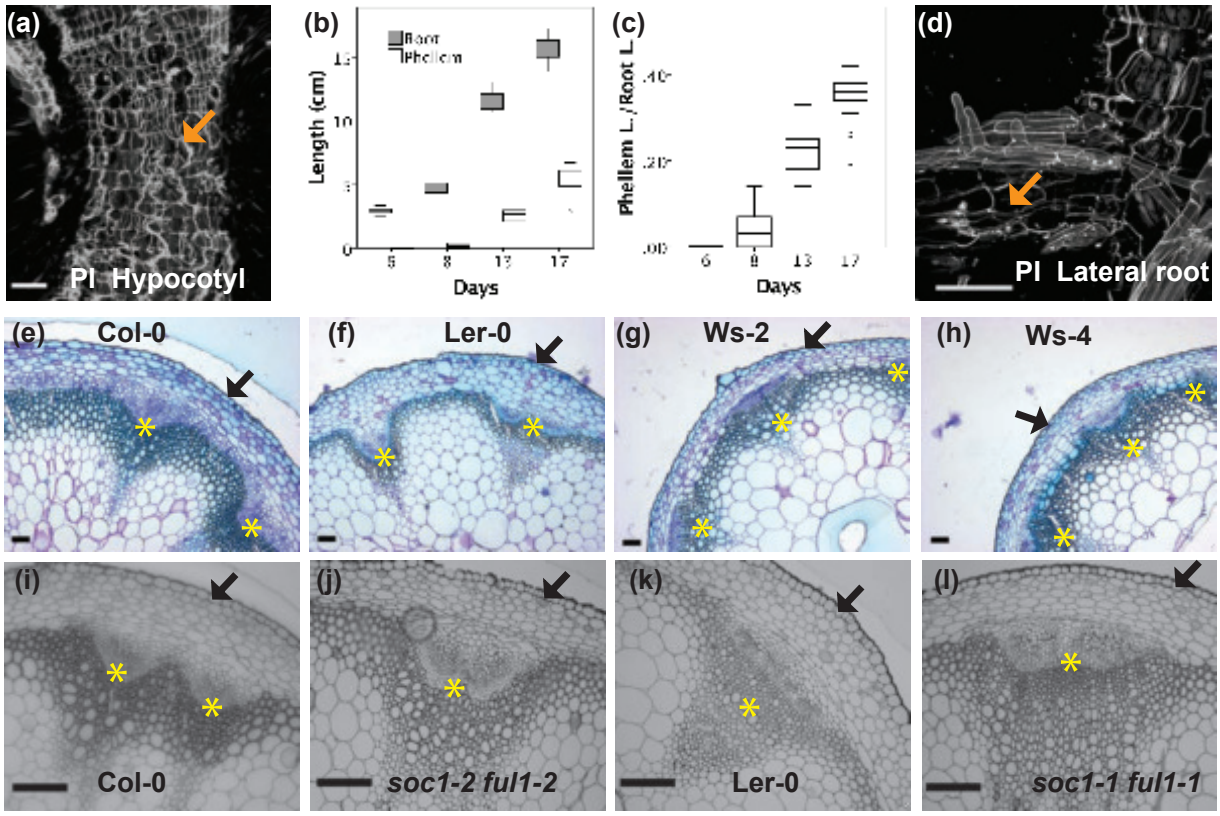

Fig. S1 Periderm formation in *Arabidopsis*.

(a) 3D reconstruction of a Z-stack of a 25-day-old hypocotyl stained with PI. PI stains the outer side of phellem cells (as it does not penetrate the phellem). Phellem cells (orange arrow) cover the hypocotyl entirely. (b) A periderm is formed in the uppermost part of the root. Quantification of root length and phellem length in Col-0 plants at different days after sowing (das) *(in vitro*; continuous light) (6 das n=17; 8 das n=17; 13 das n=17; 17 das n=18). (c) Periderm extension can be quantified as the ratio of phellem length/ root length. Ratio of phellem length/ root length of b. (d) 3D reconstruction of a Z-stack of a 25-day-old root stained with PI showing a primary and a lateral root. Phellem cells (orange arrow) cover both the lateral and primary root. (e-h) Plastic cross-sections of the base of 3-month-old stems. Plants were grown in soil under long day conditions (LD). (e) Col-0. (f) Ler-0. (g) Ws-2. (h) Ws-4. A periderm is not formed and the epidermis is still visible (black arrow). (i-l) Plastic cross-sections of the stem base: (i) Col-0 (3-month-old), (j) *soc1-2 ful1-2* (6-month-old), (k) Ler-0 (3-month-old) and (l) *soc1-1 ful1-1* (3-month-old). Plants were grown in soil LD. A periderm is not even formed in *soc1 ful1* double

mutants (epidermis: black arrow). White and black scale bar: 100µm. Yellow asterisk: vascular bundle.

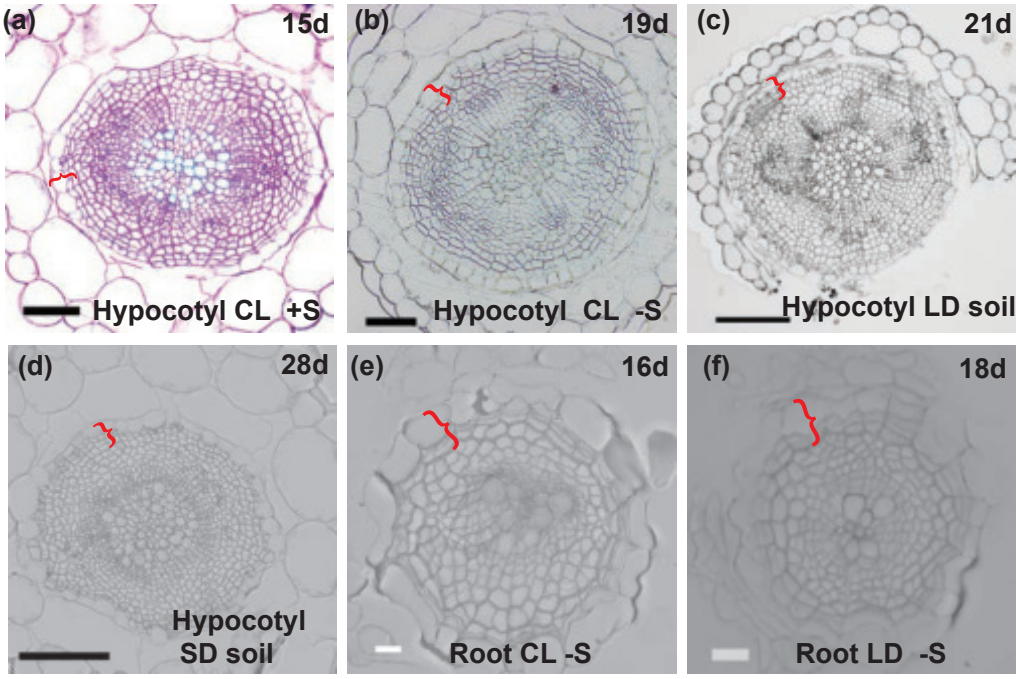

(g)

Conditions	Flowering time	Periderm
CL; *in vitro* (1/2MS with 1% sugar)	20-21d	At 10-12d in the uppermost part of the root, the phellem is the outer tissue. In the hypocotyl, a ring of phellem cells is already present at 15d.
LD; soil	30-32d	In the hypocotyl, a ring of phellem cells is already present at 21d.
SD; soil	More than 42d	In the hypocotyl, a ring of phellem cells is already present at 28d.

Fig. S2 Periderm establishment in the hypocotyl and in the root grown under different conditions.

(a-d) Plastic cross-sections of Col-0 hypocotyls grown under different conditions. (a) *In vitro* on 1/2 MS agar with 1% sugar under continuous light (CL). (b) *In vitro* on 1/2 MS agar (without sugar) under CL. (c) On soil under long day (LD). (d) On soil under short day (SD). (e-f) Plastic cross-sections of Col-0 roots grown under different conditions. (e) *In vitro* on 1/2 MS agar (without sugar) under CL. (f) *In vitro* on 1/2 MS agar (without sugar) under LD. (g) Table of flowering time and periderm formation. The periderm is established before flowering. Black scale bar: 100µm, white scale bar: 20µm. Red bracket: periderm.

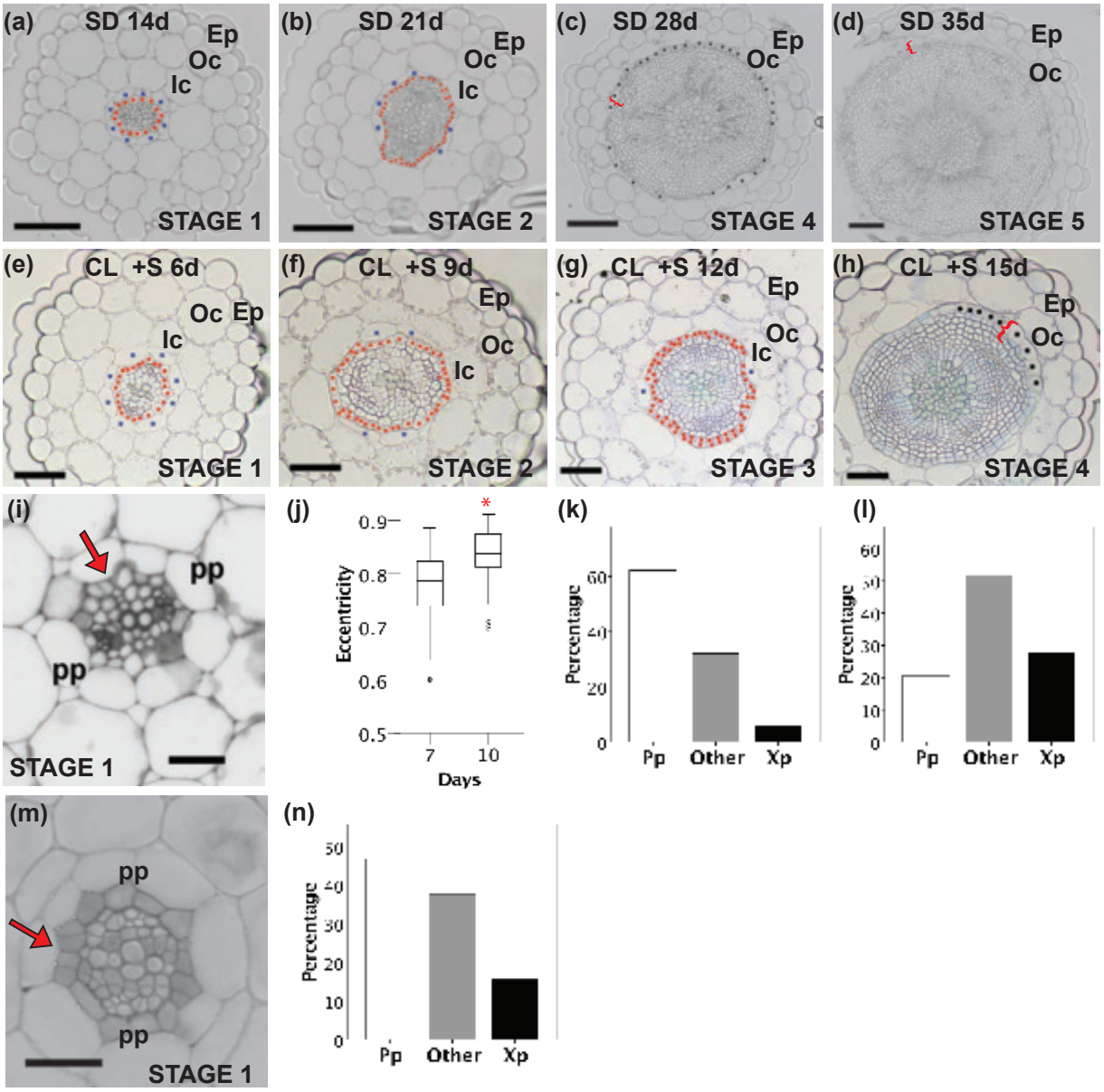

Fig. S3 Stages of periderm development in the hypocotyl of plants grown under different conditions.

(a-d) Plastic cross-sections of hypocotyls grown in soil under short day (SD) conditions at different time points. (a) 14-day-after-sowing (das)/STAGE 1. (b) 21das/STAGE 2. (c) 28 das/STAGE 4. (d) 35 das/STAGE 5. (e-h) Plastic cross-sections of hypocotyls grown *in vitro* on 1/2 MS with 1% sugar under continuous light (CL) at different time points. (e) 6-day-old/STAGE 1. (f) 9-day-old/STAGE 2. (g) 12-day-old/STAGE 3. (h) 15-day-old/STAGE4. Red bracket: periderm, red dot: pericycle/phellogen, blue square: endodermis, black square: phellem,

Ep: epidermis, Oc: outer cortex, Ic: inner cortex. (i) Plastic cross-section of a 4 day-old hypocotyl at STAGE 1 showing that the first pericycle divisions occur at the xylem poles (red arrow, pp: phloem poles). (j) Quantification of the eccentricity of endodermal cells of 7-day-old and 10-day-old hypocotyls (soil; long day) Welch's t-test (red asterisk: p=<0.001; n=120-128). (k) Quantification of the occurrence of PCD in the inner cortex at different positions. We defined 8 possible positions in the hypocotyl: 2 phloem poles (Pp), 2 xylem poles (Xp) and 4 in between poles positions (Other), thus in a random distribution, we expect 25% at Pp, 50% at Other and 25% at Xp Cross-sections from independent experiments from plants grown under different conditions were used for the quantification (n=106). (l) Quantification of the position of cortex and epidermis breaking in the hypocotyl performed as in k (n=56). (m) Cross-section of a 14-day-old root at STAGE 1 showing that the first pericycle divisions occur at the xylem poles (red arrow, pp: phloem poles). (n) Quantification of the occurrence of PCD in the root endodermis at different positions, performed as in k (n= 77). Black scale bar: 100µm, white scale bar: 20µm.

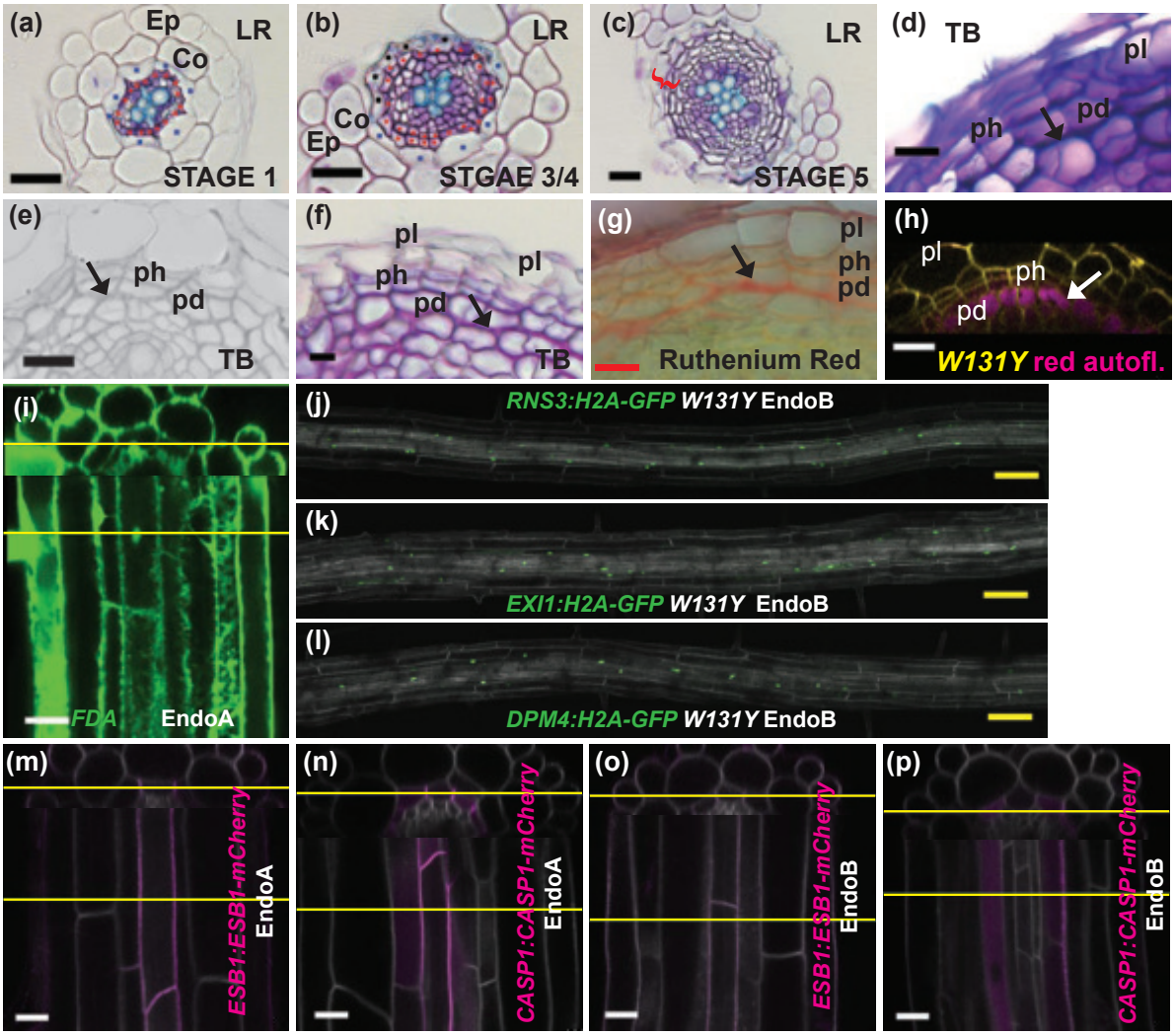

Fig. S4 Periderm formation in lateral roots, phelloderm stainings and programmed cell death in the root endodermis.

(a-c) Periderm formation in lateral roots occurs like in the main root and it is possible to identify the same stages. Plastic cross-sections of an old lateral root (LR) from a 25-day-old plant (1/2MS 1% sugar continuous light (CL)) stained with Toludine Blue (TB). Red bracket: periderm, red dot: pericycle/phellogen, blue square: endodermis, black square: phellem, Ep: epidermis, Co: cortex. (d) Vibratome section of the uppermost part of a 24-day-old root stained with TB. (e-f) Plastic sections of the uppermost part of 16-17-old-day roots stained with TB ((e) black and white picture; (f) color picture). (g) Vibratome section of the uppermost part of a 24-day-old root stained with Ruthenium Red. (h) Orthoview of a Z-stack of a 17-day-old root. Autofluorescence

in the red spectrum (ex. 561nm; em. 570-630nm; white arrow) and reporter line *W131Y*. The black arrow indicates the presumptive phelloderm-to-phloem border. pl: phellem ph: phellogen and pd: phelloderm. (i) Cross and longitudinal sections (Ortho View of a Z-stack) of a 13-day-old root stained with FDA in the region of the endodermis where lateral root are emerged (EndoA). FDA stains the epidermis, the cortex, the endodermis and the pericycle. (j) *RNS3:H2A-GFP W131Y*. (k) *EXI1:H2A-GFP W131Y*. (l) *DPM4:H2A-GFP W131Y*. (j-l) Confocal images of 12-day-old roots. Developmental programmed cell death (PCD) markers are expressed broadly in the endodermis at STAGE1 (EndoB: region of the root prior to endodermis PCD). (m-o) Cross and longitudinal sections (Ortho View of a Z-stack) of 12-day-old roots. Expression of ESB1:ESB1-mCherry (m-o) and CASP1:CASP1-mCherry (n-p) in the region of the endodermis where lateral root are emerged (m and n; EndoA) and in the region prior to endodermis PCD (o and p; EndoB). White and black scale bar: 20µm, red scale bar: 25µm and yellow scale bar: 100 µm.

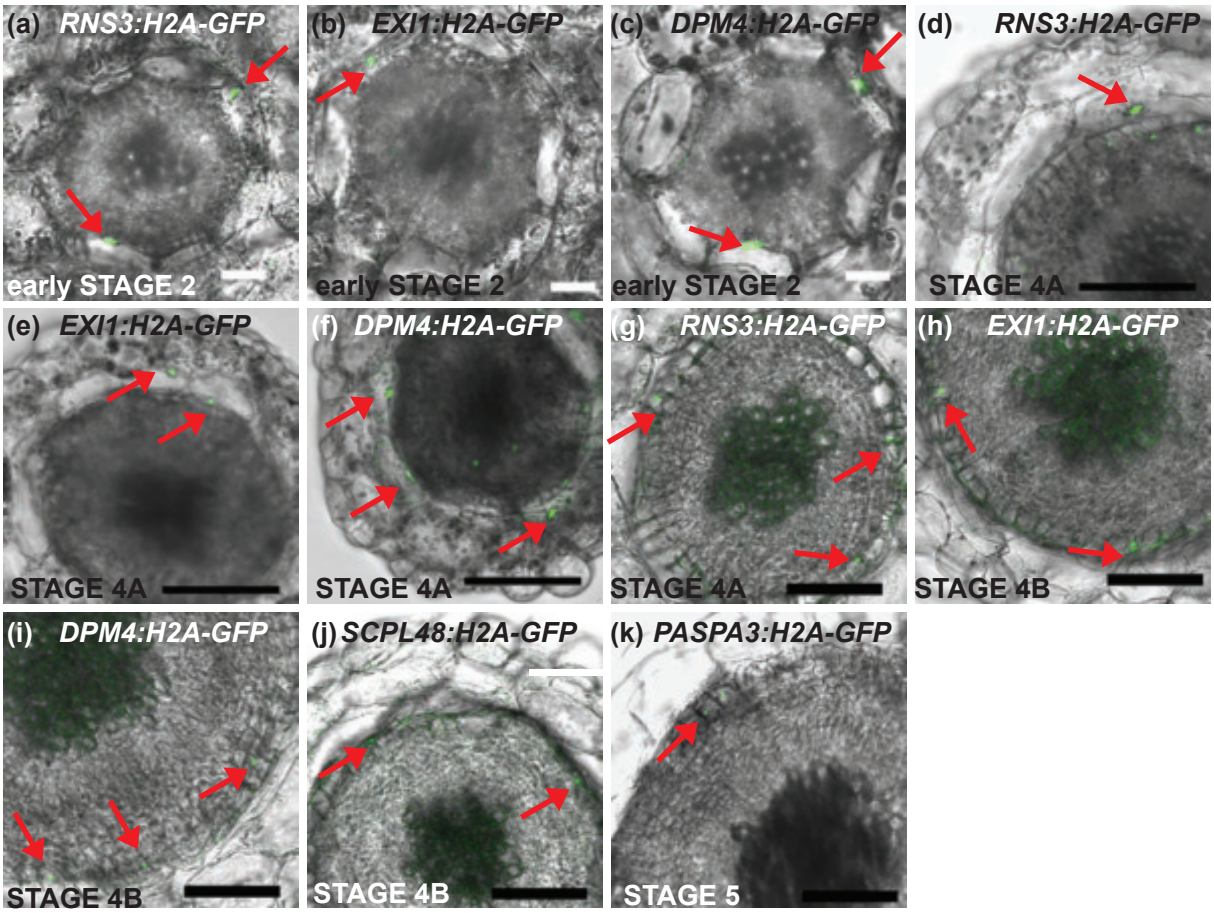

Fig. S5 Programmed cell death in the hypocotyl during periderm growth. (a-k) Developmental programmed cell death (PCD) markers are expressed (red arrows) in the endodermis (a-c), in the inner cortex (d-f) and in the phellem (g-k) in the hypocotyl prior to PCD. Vibratome sections of the hypocotyl of *RNS3:H2A-GFP* (a,d,g), *EXI1:H2A-GFP* (b,e,h) and *DPM4:H2A-GFP* (c,f,i) at 12, 18 and 21 das respectively. Vibratome sections of the hypocotyl of *SCPL48:H2A-GFP* (j) and *PASPA3:H2A-GFP* (k) at 21 das. White scale bar: 20µm, black scale bar: 100µm.

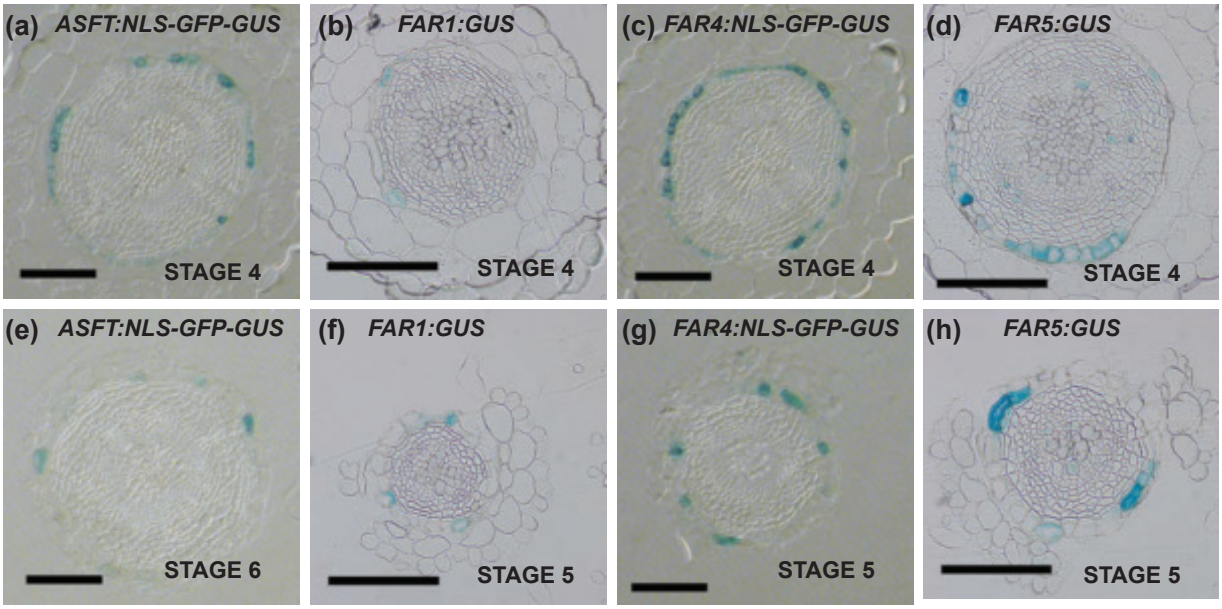

Fig. S6 Several suberin biosynthesis genes are expressed in the phellem.

Plastic cross-sections of GUS staining of 17-day-old hypocotyls (a-d) and roots (e-h). Plants were grown in vitro on 1/2MS with 1% sugar under continuous light. (a,e) *ASFT:NLS-GFP-GUS*. (b,f) *FAR1:GUS*. (c,g) *FAR4:NLS-GFP-GUS*. (d,h) *FAR5:GUS*. Black scale bar: 100µm.

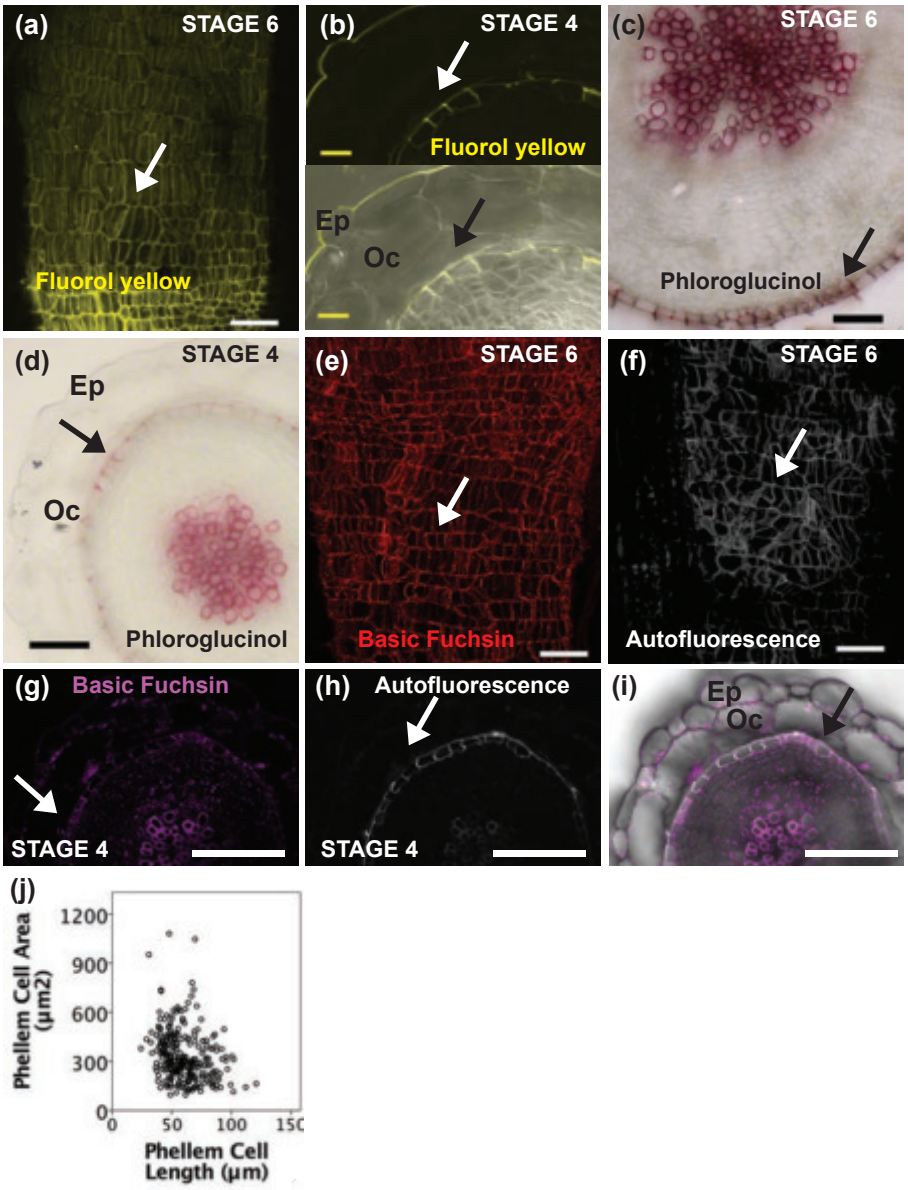

Fig. S7 Chemical composition of hypocotyl phellem cells.

(a,c,e-f) 35-day-old hypocotyls at STAGE 6 of periderm development. Plants were grown in soil under long day conditions. (b,d,g-i) Hypocotyls at STAGE 4 of periderm development. Vibratome sections of 19-day-old plants. (a,e-f) 3D reconstruction of a Z–stack. (a-b) Fluorol yellow (FY) staining shows suberin deposition in phellem cells. (b) Confocal image of FY staining. Upper panel: FY channel, Lower panel: overlay of the transmitted light and FY channels (c-d) Vibratome sections stained with Phloroglucinol (lignin staining, purple coloration). (e,g) Basic Fuchsin staining shows lignin deposition in phellem cells. (f,h)

Autofluorescence (ex. 405nm; em. 420-500nm) of phellem cells. (g-i) Confocal images of Basic Fuchsin staining. (g) Basic Fuchsin channel. (h) Autofluorescence channel. (i) Overlay of the autofluorescence, transmitted light and Basic Fuchsin channels. (j) Plot of phellem cell length *vs.* phellem cell area. White bar: 100µm, black scale bar: 50µm and yellow scale bar: 20µm. The black and the white arrows indicate phellem cells. Ep: epidermis, Oc: outer cortex.

9.3 Auxin signaling regulates the periderm development in *Arabidopsis thaliana*

Anna Wunderling, Dagmar Ripper, Stefan Mahn, Joop Vermeer, Laura Ragni

unsubmitted

Title: Auxin signaling regulates periderm development in *Arabidopsis thaliana*

Authors: Anna Wunderling[1], Dagmar Ripper[1], Stefan Mahn, Joop Vermeer, [2] Laura Ragni[1,3].

Affiliations:

[1]ZMBP- Center for Plant Molecular Biology, University of Tübingen, Auf der Morgenstelle 32, D-72076 Tübingen, Germany

[2] University of Zurich, Switzerland

[3] Corresponding author: laura.ragni@zmbp.uni-tuebingen.de +49 (0)7071 - 29 76677

Word count for each section, number of figure and supplemental information:

Total word count of the Main body	4510	**N. of figures in color**	7
Summary	104	**N. of tables**	0
Introduction	895	**N. of supplemental figures**	4
Material and methods	596		
Results	1994		
Discussion	892		
Acknowledgments	29		

Summary

- The periderm surrounds the vascular cylinder and acts as the first line of defense during secondary growth.
- Auxin accumulates in the phellogen and auxin signaling is required for periderm formation.
- Both Lateral roots (LR) and the phellogen arise from the pericycle and many LR regulators are expressed during periderm development and mutants in early LR regulators such as *IAA28*, *GATA23*, *ARF7 ARF19* display altered periderm formation.
- However, a periderm can be formed even in the absence of LRs and LRs can develop in plants with an impaired periderm although both organs arise from the pericycle.
- Periderm development and lateral root formation are competing processes.

Keywords: *Arabidopsis*, Endodermis, Periderm, Phellem, Secondary growth, Lateral root formation, Auxin.

Introduction

The periderm surrounds the vascular cylinder and acts as the first line of defense of plants during secondary growth. It is formed by a lateral meristem, the phellogen/ cork cambium, that divides in a bidirectional manner to produce inwards the phelloderm cells and outwards the phellem/cork cells (Esau, 1977). These three tissues together are referred to as the periderm. Likewise the epidermis during the primary development, the periderm is a protection against biotic and abiotic stress during secondary growth. It effectively restricts gas exchange, water loss and pathogen infestation (Groh *et al.*, 2002; Lendzian, 2006; Lulai and Freeman, 2001).

Stems, branches, and roots of most woody eudicotyledons, and gymnosperms develop a periderm that replaces the epidermis once it can no longer accommodate to radial growth. Also underground stems such as the potato tuber can form a periderm. In the herbaceous model plant species Arabidopsis, a periderm is present in the mature main root, lateral roots and the hypocotyl, whereas it has not been reported in stems (Wunderling et al. 2018). Periderm development can be followed along the same root as it represents a gradient of secondary growth. Root periderm of most plant species including Arabidopsis arises from the pericycle, an inner tissue that is surrounded by several cell layers (ground tissues and epidermis), and becomes the external tissue protecting the vasculature (Wunderling et al., 2018; Esau, 1977). In Arabidopsis, we recently described 5 distinct stages of periderm development taking also in consideration the fate of the epidermis, cortex and endodermis. For instance, the endodermis undergoes programmed cell death during stage 2 whereas the epidermis and the cortex break during stage 3/4 and are abscised from the root in stage 5. At maturity (stage 6) the periderm consists of three to four cell layers comprising the phellem, the phellogen and one layer of phelloderm cells. Upon periderm formation the endodermis undergoes PCD while the epidermis and the cortex/outer cortex are abscised from the root.

Periderm development shares some mutual characteristics with lateral root (LR) formation however it is not known whether they share the same regulatory networks. LRs and the periderm both arise from the pericycle (Wunderling et al., 2018; Malamy and Benfey, 1997) and cell elimination contributes to organ growth during both processes. Endodermal cells undergo PCD during periderm development (Wunderling et al., 2018) and similarly during LR emergence, some LR primordia- overlying endodermal cells undergo cell death (Escamez et al., 2018).

LRs are formed from xylem pole pericycle cells, the so-called founder cells (Malamy and Benfey, 1997). The LR founder cells are primed by auxin (De Smet et al., 2007; Moreno-

Risueno et al., 2010; Van Norman et al., 2013) and auxin plays a critical root during the lateral root development (Lavenus et al., 2013).

Different auxin signaling modules, consisting of Aux/ INDOLE-3-ACETIC ACID INDUCIBLEs *(*Aux/IAA) and AUXIN RESPONSE FACTOR (ARF) proteins regulate different steps of lateral root formation (De Rybel et al., 2010). LR priming is controlled by an IAA28-dependent auxin signaling module. One target of this group is *GATA23*, encoding a transcription factor that triggers the acquisition of lateral root founder cell identity (De Rybel et al., 2010). The divisions of LR founder cells are regulated by an auxin signaling module that involves IAA14/SLR, ARF7 and ARF19 (Fukaki et al., 2005; Okushima et al., 2005a, 2007; Wilmoth et al., 2005; Lee et al., 2009; Goh et al., 2012). Signaling targets of this group are genes encoding the LBD transcription factors LBD16, 18, 29, and 33 as well as ARF19 itself (Okushima et al., 2005a, 2007). Together with a third group consisting of IAA12/BDL and ARF5/MP, the IAA14/SLR module is also important for LR initiation and LR primordia patterning (Vanneste et al., 2005; De Smet, 2010). ARF6 and ARF8 is predicted to positively regulate a group of genes involved in lateral root fomation. (Lavenus et al., 2015)

Auxin signaling is not only involved in LR formation but also in vascular stem cell initiation and cambium maintenance. For example the auxin responsive transcription factor MONOPTEROS (MP)/AUXIN RESPONSE FACTOR5 (ARF5) is essential for the specification of vascular stem cells during embryogenesis (Hardtke and Berleth, 1998) and plays a role in cambium homeostasis by restricting the number of stem cells in a cell-autonomous fashion (Brackmann et al., 2018)

The similarities between LR formation and periderm development as well as the fact that auxin signaling is involved in secondary growth led us to investigate the role of auxin and LR regulators during periderm development. Here we demonstrate that in the Arabidopsis root auxin accumulates within the phellogen and auxin signaling is required for periderm formation as locally impaired auxin signaling results in periderm disorganization. Furthermore, many LR regulators are expressed during periderm development (*GATA23*, *ARF7, ARF19*, *ARF17*, *ARF6* and *LBD16*). However only mutants in early LR regulators such as *IAA28*, *GATA23*, *ARF7 ARF19* display periderm phenotypes. In case of *iaa18*, *slr-1* and *CASP1::shy2.2* the periderm development is accelerated and decelerated for *iaa28* and *GATA23 RNAi* as well as nearly abolished in *sur1* mutants. Furthermore the periderm of *iaa28-1* is not and of *arf7 arf19* very weakly able to respond to an exogenous auxin application. In contrast, a periderm can be formed even in the absence of lateral roots and lateral roots can develop in plants with an impaired

periderm although both organs arise from the pericycle. This indicates that periderm development and lateral root formation are competing processes.

Materials and Methods

Plant material and growth

Transgenic plant lines are in Col-0 background unless it is specified otherwise in the text or figures. Plants used for microscopy and periderm extension experiments were grown under continuous light condition *in vitro* on 1/2MS plates supplemented with 1% sugar unless it is specified otherwise in the text or figures (on soil under long-day conditions). For NAA and NPA treatments, plants were transferred after 7 days of growth on 1/2MS 1% sugar to 1/2MS 1% sugar 5µM NPA/ 10µM NPA / 0,1 µM NAA / 1µM NAA / mock respectively. *35S::D2-VENUS* (N799173 Brunoud et al., 2012), *35S::m-D2-VENUS* (N799174 Brunoud et al., 2012), *R2D2 (RPS5A::m-D2-dTomato RPS5A::D2VENUS*) (from Dolf Wejers; Liao et al., 2015), *DR5::ERGFP* (Ulmasov et al., 1997), *GATA23::NLS-GFP-GUS* (from Bert de Rybel; De Rybel et al., 2010) *UBQ10:eYFP-NPSN12* (*W131Y*) (Geldner et al., 2009), *ARF7::NLS-3xGFP* (N67080; Rademacher et al., 2011) *W131Y*, *ARF19::NLS-3xGFP* (N67104; Rademacher et al., 2011), *ARF17::NLS-3xGFP* (N67100; Rademacher et al., 2011) *W131Y*, *ARF8::NLS-3xGFP* (N67082; Rademacher et al., 2011) *ARF6::ARF6-GFP* (from Dolf Weijers) *W131Y*, *LBD16::GUS* (N68141), *PER15::NLS-GFP-GUS* (from Joop Vermeer),*slr-1* (from Charles Melnyk), *bdl-.2* (from Charles Melnyk), *iaa18-1* (from Charles Melnyk; Ploense et al., 2009), *iaa28-1* (from Charles Melnyk; Rogg et al., 2001), axr3-1 (from Charles Melnyk; N57504), *alf4-1* (from Charles Melnyk; DiDonato et al., 2004), *axr1-12* (from Charles Melnyk; Timpte et al., 1995), *arf7 arf19* (N24629; Okushima et al., 2007), *sur1-1/rty1-1 +DR5::GUS* (N16708; Stepanova et al., 2007), *CASP1::shy2-2* and *PER15::shy2.2* were gifts from J. Vermeer (University of Zurich, Switzerland), *GATA23 RNAi line 1-2* and *7-3* (from Tom Beeckman; De Rybel et al., 2010), .

Histology and staining

Root and hypocotyl plastic cross-sections were obtained as described in (Barbier de Reuille & Ragni, 2017) 0.5 mm below or above the hypocotyl-root-junction, stained with 0.1 % toluidine blue and imaged with a Zeiss Axio M2 imager microscope or a Zeiss Axiophot microscope. The GUS assay was performed according to (Beisson et al., 2007).

Confocal Microscopy

Confocal images where acquired from whole-mount samples with a Zeiss LSM880. For green fluorescent protein (GFP): excitation wavelength (ex.) 488 nm; emission (em.) 490–510 nm. For yellow fluorescent protein (YFP) and mCitrine: ex. 514 nm; em. 520–540 nm. For mCherry: ex. 561 nm; em. 570–630 nm. For phellem autofluorescence: ex. 405 nm; em. 420–500 nm or ex. 405 nm; em. 420–460 nm if combined with GFP or YFP. 3D reconstructions and Ortho Views of a Z-stack were obtained using the ZEN Black pro software.

Image analyses and statistical analyses

Periderm extension was measured as described in Wunderling et al., 2018. The ratio of phellem length to root length was calculated from at least 15 roots per time point and plant line. Root diameter and periderm cell layers were measured on plastic cross-sections of most mature root parts. All statistical analyses were performed using IBM SPSS Statistics version 24 (IBM). Datasets were at first tested for homogeneity of variances using Levene's Test of Equality of Variances. Then the significant differences between two datasets were calculated using a Welch's t-test in case of a non-homogenous variance or a Student's t-test if the variance is homogeneous. The threshold for significance was set to a p-value < 0.05.

Molecular cloning

The *PER15* promoter was amplified from genomic DNA with the primers: *A-pPER15* (AACAGGTCTCAACCTCATAACCTCTGAATTAAGCCA) and *Br-pPER15R* (AACAGGTCTCATGTTTGTCAAATTTTCCGCTAGCTA) and cloned into *pGG-A0* using the GreenGate cloning system (Lampropoulos et al., 2013). The *SYP122* coding sequence was recloned into *pGG-D0*. To obtain the line *PER15::mCherry-SYP122*, the final GreenGate reaction was assembled in pGGZ003 using also the published and publicly available modules: *pGGB003*, *pGGC015*, *pGGE001* and *pGGF005* (Lampropoulos et al., 2013).

Results

Auxin promotes the periderm development

To determine whether auxin signaling regulates periderm development in Arabidopsis, at first we analyzed the auxin concentration and activity pattern during periderm formation. Therefore we examined several transgenic auxin concentration and activity reporter lines using confocal fluorescence microscopy. The ratiometric auxin sensor reporter *R2D2* shows that auxin accumulates at high levels in the phellogen (red arrows) and in the stele of a mature root (Fig.

1b,c), whereas in the phellem auxin levels are lower. Consistently, auxin signaling takes place within phellogen cells (black arrows) and stele as demonstrated by *DR5::ERGFP* expression (Fig. 1d). To investigate whether auxin is required for proper periderm development, we first tested the effect of NPA, auxin transport inhibitor, on periderm growth. Consistently with previous results, NPA-treated plants had significantly shorter roots (Fig. 1e) and ceased to form LRs. We analyzed periderm extension using the ratio of phellem length to root length as an indirect measurement of periderm dynamics. Periderm extension was significantly reduced in 10µM NPA- treated plants compared to mock control and 5µM NPA- treated plants (Fig. 1g). However, both 5 and 10 µM NPA-treated plants display the same root length that was significantly shorter than for the mock control (Fig. 1e). Root cross-sections of plants of both NPA treatments show a smaller root diameter (Fig. 1i,j) compared to untreated Col-0 plants (Fig. 1h) and have still some cortex and epidermis cells attached to the periderm (Fig. 1i,j) while the periderm is already the outside tissue in mock-treated plants (Fig. 1h). This suggests that a severely inhibited auxin transport and signaling leads to a reduced periderm development.

To corroborate these results we examined the opposite situation using an exogenous auxin application. Therefore we treated plants with NAA, a synthetic auxin that effects an over-proliferation of lateral roots. The periderm extension is significantly higher in 1µM NAA-treated plants than in mock- or 0.1 µM NAA- treated plants (Fig. 1m) and also the phellem length itself is significantly larger in 1µM NAA- treated plants than in mock- treated plants (Fig 1l) although the root length is significantly shorter (Fig. 1k). 1µM NAA-treated plants show a closed ring of phellem cells in root cross-sections (Fig. 1p) at a stage when the ring is not yet closed in mock- or 0.1 µM NAA-treated plants (Fig. 1n,o). This indicates that a high concentration of auxin and increased auxin signaling accelerates periderm development. In conclusion, an altered auxin signaling indeed effects periderm development suggesting that the periderm is regulated by auxin.

LR regulators are expressed during periderm development

As we have shown that auxin accumulates in the phellogen and has an effect on periderm development we further analyzed if the periderm shares more molecular regulators with LR formation. At first we determined if molecular regulators of lateral root formation are expressed in the periderm (Fig. 2). *IAA28,* which controls LR priming is expressed in the periderm only in the root and not in the hypocotyl (preliminary). *GATA23* was shown to control lateral root founder cell specification downstream of IAA28 (De Rybel et al., 2010) and is expressed in the periderm of roots (Fig. 2a,d) and hypocotyls (Fig. 2e,f) throughout periderm development.

ARF7 and *ARF19* are involved in several steps of LR formation and are also expressed throughout root periderm development (Fig. 2b,c). *LBD16* is a target of ARF7 and ARF19 in LR formation (Okushima et al., 2007) and is expressed in the periderm of root (Fig. 2i) and hypocotyl (Fig. 2j). ARF6 and ARF8 are promoting adventitituous root formation and are also expressed in the phellem and phellogen of roots (Fig. 2g).

Mutants in early LR regulators show periderm defects

As several LR regulators are expressed in the periderm we determined their role during periderm development. Therefore we used transgenic plant lines that are mutated in regulatory genes of the auxin-dependent early LR formation. At first we investigated the dominant mutant *iaa28-1,* which suppresses LR initiation as the protein cannot be degraded in the presence of auxin (Rogg et al., 2001). *iaa28-1* plants show a significantly decreased periderm extension (Suppl. Fig. 1c) and a delay in periderm development in the root with only few differentiated phellem cells in cross-sections (Fig. 3b) while the *Ws* control already has a ring of phellem cells (Fig. 3a). GATA23 controls LR founder cell identity downstream of IAA28 and *GATA23 RNAi* lines have a decreased LR density (De Rybel et al., 2010). In the strongest line we could observe a mild reduction in periderm extension (white box Fig. 5 o, line 1-2 stronger, 7-3 weaker) compared to Col-0 suggesting a decelerated periderm development (preliminary results). The gain-of-function mutation *slr-1* decreases auxin-inducible gene expression (Fukaki et al, 2002) and *slr-1* mutants do not have lateral roots. Periderm extension is significantly increased in *slr-1* compared to *Col-0* (Suppl. Fig. 1i) indicating an accelerated periderm development *slr-1* plants show a disorganized xylem in root cross-sections (Fig. 3f) although the overall secondary growth is comparable to *Col-0* (Fig. 3e) with a tendency to a larger root diameter than *Col-0* (Suppl. Fig. 2a) but the same number of periderm cell layers (4 layers in slr-1 and *Col-0*) and a normally developed periderm in root cross-sections (Fig. 3f). Also plants with the gain-of-function mutation *iaa18* show a significantly increased periderm extension (Suppl. Fig. 1f) and the periderm in root cross-sections already shows a ring of phellem cells (Fig 3d), which is not yet closed in Ler control roots (Fig. 3c) suggesting an accelerated periderm development. IAA18, IAA14 and most likely IAA28 negatively regulate ARF7 and ARF19 transcriptional activators that positively regulate lateral root formation (Uehara et al. 2008). In the *arf7 arf19* double mutant, several auxin-responsive genes (e.g. *IAA5*, *LBD16*, *LBD29* and *LBD33*) are no longer up-regulated by auxin and thus, LR formation is not initiated. We were able to show that these plants still have a normally developed periderm with phellem cell differentiation in root cross-sections (Fig. 3h) like *Col-0* (Fig. 3g). The periderm extension of *arf7 arf19* (Suppl Fig. 1i) is similar to *Col-0* whereas the *arf7 arf19* root diameter has a tendency to be smaller than in

Col-0 (Suppl. Fig. 2a) and the number of periderm cell layers is reduced in *arf7 arf19* (3 -4 layers) roots than in *Col-0* (4 layers). Furthermore we found a periderm present in roots of plants with defects in less important regulators of LR formation, *alf4-1*, *axr1-12*, *bdl-2* and *axr3-1* (Suppl. Fig3). In root cross-sections of *alf4-1* the periderm seems to comprise one more cell layer than in *Col-0* and the periderm area seems to be larger (preliminary results).

A transgenic line with an impaired auxin-signaling pathway outside of the pericycle/periderm is *CASP1::shy2-2*. It harbors a dominant version of *short hypocotyl 2* (*shy2)/iaa3* that cannot be degraded and is expressed in the endodermis. This causes endodermis cells to stay turgid and block lateral root emergence and thus lateral roots are not even initiated (Vermeer et al., 2014). We found the periderm extension to be increased in *CASP1::shy2-2* compared to *Col-0* plants (Fig. 4c) while the root length is the same for both (Fig. 4a). In root cross-sections *CASP1::shy2-2* plants show a normal periderm that even develops faster than in *Col-0* with an early phellem cell differentiation (Fig. 4e red arrows: phellem cells). At a later stage the ring of phellem is normally differentiated (Fig. 4f,g). Additionally, the root diameter of *CASP1::shy2-2* cross-sections is larger than in *Col-0* plants (Suppl. Fig. 2b) with an increased number of periderm cell layers (3 or 4 in *CASP1::shy2-2*, 3 in *Col-0*). These results indicate that the periderm development of *CASP1::shy2-2* is accelerated compared to *Col-0*.

In conclusion, plants with impaired auxin-dependent early LR regulators develop a periderm but show some periderm phenotypes like an accelerated (*iaa18*, *slr-1*) or decelerated (*iaa28*) periderm development compared to control plants or an additional periderm cell layer (*alf-4-1*).

Since many mutants and transgenic lines with no emerged lateral roots display a normal periderm organization, we next examined whether their periderm could still respond to an auxin treatment. Periderm extension is significantly increased with 1 µM NAA treatment compared to mock in *iaa18-1* roots and the increase is comparable to the NAA-induced increase in *Ler* control plants (Fig 5c). In contrast, periderm extension does not increase with the NAA treatment in *iaa28-1* roots while there is a significant increase of periderm extension in *Ws*-control roots upon NAA treatment (Fig. 5c). Furthermore, *CASP1::shy2-2* roots display a strong increase in periderm extension upon NAA treatment like the *Col-0* control but there is only a mild increase in *arf 7 arf 19* double mutant roots (Fig. 5l). Additionally both *GATA23 RNAi* lines show an increased periderm extension in roots upon NAA treatment like the *Col-0* control (Fig. 5o). These results suggest that the periderm of *iaa18-1*, *CASP1::shy2-2* and *GATA23 RNAi*

lines is still able to respond to auxin while the periderm of *iaa28-1* and *arf7 arf19* is not able to respond to auxin.

Over-proliferation of adventitious roots nearly eliminates periderm

Next, we examined the periderm of *superroot 1* (*sur1*) mutants that display an over-proliferation of adventitious roots due to an overproduction of auxin in the hypocotyl (Pacurar et al., 2014). Periderm extension is strongly reduced in the root of *sur1* mutants compared to *Col-0* (Suppl. Fig. 1l). Cross-sections show that secondary growth and also periderm development is very delayed in *sur1* mutants compared to wild type plants in the root (Fig. 6b) and in the hypocotyl (Fig. 6d). Because of the abundance of adventitious roots in the hypocotyl, a periderm cannot be distinguished in cross-sections (Fig. 6d). This suggests that the over-proliferation of adventitious roots caused by auxin overproduction in the hypocotyl inhibit the periderm formation.

Locally blocking auxin signaling in the periderm results in a disorganized/delayed periderm development

Next we examined plants that have an altered auxin signaling in the periderm using the periderm-specific promoter *PEROXIDASE 15* (*PER15*) to express the dominant version of SHY2/IAA3 that cannot be degraded in presence of auxin. The *PER15* promoter is mainly active in the pericycle when periderm formation begins and at later stages in the phellem and phellogen of roots (Suppl. Fig 4a,b) and hypocotyls (Suppl. Fig 4c). *PER15:shy2-2* plants displayed a normal root growth with an even longer primary root length compared to *Col-0* plants (Fig. 7a). However lateral root density was slightly reduced in *PER15::shy2-2* plants (Suppl. Fig. 4p) and the distribution of lateral root stages was shifted towards early stages in *PER15::shy2.2* compared to *Col-0*. The mild defects in LR formation may be explained by the fact that the *PER15* promoter is active in the endodermis when lateral roots are emerging, thus it partially recapitulates the phenotype of *CASP1:shy2-2* plants (Vermeer et al., 2014). But still, periderm extension was strongly decreased in *PER15::shy2-2* plants compared to *Col-0* (Fig. 7c). Analyzing cross-sections, at an early stage when the pericycle is still present, no obvious phenotype is visible between the hypocotyl of *PER15::shy2-2* (Suppl. Fig. 4e) and *Col-0* (Suppl. Fig. 4d). At a later stage, we found missing periderm cells at phloem poles and abnormal division planes of cells in the periderm of the root (Fig. 7e,g, red arrows) and hypocotyl (Suppl. Fig. 4g,i red arrows). At very late stages of periderm development, the periderm became even more disorganized in *PER15::shy2-2* roots (Fig. 7g) and hypocotyls (Suppl. Fig. 4i,k,m). Even the vascular cambium cells were missing at the sites in correspondence with the original xylem

poles in *PER1::shy2-2* roots (Fig. 7g black arrows) and hypocotyls (Suppl. Fig. 4i black arrows). We furthermore found that the mentioned characteristics of the *PER15::shy2-2* phenotype were stronger on soil than in vitro. Additionally, *PER15::shy2-2* plants were not resistant to mechanical stress. When the shoot reached around 15cm, plants were falling to one side pulling their roots out of the soil from even the lightest touch (Suppl. Fig. 4r red arrow). Overall, these results show that blocking auxin signaling in the pericycle and phellogen leads to a severely disorganized periderm suggesting that auxin plays an important role in periderm development.

Discussion

Auxin promotes periderm development

Auxin is involved in many plant developmental programs such as lateral root development (Lavenus et al., 2013) and vascular stem cell initiation (Hardtke CS, Berleth T 1998; Friml et al., 2003). It has for example a pivotal role in promoting cambium activity and auxin-dependent cambium stimulation requires the homeobox transcription factor WUSCHEL RELATED HOMEOBOX 4 (WOX4) (Suer et al., 2011). The auxin responsive transcription factor MONOPTEROS (MP)/ARF5 is essential for the specification of vascular stem cells. It is expressed in the procambial cells during early embryogenesis and its expression is upregulated by auxin (Hardtke and Berleth 1998). Furthermore, the major auxin efflux carrier, PIN-FORMED1 (PIN1) protein, is polarly localized in the inner cells of the pro-embryo before they turn into procambial cells during early embryogenesis (Friml, 2003). It furthermore was proposed by Beckman (2000) that during stress response an accumulation of IAA leads to a reaction of the periderm inducing peridermal defense. And also in 2016 it was shown by Lulai et al. that wounding induces changes of the auxin content in potato tubers followed by a wound periderm formation. This is in line with the results of this study that auxin plays a role in periderm development. In this study we found that auxin accumulates in the phellogen and phellem and an auxin response takes place in the phellogen. Furthermore plants with an altered auxin signaling specifically in the pericycle/periderm display a severely disorganized periderm (*PER15::shy2-2*). This indicates that auxin also plays a role in the periderm development.

Periderm development shares molecular regulators of LR formation

Thus, periderm development shares auxin as a molecular regulator with LR formation in addition to previously known mutual characteristics. Our results furthermore demonstrate that

also many auxin signaling dependent LR regulators are expressed in periderm tissues: *GATA23*, *ARF7*, *ARF19*, *ARF17*, *ARF6* and *LBD16*. Consequently, plants with defects in auxin signaling dependent LR regulators show differences in periderm development compared to control plants. Periderm development is decelerated for *iaa28* and *GATA23 RNAi*. Furthermore the periderm of *iaa28-1* and *arf7 arf19* does not respond to exogenous auxin application. These results demonstrate that auxin plays an important role not only in lateral root formation but has also a very important positive role for the periderm development. Furthermore the periderm seems to share some of the LR regulators, e.g *IAA28, GATA23*, *ARF7, ARF19*.

Competition between periderm and LRs

Both processes of LR formation and periderm development are regulated by auxin and display some developmental molecular regulators in common. Nevertheless it is striking thatperiderm development is accelerated in plants with severe defects in LR formation leading to a severely decreased LR density or absence of LRs (*iaa18*, *slr-1* and *CASP1::shy2-2*). Maybe this is the case because *IAA18* and *IAA14/SLR* are not expressed in the periderm (preliminary) and *CASP1::shy2-2* does not perturb auxin signaling in the periderm but only in the endodermis. In contrast, *sur1* displays an over-proliferation of adventitious roots accompanied by a nearly abolished periderm. Additionally, plants with an impaired auxin-signaling specifically in the pericycle (*PER15::shy2-2*) display a very disorganized periderm but nearly normal lateral root formation. These results indicate a competition between lateral/adventitious root formation and periderm development possibly with a molecular switch in between both processes.

A competition and molecular switch between periderm development and LR formation would be reasonable for a fast adaptation of the plant to respond to its environment. This adaptation potentially includes a change from increasing water-uptake by LR growth to increasing protection by periderm growth and vice versa. It has been shown indeed that environmental factors like drought or salt stress lead to an increased suberization of apoplastic transport barriers in the root endodermis (North and Nobel, 1994; Reinhardt and Rost, 1995). Furthermore an increase in suberin contents was observed in endodermal and/or exodermal root cells of Castor bean (*Ricinus communis L.*) plants after exposure to salt conditions (Schreiber et al., 2005). With this increase in suberin contents in roots Castor bean plants increase their apoplastic transport barriers in adaptation to salt stress in order to minimize NaCl uptake (Schreiber et al., 2005). It would be interesting to investigate periderm development and suberin content as well as LR number and density of stress-treated plants compared to control plants.

It further would be interesting to investigate the competition between periderm development and LR formation on a molecular level regarding a molecular switch. A competition between cell fates has already been found in the Arabidopsis root epidermis, where MYB transcription factors *WEREWOLF* (*WER*) and *CAPRICE* (*CPC*) compete about nonhair cell fate (WER) and hair cell fate (CPC) (Song et al., 2011). Even auxin could be involved in this competition as Lavenus et al., 2015 have shown that an auxin-dependent switch could control the differentiation between meristematic cells and flank cells of LR primordia. Furthermore, alternative positive feedback loops within cell types coupled by inhibitory pathways connecting neighboring cells are a part of developmental decisions as different as the choice between lysis and lysogeny in bacteriophage λ, heterocyst differentiation in blue-green algae, macrochaete differentiation in Drosophila, and epidermal patterning systems in plants (Larkin et al., 2003). Likewise, a molecular switch between phellogen and LR primordial cell fate/identity of the pericycle could also be formed by different transcription factors (*MYB* and/or *NAC*), an auxin signaling network of ARFs and IAAs and involve positive feedback loops within cell types coupled by inhibitory pathways.

Acknowledgements

L.R. is indebted to the Baden-Württemberg Stiftung for financial support of this research project by the Elite program for Postdocs. This work was supported by the DFG (grant RA-2590/1-1).

Author contributions

A.W. and L.R. designed the research; A.W., D.R., S.M., J.V. and L.R. performed the experiments; A.W., and L.R. analyzed and discussed the data; A.W. wrote the paper with the help of L.R.

Figure legends

Fig. 1: An auxin response takes place in the periderm. (a) *35S::D2VENUS* (b) *35s::mD2VENUS* (control) (c) *R2D2* (*RPS5A::D2VENUS RPS5A::mD2-Tomato*) (d) *DR5::ERGFP W131Y*. (a,b,c,d) Cross and longitudinal sections (Ortho View of a Z-stack) of 14-d-old roots. (e-g) Box plots of the root length (e), length of the phellem-covered root part (f) and ratio of phellem length to root length (g) of mock, 5µM and 10µM NPA-treated Col-0 12-d-old roots shown in h-j. (h-j) Plastic cross-sections of (h) mock, (i) 5µM and (j) 10µM NPA-treated 12-d-old Col-0

roots. (k-m) Box plots of the root length (k), length of the phellem-covered root part (l) and ratio of phellem length to root length (m) of mock, 0.1µM and 1µM NAA-treated 12-d-old Col-0 roots shown in n-p. (n-p) Plastic cross-sections of (n) mock, (o) 0.1µM and (p) 1µM NAA-treated 12-d-old Col-0 roots. Box plots: the dark line in the middle of the boxes is the median, the bottom and top of the box indicates the 25th and 75th percentiles, whiskers are within 1.5 times the interquartile range, the empty dots are outliers. (e-g, k-m) Student's t-test ($p < 0.05$; n =19–21). Black scale bars, 50 µm. White scale bars 20µm.

Fig. 2: Regulators of lateral root formation are expressed in the periderm. (a,d-f) *GATA23::NLS-GFP-GUS W131Y*, (b) *ARF7::NLS-3xGFP W131Y*, (c) *ARF19::NLS-3xGFP* autofluorescence, (g) *ARF8::NLS-3xGFP W131Y*, (h) *ARF6::ARF6-GFP W131Y*, (i,j) *LBD16::GUS*. (a-c,h) Cross and longitudinal sections (Ortho View of a Z-stack) of 12-d-old roots, (g) 3D reconstruction of Z-Stacks of 12-d-old roots. (d-f, i,j) Plastic cross-sections of GUS-stained 12-d-old (d,e,i,j) and 17-d-old (f,k) roots (d,i) and hypocotyls (e,f,j). Black scale bars, 50 µm. White scale bars 20µm.

Fig. 3: Plants with defects in regulators of the auxin-dependent LR formation still develop a normal periderm. (a, b) Plastic cross-sections of 12-d-old *Ws-2* (a) and *iaa28-1* (b) roots. (c,d) Plastic cross-sections of 12-d-old *Ler* (c) and *iaa18-1* (d) roots. (e-h) Plastic cross-sections of 19-d-old (e,f) *Col-0* (e), *slr-1* (f) and 15-d-old (g,h) *Col-0* (g) and *arf7 arf19* (h) roots. Scale bars, 50 µm.

Fig. 4: Plants with an impaired auxin-signaling pathway outside of the pericycle/periderm show an accelerated periderm development. (a-d) Plastic cross-sections of 9-d-old (a,b) and 15-d-old (c, d) *Col-0* (a, c) and *CASP1::shy2.2* (b, d) roots. (e-h) Box plots of the root length (e), length of the phellem-covered root part (f) and ratio of phellem length to root length (g) of 12-d-old *Col-0* and *CASP1::shy2.2* roots (n=20). Student's t-test $p < 0.05$. Box plots: the dark line in the middle of the boxes is the median, the bottom and top of the box indicates the 25th and 75th percentiles, whiskers are within 1.5 times the interquartile range. (a-d) Bars, 50 µm.

Fig. 5: The response of the periderm of auxin-impaired plants to an exogeous auxin-treatment. (a-o) Box plots of the root length (a,j,m), length of the phellem-covered root part (b,k,n) and ratio of phellem length to root length (c,l,o) of 12-d-old *Ws*, *iaa28-1*, *Ler* and *iaa18-1* (a-c, n=16-21), 12-d-old *Col-0*, *arf7 arf19* and *CASP1::shy2.2* roots (j-l; n=20) and 13-d-old *Col-0* and two independent *GATA23 RNAi* lines (*1-2* and *7-3*) (m-o; n=14-20). Student's t-test $p < 0.05$. Box plots: the dark line in the middle of the boxes is the median, the bottom and top of the box indicates the 25th and 75th percentiles, whiskers are within 1.5 times the interquartile range, the empty dots are outliers.

Fig. 6: Plants with over-proliferation of adventitious roots are nearly without periderm. (a-d) Plastic cross-sections of 19-d-old *Col-0* (a,c) and *sur1* (b,d) roots (a,b) and hypocotyls (c,d). Scale bars, 50 µm.

Fig. 7: A perturbed auxin signaling in pericycle and periderm leads to a severely disorganized periderm. (a-c) Box plots of the root length (a), length of the phellem-covered root part (b) and ratio of phellem length to root length (c) of 12-d-old *PER15::shy2.2* and *Col-0* roots. (d-g) Plastic cross-sections of 9-d-old (d,e) and 15-d-old (f,g) roots of *PER15::shy2.2* (e,g; red arrows: missing periderm cells; g: black arrows: missing vascular cambium cells) and *Col-0* (d,f). Box plots: the dark line in the middle of the boxes is the median, the bottom and top of the box indicates the 25th and 75th percentiles, whiskers are within 1.5 times the interquartile range, the empty dots are outliers. Student's t-test ($p < 0.05$; n =19–21). Black scale bars, 50 µm.

References

Beckman CH. 2000. Phenolic-storing cells: keys to programmed cell death and periderm formation in wilt disease resistance and in general defence responses in plants? *Physiological and Molecular Plant Pathology* **57**, 101-110.

Brackmann K, Qi J, Gebert M, Jouannet V, Schlamp T, Grünwald K, Wallner E-S, Novikova DD, Levitsky VG, Agustí J, Sanchez P, Lohmann JU, Greb T. 2018. Spatial specificity of auxin responses coordinates wood formation. *Nat Commun* **9**: 875.

Brunoud G, Wells DM, Oliva M, Larrieu A, Mirabet V, Burrow AH, Beeckman T, Kepinski S, Traas J, Bennett MJ, Vernoux T. 2012. A novel sensor to map auxin response and distribution at high spatio-temporal resolution. *Nature* **482**, 103–106.

Caritat A, Gutierrez E, Molinas M. 2000. Influence of weather on cork-ring width. *Tree Physiology* **20**, 893-900.

De Rybel B, Vassileva V, Parizot B, Demeulenaere M, Grunewald W, Audenaert D, Van Campenhout J, Overvoorde P, Jansen L, Vanneste S, Moller B, Wilson M, Holman T, Van Isterdael G, Brunoud G, Vuylsteke M, Vernoux T, De Veylder L, Inze D, Weijers D, Bennett MJ, Beeckman T. 2010. A novel aux/IAA28 signaling cascade activates GATA23-dependent specification of lateral root founder cell identity. *Curr Biol* **20**, 1697-1706.

De Smet I, Lau S, Voss U, Vanneste S, Benjamins R, Rademacher EH, Schlereth A, De Rybel B, Vassileva V, Grunewald W, Naudts M, Levesque MP, Ehrismann JS, Inze D, Luschnig C, Benfey PN, Weijers D, Van Montagu MC, Bennett MJ, Jurgens G, Beeckman T. 2010. Bimodular auxin response controls organogenesis in Arabidopsis. *Proc Natl Acad Sci U S A* **107**, 2705-2710.

De Smet I, Tetsumura T, De Rybel B, Frei dit Frey N, Laplaze L, Casimiro I, Swarup R, Naudts M, Vanneste S, Audenaert D, Inze D, Bennett MJ, Beeckman T. 2007. Auxin-dependent regulation of lateral root positioning in the basal meristem of Arabidopsis. *Development* **134**, 681-690.

DiDonato RJ, Arbuckle E, Buker S, Sheets J, Tobar J, Totong R, Grisafi P, Fink GR, Celenza JL. 2004. Arabidopsis ALF4 encodes a nuclear-localized protein required for lateral root formation. *Plant J* **37(3)**:340-53.

Esau K. 1977. *Anatomy of seed plants.* New York, NY, USA: John Wiley & Sons.

Fagerstedt KV, Saranpaa P, Tapanila T, Immanen J, Serra JA, Nieminen K. 2015. Determining the Composition of Lignins in Different Tissues of Silver Birch. *Plants (Basel)* **4**, 183-195.

Friml J. 2003. Auxin transport - shaping the plant. *Curr Opin Plant Biol* **6(1)**:7-12.

Fukaki H, Tameda S, Masuda H, Tasaka M. 2002. Lateral root formation is blocked by a gain-of-function mutation in the SOLITARY-ROOT/IAA14 gene of Arabidopsis. *Plant J* **29(2)**:153-68.

Fukaki H, Nakao Y, Okushima Y, Theologis A, Tasaka M. 2005. Tissue-specific expression of stabilized SOLITARY-ROOT/IAA14 alters lateral root development in Arabidopsis. *Plant J* **44**, 382-395.

Geldner N, Dénervaud-Tendon V, Hyman DL, Mayer U, Stierhof YD, Chory J. 2009. Rapid,combinatorial analysis of membrane compartments in intact plants with a multicolor marker set. *Plant J* **59(1)**:169-78.

Goh T, Joi S, Mimura T, Fukaki H. 2012. The establishment of asymmetry in Arabidopsis lateral root founder cells is regulated by LBD16/ASL18 and related LBD/ASL proteins. *Development* **139**, 883-893.

Groh B, Hubner C, Lendzian KJ. 2002. Water and oxygen permeance of phellems isolated from trees: the role of waxes and lenticels. *Planta* **215**, 794-801.

Hardtke CS, Berleth T. 1998. The Arabidopsis gene MONOPTEROS encodes a transcription factor mediating embryo axis formation and vascular development. *EMBO J* **17(5)**:1405-11.

Larkin JC, Brown ML, Schiefelbein J. 2003. HOW DO CELLS KNOW WHAT THEY WANT TO BE WHEN THEY GROW UP? Lessons from Epidermal Patterning in Arabidopsis. *Annu Rev Plant Biol* **54**:403–30.

Lavenus J, Goh T, Roberts I, Guyomarc'h S, Lucas M, De Smet I, Fukaki H, Beeckman T, Bennett M, Laplaze L. 2013. Lateral root development in Arabidopsis: fifty shades of auxin. *Trends Plant Sci* **18**, 450-458.

Lavenus J, Goh T, Guyomarc'h S, Hill K, Lucas M, Voß V, Kenobi K, Wilson MH, Farcot E, Hagen G, Guilfoyle TJ, Fukaki H, Laplaze L, Bennett MJ. 2015. Inference of the Arabidopsis Lateral Root Gene Regulatory Network Suggests a Bifurcation Mechanism That Defines Primordia Flanking and Central Zones. *The Plant Cell* **27**: 1368–1388.

Lee HW, Kim NY, Lee DJ, Kim J. 2009. LBD18/ASL20 regulates lateral root formation in combination with LBD16/ASL18 downstream of ARF7 and ARF19 in Arabidopsis. *Plant Physiol* **151**, 1377-1389.

Lendzian KJ. 2006. Survival strategies of plants during secondary growth: barrier properties of phellems and lenticels towards water, oxygen, and carbon dioxide. *J Exp Bot* **57**, 2535-2546.

Liao C-Y, Smet W, Brunoud G, Yoshida S, Vernoux T, Weijers D. 2015. Reporters for sensitive and quantitative measurement of auxin response. *Nat Methods* **12(3)**: 207–210.

Lourenco A, Rencoret J, Chemetova C, Gominho J, Gutierrez A, Del Rio JC, Pereira H. 2016. Lignin Composition and Structure Differs between Xylem, Phloem and Phellem in Quercus suber L. *Front Plant Sci* **7**, 1612.

Lucas M, Kenobi K, von Wangenheim D, Vobeta U, Swarup K, De Smet I, Van Damme D, Lawrence T, Peret B, Moscardi E, Barbeau D, Godin C, Salt D, Guyomarc'h S, Stelzer EH, Maizel A, Laplaze L, Bennett MJ. 2013. Lateral root morphogenesis is dependent on the mechanical properties of the overlaying tissues. *Proc Natl Acad Sci U S A* **110**, 5229-5234.

Lulai EC, Freeman TP. 2001. The Importance of Phellogen Cells and their Structural Characteristics in Susceptibility and Resistance to Excoriation in Immature and Mature Potato Tuber (Solanum tuberosum L.) Periderm. *Annals of Botany* **Volume 88**, 555-561.

Lulai EC, Suttle JC, Olson LL, Neubauer JD, Campbell LG, Campbell MA. 2016. Wounding induces changes in cytokinin and auxin content in potato tuber, but does not induce formation of gibberellins. *Journal of Plant Physiology* **191**, 22-28.

Malamy JEB, P.N. 1997. Organization and cell differentiation in lateral roots Arabidopsis thaliana. *Development* **124**, 33-44.

Marques AV, Pereira H. 2013. Lignin monomeric composition of corks from the barks of Betula pendula, Quercus suber and Quercus cerris determined by Py–GC–MS/FID. *Journal of Analytical and Applied Pyrolysis* **100**, 88-94.

Miguel A. Moreno-Risueno JMVN, Antonio Moreno, Jingyuan Zhang, Sebastian E. Ahnert, Philip N. Benfey. 2010. Oscillating Gene Expression Determines Competence for Periodic Arabidopsis Root Branching. *Science* **329**, 1306-1311.

North GB and Nobel PS. 1994. Changes in root hydraulic conductivity for two tropical epiphytic cacti as soil moisture varies. *Am J Bot*. **81**, 46–53.

Okushima Y, Fukaki H, Onoda M, Theologis A, Tasaka M. 2007. ARF7 and ARF19 regulate lateral root formation via direct activation of LBD/ASL genes in Arabidopsis. *Plant Cell* **19**, 118-130.

Okushima Y, Overvoorde PJ, Arima K, Alonso JM, Chan A, Chang C, Ecker JR, Hughes B, Lui A, Nguyen D, Onodera C, Quach H, Smith A, Yu G, Theologis A. 2005. Functional genomic analysis of the AUXIN RESPONSE FACTOR gene family members in Arabidopsis thaliana: unique and overlapping functions of ARF7 and ARF19. *Plant Cell* **17**, 444-463.

Pacurar DI, Pacurar ML, Bussell JD, Schwambach J, Pop TI, Kowalczyk M, Gutierrez L, Cavel E, Chaabouni S, Ljung K, Fett-Neto AG, Pamfil D, Bellini C. 2014. Identification of new adventitious rooting mutants amongst suppressors of the Arabidopsis thaliana superroot2 mutation. J Exp Bot **65(6)**:1605-18.

Pereira H. 1988. Chemical composition and variability of cork from Quercus suber L. *Wood Science and Technology* **22**, 211-218.

Pereira H. 2007. *Cork: Biology, Production and Uses*. Amsterdam: Elsevier.

Ploense SE, Wu MF, Nagpal P, Reed JW. 2009. A gain-of-function mutation in IAA18 alters Arabidopsis embryonic apical patterning. *Development* **136(9)**:1509-17.

Rademacher EH, Möller B, Lokerse AS, Llavata-Peris CI, van den Berg W, Weijers D. 2011. A cellular expression map of the Arabidopsis AUXIN RESPONSE FACTOR gene family. *The Plant Journal* **68**, 597–606.

Reinhardt DH and Rost TL. 1995. Salinity accelerates endodermal development and induces an exodermis in cotton seedling roots. *Environ Exp Bot* **35**, 563–574.

Rogg LE, Lasswell J, Bartel B. 2001. A Gain-of-Function Mutation in IAA28 Suppresses Lateral Root Development. *The Plant Cell* **13**, 465–480.

Sacha Escamez BB, Hardy Hall, Domenique André, Béatrice Berthet, Ute Voß, Amnon Lers, Alexis Maizel, Malcolm Bennett and Hannele Tuominen. 2018. Cell death in cells overlying lateral root primordia contributes to organ growth in Arabidopsis.

Schreiber L, Franke R, Hartmann K. 2005. Effects of NO3 deficiency and NaCl stress on suberin deposition in rhizo- and hypodermal (RHCW) and endodermal cell walls (ECW) of castor bean (Ricinus communis L.) roots. *Plant and Soil* **269**, 333-339.

Serra O, Hohn C, Franke R, Prat S, Molinas M, Figueras M. 2010. A feruloyl transferase involved in the biosynthesis of suberin and suberin-associated wax is required for maturation and sealing properties of potato periderm. *Plant J* **62**, 277-290.

Serra O, Soler M, Hohn C, Franke R, Schreiber L, Prat S, Molinas M, Figueras M. 2009a. Silencing of StKCS6 in potato periderm leads to reduced chain lengths of suberin and wax compounds and increased peridermal transpiration. *J Exp Bot* **60**, 697-707.

Serra O, Soler M, Hohn C, Sauveplane V, Pinot F, Franke R, Schreiber L, Prat S, Molinas M, Figueras M. 2009b. CYP86A33-targeted gene silencing in potato tuber alters suberin composition, distorts suberin lamellae, and impairs the periderm's water barrier function. *Plant Physiol* **149**, 1050-1060.

Song S-K, Ryu KH, Kang YH, Song JH, Cho Y-H, Yoo S-D, Schiefelbein J, Lee MM. 2011. Cell Fate in the Arabidopsis Root Epidermis Is Determined by Competition between WEREWOLF and CAPRICE. *Plant Physiology* **157**(3):1196-1208.

Stepanova AN, Yun J, Likhacheva AV, Alonso JM. 2007. Multilevel Interactions between Ethylene and Auxin in Arabidopsis Roots. *The Plant Cell* **19**: 2169–2185.

Suer S, Agusti J, Sanchez P, Schwarz M, Greb T. 2011. WOX4 Imparts Auxin Responsiveness to Cambium Cells in Arabidopsis. *Plant Cell* **23**(9): 3247–3259.

Timpte C, Lincoln C, Pickett FB, Turner J, Estelle M. 1995. The AXR1 and AUX1 genes of Arabidopsis function in separate auxin-response pathways. *Plant J* **8(4)**:561-9.

Uehara T, Okushima Y, Mimura T, Tasaka M, Fukaki H. 2008. Domain II mutations in CRANE/IAA18 suppress lateral root formation and affect shoot development in Arabidopsis thaliana. *Plant Cell Physiol* **49(7)**:1025-38.

Van Norman JM, Xuan W, Beeckman T, Benfey PN. 2013. To branch or not to branch: the role of pre-patterning in lateral root formation. *Development* **140**, 4301-4310.

Vanneste S, De Rybel B, Beemster GT, Ljung K, De Smet I, Van Isterdael G, Naudts M, Iida R, Gruissem W, Tasaka M, Inze D, Fukaki H, Beeckman T. 2005. Cell cycle progression in the pericycle is not sufficient for SOLITARY ROOT/IAA14-mediated lateral root initiation in Arabidopsis thaliana. *Plant Cell* **17**, 3035-3050.

Vermeer JE, von Wangenheim D, Barberon M, Lee Y, Stelzer EH, Maizel A, Geldner N. 2014. A spatial accommodation by neighboring cells is required for organ initiation in Arabidopsis. *Science* **343**:178-83.

Waisel Y. 1995. Developmental and functional aspects of the periderm. In: Iqbal M, ed. The *cambial derivatives*. Stuttgart, Germany: Gebruder Borntraeger Verlagsbuchhandlung, 293–315.

Wilmoth JC, Wang S, Tiwari SB, Joshi AD, Hagen G, Guilfoyle TJ, Alonso JM, Ecker JR, Reed JW. 2005. NPH4/ARF7 and ARF19 promote leaf expansion and auxin-induced lateral root formation. *Plant J* **43**, 118-130.

Wunderling A, Ripper D, Barra-Jimenez A, Mahn S, Sajak K, Targem MB, Ragni L. 2018. A molecular framework to study periderm formation in Arabidopsis. *New Phytol* **219**, 216-229.

Figure 1

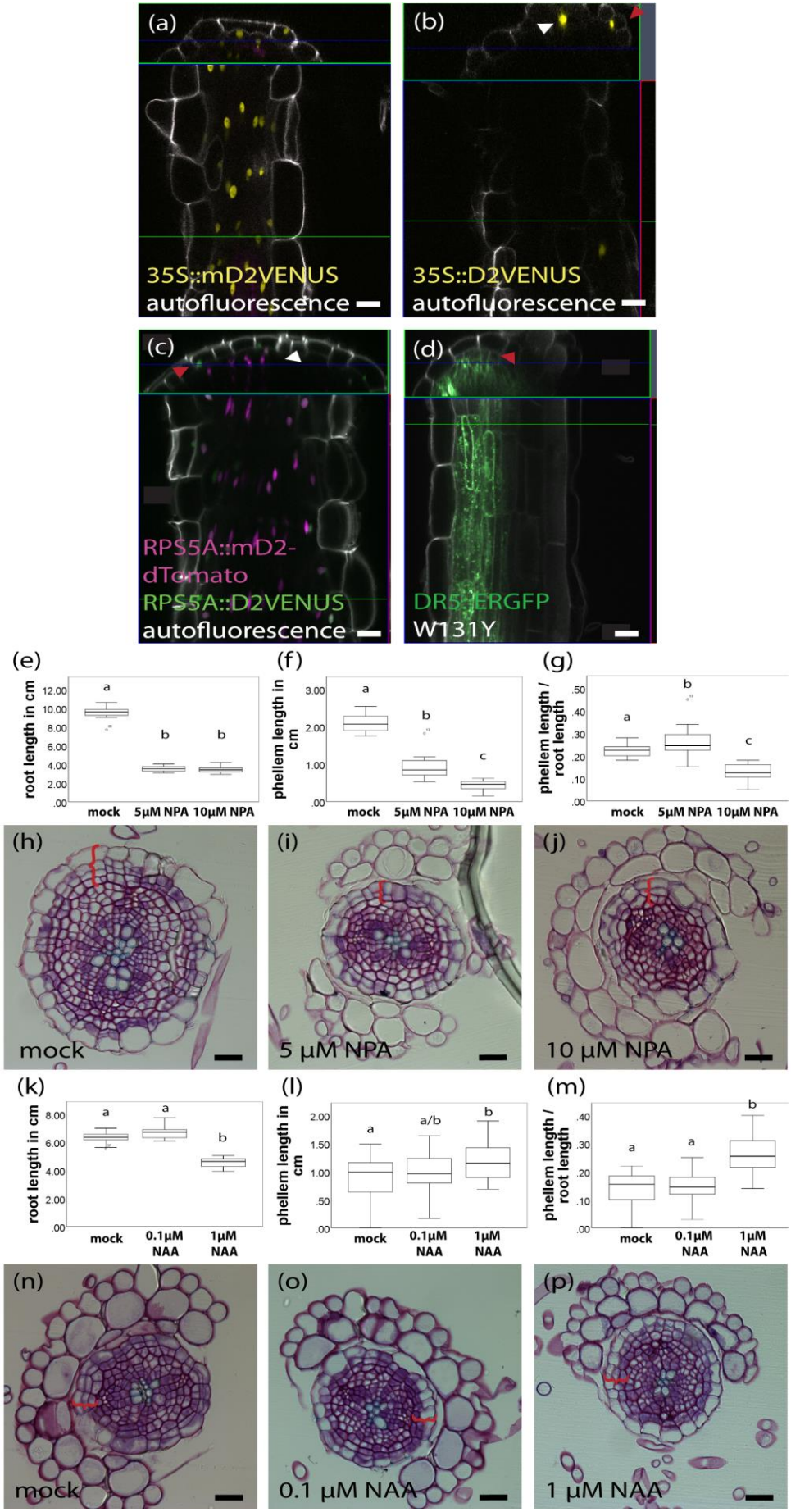
(a)
35S::mD2VENUS
autofluorescence
(b)
35S::D2VENUS
autofluorescence
(c)
RPS5A::mD2-dTomato
RPS5A::D2VENUS
autofluorescence
(d)
DR5::ERGFP
W131Y
(e)
root length in cm
mock
5μM NPA
10μM NPA
(f)
phellem length in cm
(g)
phellem length / root length
(h)
mock
(i)
5 μM NPA
(j)
10 μM NPA
(k)
root length in cm
0.1μM NAA
1μM NAA
(l)
phellem length in cm
(m)
phellem length / root length
(n)
mock
(o)
0.1 μM NAA
(p)
1 μM NAA

Figure 2

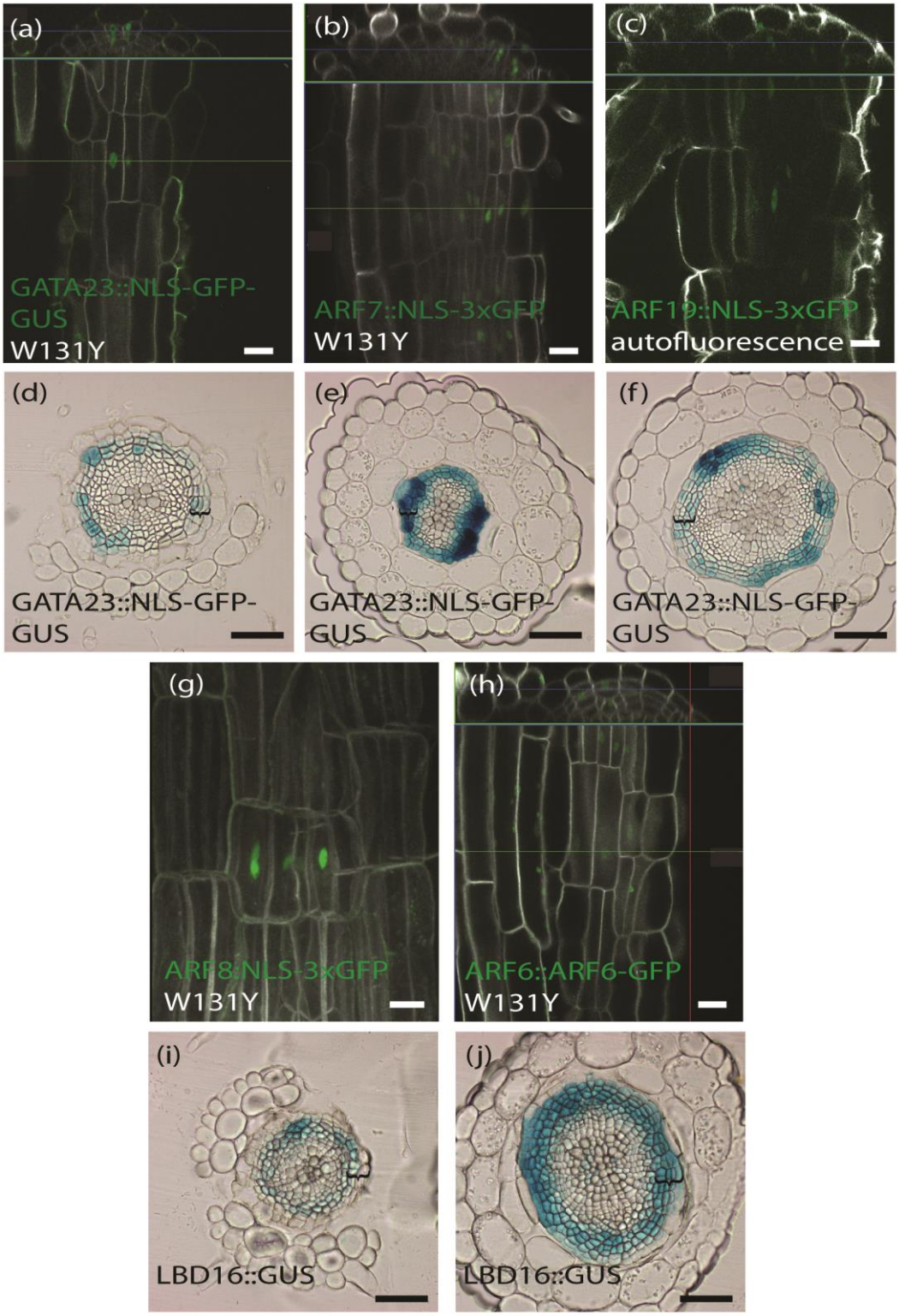
(a)
GATA23::NLS-GFP-GUS
W131Y
(b)
ARF7::NLS-3xGFP
W131Y
(c)
ARF19::NLS-3xGFP
autofluorescence
(d)
GATA23::NLS-GFP-GUS
(e)
GATA23::NLS-GFP-GUS
(f)
GATA23::NLS-GFP-GUS
(g)
ARF8::NLS-3xGFP
W131Y
(h)
ARF6::ARF6-GFP
W131Y
(i)
LBD16::GUS
(j)
LBD16::GUS

Figure 3

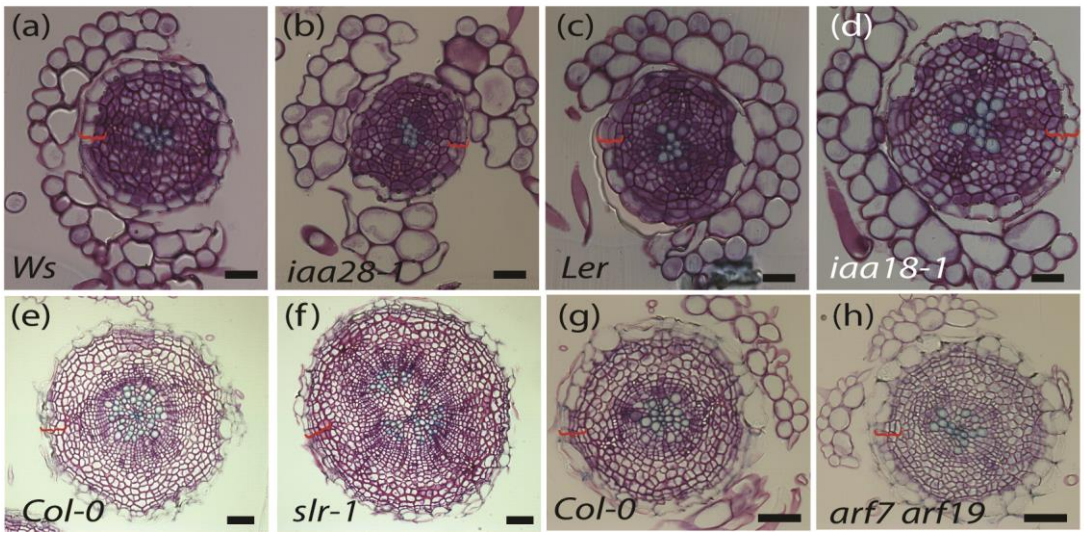

Figure 4

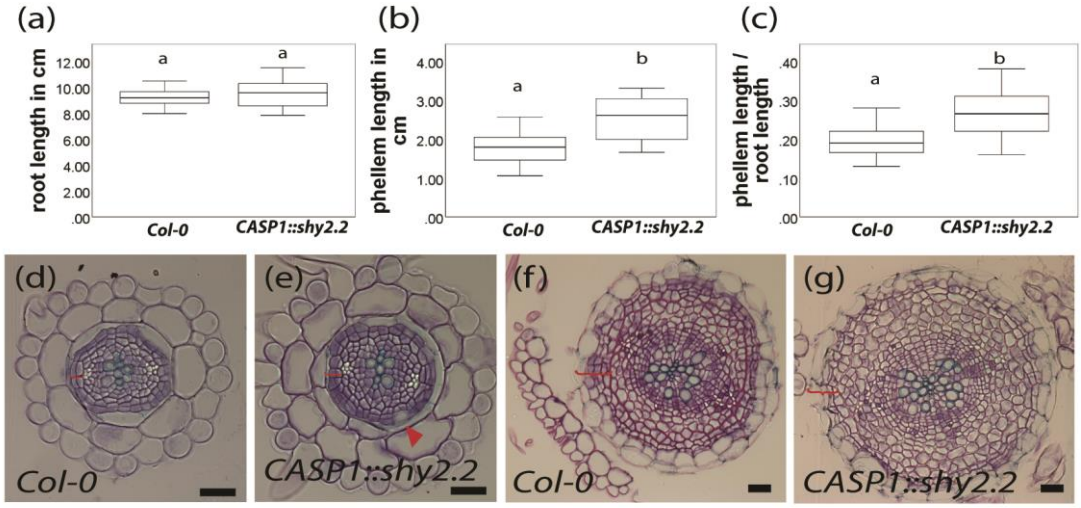
(a)
root length in cm
12.00
10.00
8.00
6.00
4.00
2.00
.00
a
a
Col-0
CASP1::shy2.2
(b)
phellem length in cm
4.00
3.00
2.00
1.00
.00
a
b
Col-0
CASP1::shy2.2
(c)
phellem length / root length
.40
.30
.20
.10
.00
a
b
Col-0
CASP1::shy2.2
(d)
Col-0
(e)
CASP1::shy2.2
(f)
Col-0
(g)
CASP1::shy2.2

Figure 5

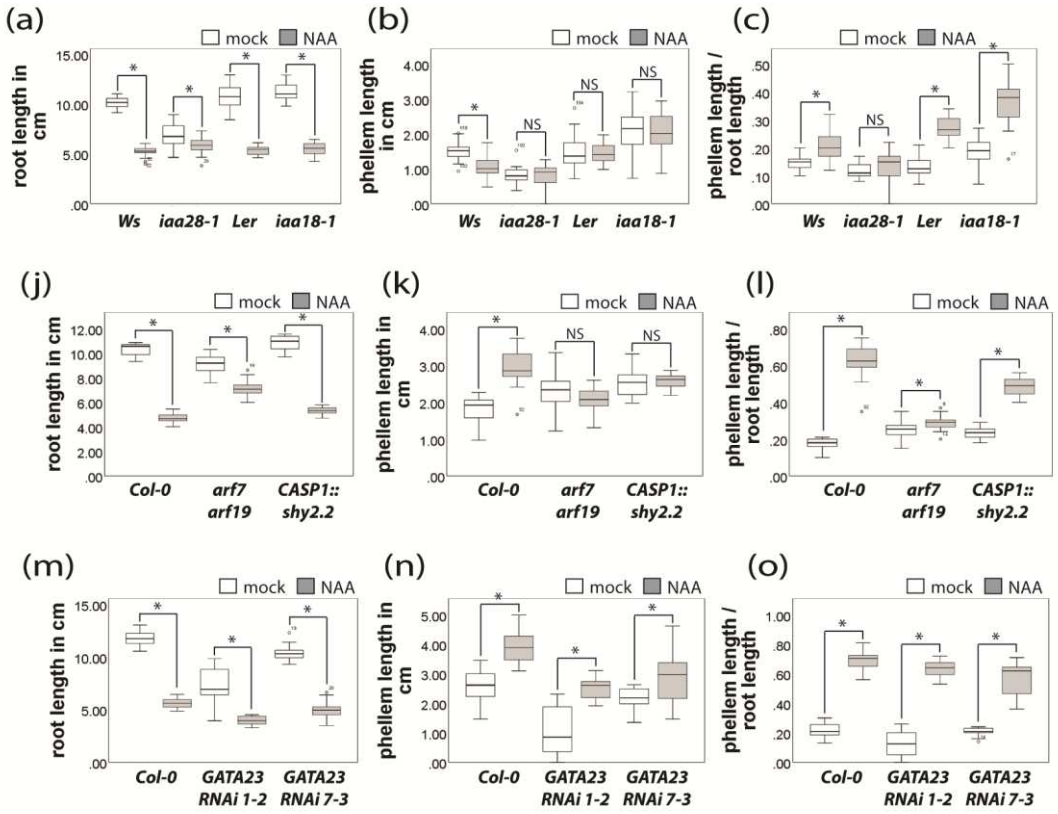
(a)
mock
NAA
root length in cm
15.00
10.00
5.00
.00
Ws
iaa28-1
Ler
iaa18-1
(b)
mock
NAA
phellem length in cm
4.00
3.00
2.00
1.00
.00
NS
Ws
iaa28-1
Ler
iaa18-1
(c)
mock
NAA
phellem length / root length
.50
.40
.30
.20
.10
.00
NS
Ws
iaa28-1
Ler
iaa18-1
(j)
mock
NAA
root length in cm
12.00
10.00
8.00
6.00
4.00
2.00
.00
Col-0
arf7 arf19
CASP1:: shy2.2
(k)
mock
NAA
phellem length in cm
4.00
3.00
2.00
1.00
.00
NS
Col-0
arf7 arf19
CASP1:: shy2.2
(l)
mock
NAA
phellem length / root length
.80
.60
.40
.20
.00
Col-0
arf7 arf19
CASP1:: shy2.2
(m)
mock
NAA
root length in cm
15.00
10.00
5.00
.00
Col-0
GATA23 RNAi 1-2
GATA23 RNAi 7-3
(n)
mock
NAA
phellem length in cm
5.00
4.00
3.00
2.00
1.00
.00
Col-0
GATA23 RNAi 1-2
GATA23 RNAi 7-3
(o)
mock
NAA
phellem length / root length
1.00
.80
.60
.40
.20
.00
Col-0
GATA23 RNAi 1-2
GATA23 RNAi 7-3

Figure 6

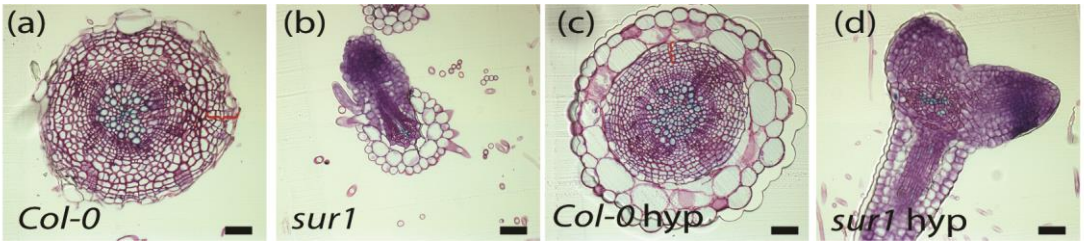

Figure 7

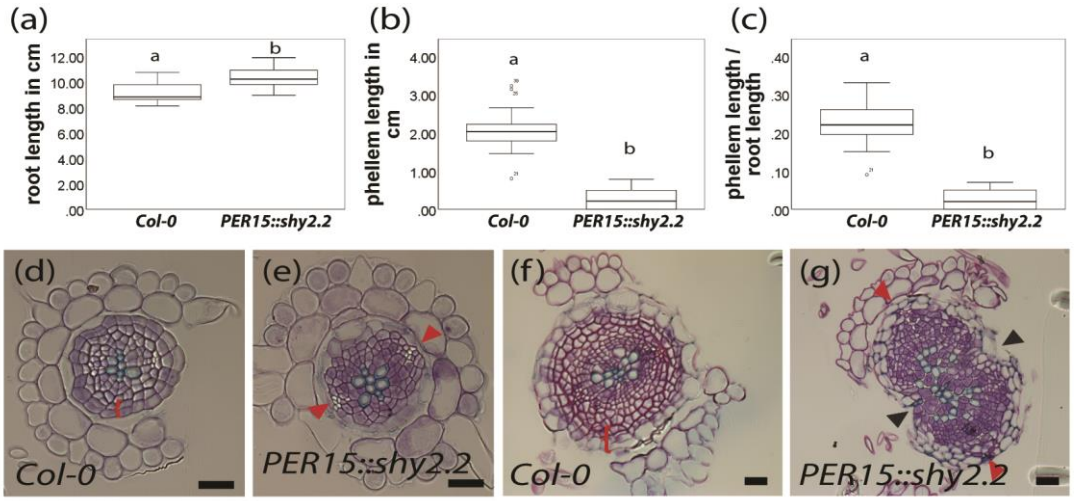
(a)
root length in cm
12.00
10.00
8.00
6.00
4.00
2.00
.00
a
b
Col-0
PER15::shy2.2
(b)
phellem length in cm
4.00
3.00
2.00
1.00
.00
a
b
Col-0
PER15::shy2.2
(c)
phellem length / root length
.40
.30
.20
.10
.00
a
b
Col-0
PER15::shy2.2
(d)
Col-0
(e)
PER15::shy2.2
(f)
Col-0
(g)
PER15::shy2.2

The following Supporting Information is available for this article:

Fig. S1: Periderm extension of auxin-signaling impaired mutants.

Fig. S2: Altered root diameter of plants with impaired auxin-dependent LR-regularors.

Fig. S3: Plants with defects in less important regulators of the auxin-dependent LR formation develop a periderm.

Fig. S4: *PER15* expression pattern and *PER15::shy2.2* phenotype.

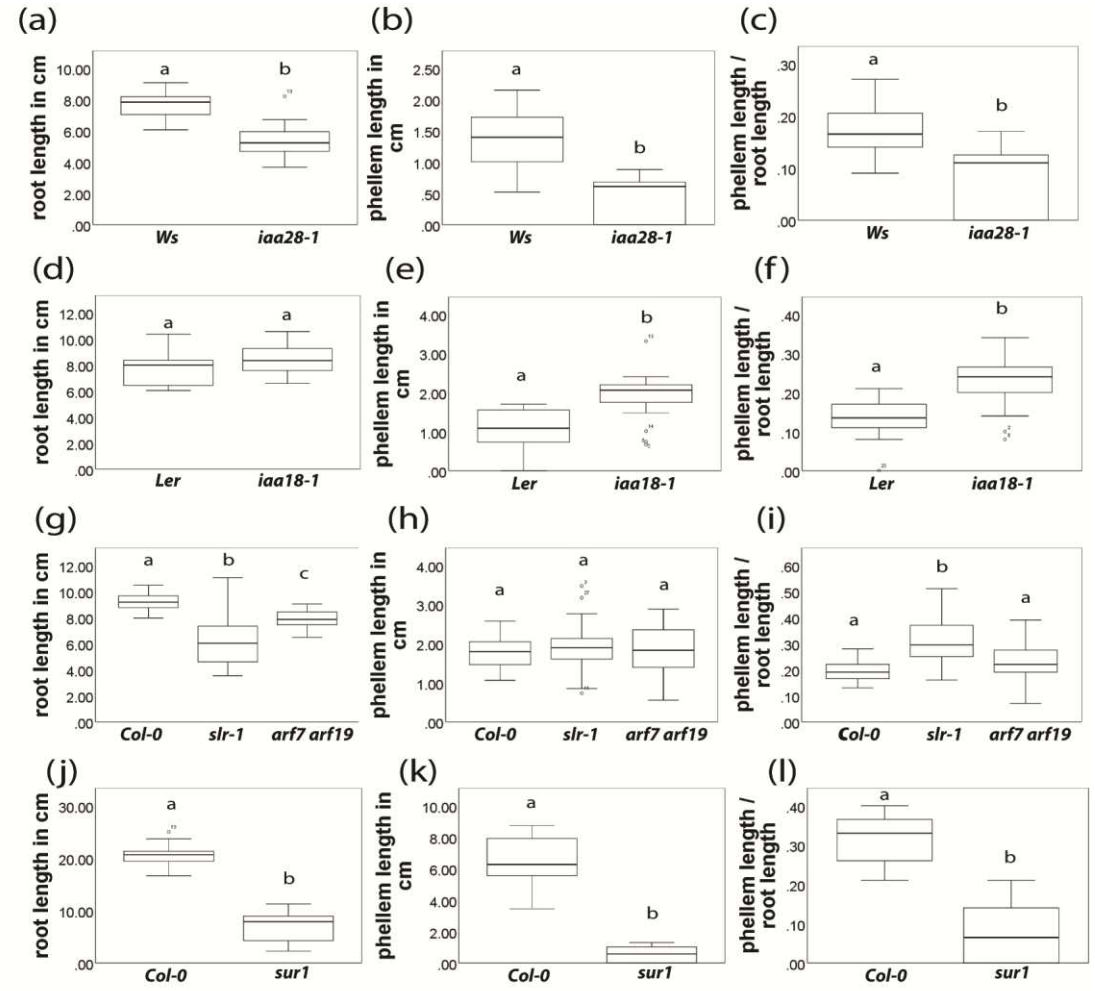

Fig. S1: Periderm extension of auxin-signaling impaired mutants. Box- plots of the root length (a,d,g,j), length of the phellem-covered root part (b,e,h,k) and ratio of phellem length to root length (c,f,i,l) of 12-d-old *Ws-2* and *iaa28-1* roots (a-c, n=20), 12-d-old *Ler* and *iaa18-1* roots (d-f, n=14,20), 12-d-old Col-0, *slr-1* and *arf7 arf19* roots (g-i, n=20-28), 19-d-old *Col-0* and *sur1* roots (j-l, n=20). Student's t-test $p < 0.05$. Box plots: the dark line in the middle of the boxes is the median, the bottom and top of the box indicates the 25th and 75th percentiles, whiskers are within 1.5 times the interquartile range, the empty dots are outliers.

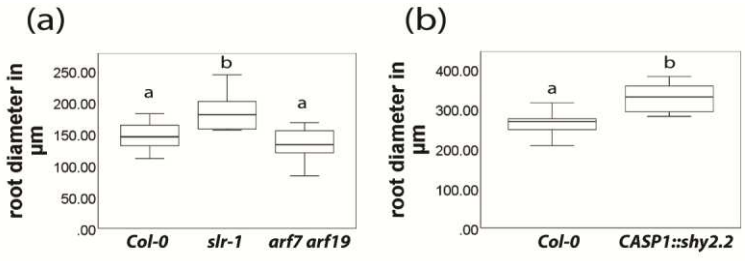

Fig. S2: Altered root diameter of plants with impaired auxin-dependent LR-regularors. (a,b) Root diameter of (a) 12-d-old *Col-0*, *slr-1* and *arf7 arf19* (n=9-18) and (b) 11-d-old *Col-0* and *CASP1::shy2.2* (n=8). Student's t-test $p < 0.05$. Box plots: the dark line in the middle of the boxes is the median, the bottom and top of the box indicates the 25th and 75th percentiles, whiskers are within 1.5 times the interquartile range.

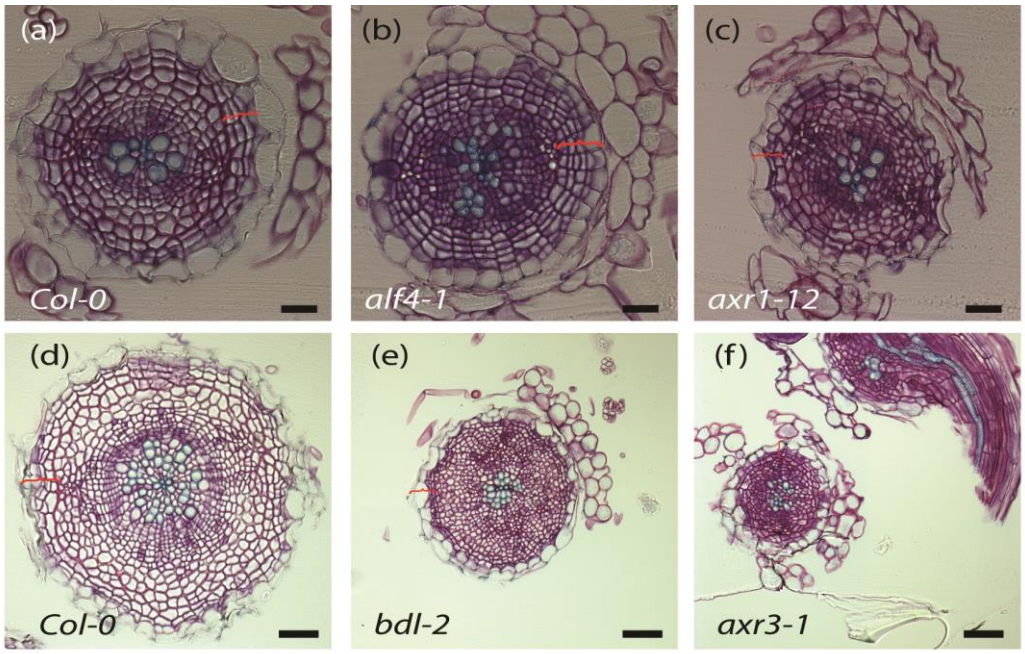

Fig. S3: Plants with defects in less important regulators of the auxin-dependent LR formation develop a periderm. Plastic cross-sections of 14-d-old (a-c) *Col-0* (a), *alf4-1* (b) and *axr1-12* (c) and 19-d-old (d-f) *Col-0* (d), *bdl-2* (e) and *axr3-1* (f) roots.

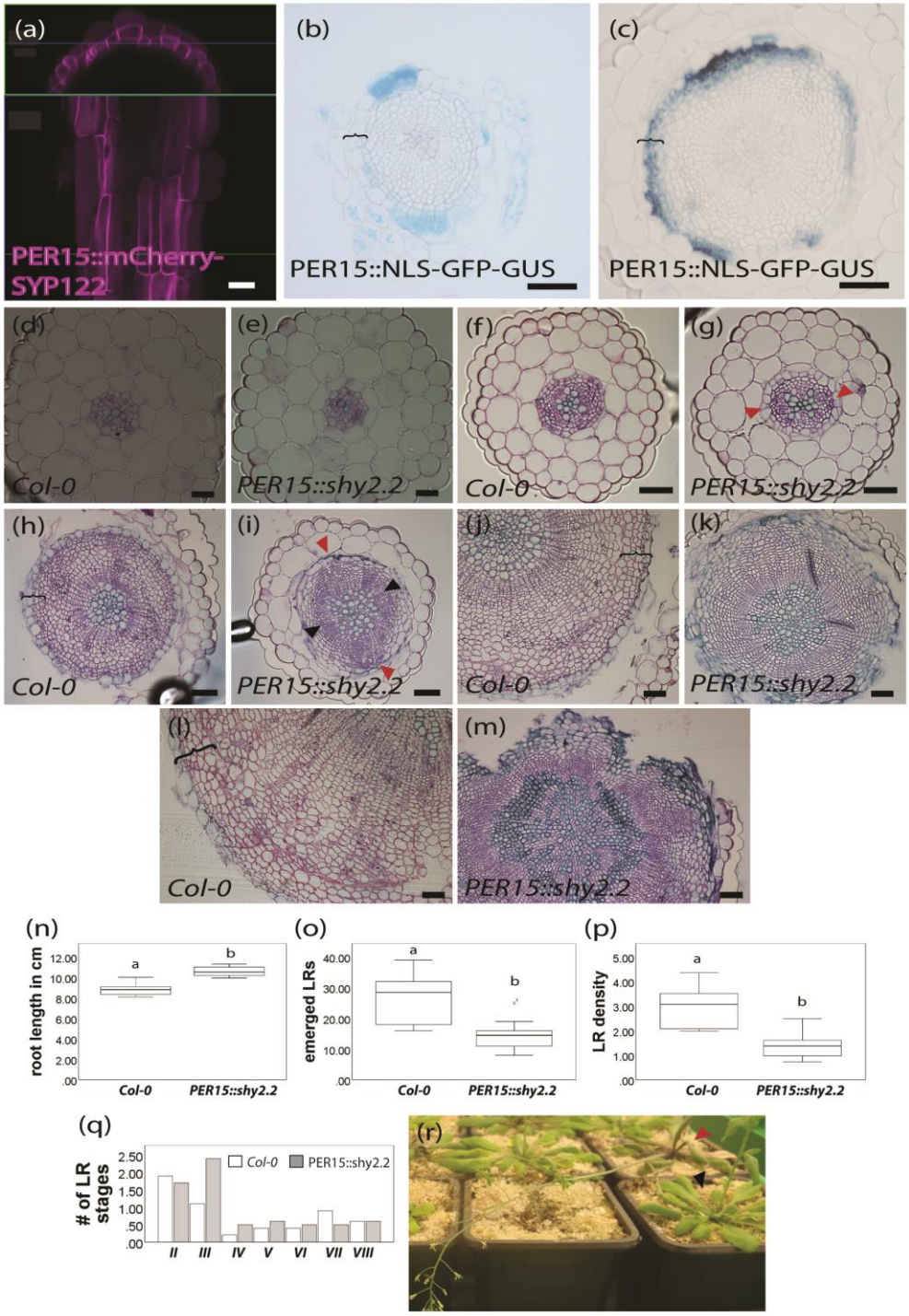

Fig. S4: *PER15* expression pattern and *PER15::shy2.2* phenotype. (a) *PER15::mCherry-SYP122*, (b,c) *PER15::NLS-GFP-GUS* (a) Cross and longitudinal sections (Ortho View of a Z-stack) of a 12-d-old root. (b,c) Plastic cross-sections of a GUS-stained 22-d-old root (b) 17-d-old hypocotyl (c). (d-m) Plastic cross-sections of 7 (d,e), 14 (f,g), 21 (h,i), 28 (j,k), 35 (l,m) -d-old hypocotyls of *Col-0* (d,f,h,j,l) and *PER15::shy2.2* (e,g,i,k,m; red arrows: missing periderm cell; black arrows: missing vascular cambium cells) plants grown on soil under long day conditions. (n-p) Box plots of root length (n), number of emerged LRs (o) and LR density (p) of 12-d-old *PER15::shy2.2* and *Col-0* roots (n=10, 2 repetitions). (q) Number of stages of LR in 12-d-old *PER15::shy2.2* (grey bars) and *Col-0* (white bars) roots (n=10, 2 repetitions). (r) *PER15::shy2.2* (red arrowhead) plant showing a lodging phenotype (black arrowhead: *Col-0*).

Student's t-test ($p < 0.05$). Box plots: the dark line in the middle of the boxes is the median, the bottom and top of the box indicates the 25^{th} and 75^{th} percentiles, whiskers are within 1.5 times the interquartile range, the empty dots are outliers and the black stars are extreme outliers. (a) White scale bar 20 µm. (b-m) Black scale bars, 50 µm.